

Gamma-aminobutyric acid Metabolism
in
Arabidopsis thaliana

I n a u g u r a l - D i s s e r t a t i o n

zur

Erlangung des Doktorgrades

der Mathematisch-Naturwissenschaftlichen Fakultät

der Universität zu Köln

vorgelegt von

Anke Christine Hüser

aus Köln

Köln, 2009

Berichterstatter:

Prof. Dr. Ulf-Ingo Flügge

Prof. Dr. Ute Höcker

Tag der letzten mündlichen Prüfung: 16. 02. 2009

FIGURE AND TABLE INDEX.....	IV
ABSTRACT.....	VI
ZUSAMMENFASSUNG	VII
1. INTRODUCTION	1
1.1. Function and metabolism of γ-amino butyric acid (GABA).....	1
1.2. The GABA-shunt in plants.....	3
1.2.1. Glutamate Decarboxylase (GAD).....	5
1.2.2. GABA-Transaminase (GABA-T).....	7
1.2.3. Succinic Semialdehyde Dehydrogenase (SSADH).....	8
1.2.4. GHB-Dehydrogenase (GHBDH).....	9
1.3. Auxin related genes in <i>Arabidopsis thaliana</i>.....	10
1.4. Callus formation in <i>Arabidopsis thaliana</i>.....	12
1.5. GABA acts as signal molecule in various organisms	13
1.5.1. GABA signaling in the central nervous system of vertebrates.....	13
1.5.2. GABA metabolism in <i>Saccharomyces cerevisiae</i>	16
1.5.3. Repression of quorum sensing in <i>Agrobacterium tumefaciens</i>	17
1.6. Aims of this thesis	19
2. RESULTS	20
2.1. Influence of the GABA-shunt on <i>Arabidopsis</i> plant growth.....	20
2.1.1. Examination of GABA-shunt mutants	20
2.1.2. Effect of GABA-shunt metabolites on plant growth.....	23
2.1.3. Analysis of the <i>Arabidopsis</i> GHBDH-genes.....	28
2.2. Identification of other genes involved in GABA-metabolism.....	35
2.2.1. Screening of <i>ssadh</i> suppressor lines	35
2.2.2. Identification of new <i>gaba-t</i> alleles.....	37
2.2.3. Map-based cloning of three <i>ssadh</i> suppressor lines	39
2.2.3.1. Line 4.D.....	40
2.2.3.2. Line 17.J.....	43
2.2.3.3. Line 21.H.....	46

2.3.	SSA induces callus formation in Arabidopsis.....	49
2.3.1.	Callus formation is dependent on the SSA concentration.....	49
2.3.2.	Does a linkage between SSA-induced callus formation and phytohormones exist?.....	52
2.3.3.	Does SSA itself act as auxin?	55
3.	DISCUSSION.....	56
3.1.	Influence of GABA-shunt metabolites on plant growth	56
3.2.	Identification of ssadh suppressor lines	61
3.3.	SSA induces callus formation in Arabidopsis thaliana.....	63
4.	MATERIALS AND METHODS.....	65
4.1.	Materials.....	65
4.1.1.	Chemicals.....	65
4.1.2.	Enzymes.....	65
4.1.3.	Kits.....	65
4.1.4.	Antibiotics.....	65
4.1.5.	Bacteria	66
4.1.6.	Plant lines.....	66
4.1.7.	Software	67
4.1.8.	Used Equipment.....	68
4.1.9.	Consumables	69
4.2.	Methods	71
4.2.1.	Work with <i>Arabidopsis thaliana</i>	71
4.2.1.1.	Growth conditions	71
4.2.1.2.	Screening of T-DNA Insertion lines.....	71
4.2.1.3.	Crossing of <i>Arabidopsis thaliana</i> plants.....	71
4.2.1.4.	Map-based cloning in <i>Arabidopsis thaliana</i>	72
4.2.1.5.	GUS Staining.....	72
4.2.1.6.	Growth of Arabidopsis plants on sterile media	72
4.2.1.7.	Fluorescence Microscopy	74
4.2.1.8.	<i>Arabidopsis thaliana</i> cell culture	74
4.2.1.9.	Biolistic transformation	75
4.2.2.	Microbiology	76
4.2.2.1.	Work with <i>E. coli</i>	76
4.2.2.2.	Work with <i>Agrobacterium tumefaciens</i>	78
4.2.3.	Molecular biology techniques	80

4.2.3.1.	Plasmid Preparation.....	80
4.2.3.2.	Preparation of <i>Arabidopsis thaliana</i> genomic DNA.....	80
4.2.3.3.	Expression Analysis	81
4.2.3.4.	Photometric determination of nucleic acid concentrations.....	82
4.2.3.5.	PCR	82
4.2.3.6.	Gel electrophoresis	83
4.2.3.7.	Gateway-Cloning.....	83
4.2.3.8.	Restriction Digestion of Nucleic Acids	84
4.2.3.9.	Precipitation of Nucleic acids.....	84
4.2.3.10.	Sequencing	84
4.2.4.	Metabolite Analysis	85
4.2.4.1.	GC-MS measurements.....	85
5.	REFERENCES	86
6.	APPENDIX.....	99
6.1.	Features of selected ssadh suppressor lines	99
6.1.1.	Growth characteristics and metabolite contents.....	99
6.1.2.	Cluster analysis	103
6.1.3.	Phenotypes	104
6.2.	Reporter lines	110
6.3.	Phytohormone mutants	111
6.4.	Primer Sequences.....	112
6.4.1.	Screening	112
6.4.2.	Cloning.....	113
6.4.3.	RT-PCR	113
6.4.4.	Sequencing.....	115
6.4.5.	Mapping	117
6.4.5.1.	SSLP-Marker.....	117
6.4.5.2.	CAPS-Marker.....	118
6.5.	Vector Maps	119
	ABBREVIATIONS.....	120
	PUBLICATIONS.....	122

Figure and Table Index

Figure 1: Schematic representation of the GABA-shunt in plants	2
Figure 2: Comparison of Arabidopsis wild type and <i>gaba-t</i> mutant siliques	20
Figure 3: Comparison of Arabidopsis wild type and <i>ssadh</i> mutant plants	21
Figure 4: Metabolite measurement of GABA and GHB in GABA-shunt mutants	22
Figure 5: Growth of various Arabidopsis ecotypes on ½ MS supplemented with different concentrations of GABA, SSA, or GHB	24
Figure 6: Growth of wild type and <i>gaba-t</i> mutant plants on different media.....	24
Figure 7: Growth of wild type, <i>gaba-t</i> , and <i>gaba-t/ssadh</i> mutant plants.....	25
Figure 8: Growth of wild type, <i>gaba-t</i> , and <i>gaba-t/ssadh</i> plants on ½ MS supplemented with either SSA or GHB in different concentrations.....	27
Figure 9: Co-localization of AtGHBDH-1-GFP with a plasma membrane marker	28
Figure 10: Growth of wild type and two independent <i>ghbdh-1</i> lines on ½ MS supplemented with SSA or GHB.....	29
Figure 11: Phylogenetic tree of GHBDH-homologous sequences.....	30
Figure 12: Alignment of the two GHBDH protein sequences.....	31
Figure 13: AtGHBDH-2-GFP co-transformation with plastid-localized RFP	32
Figure 14: AtGHBDH-2-GFP co-transformation with plastid-localized RFP	32
Figure 15: AtGHBDH-2-GFP co-transformation with mitochondrial-localized RFP	32
Figure 16: AtGHBDH-2-GFP co-localization with Mitotracker Red	33
Figure 17: Growth of wild type and two <i>ghbdh-1/ghbdh-2</i> lines on ½ MS supplemented with SSA or GHB	34
Figure 18: Phenotypes of several independent <i>ssadh</i> suppressor mutants	36
Figure 19: Location of the EMS induced mutations in the <i>gaba-t</i> genomic sequence.....	37
Figure 20: Alignment of protein sequences from Arabidopsis and pig.....	38
Figure 21: Distribution of the used SSLP markers in the Arabidopsis genome.....	39
Figure 22: Phenotype of 4.D M ₂ plant grown under greenhouse conditions for 44 days.	41
Figure 23: Plants of the M ₃ -generation were grown under long day (A) and short day (B) conditions for 39 days.....	41
Figure 24: Analysis of the M ₃ -generation	41
Figure 25: Marker distribution with a high frequency of Col-0 fragments in line 4.D	42
Figure 26: Phenotype of 17.J M ₂ plant grown under greenhouse conditions for 44 days.	44

Figure 27: Plants of the M ₃ -generation were grown under long day (A) and short day (B) conditions for 39 days.....	44
Figure 28: Analysis of the M ₃ -generation	44
Figure 29: Marker distribution with a high frequency of Col-0 fragments in line 17.J ...	45
Figure 30: Phenotype of 21.H M ₂ plant grown under greenhouse conditions for 44 days.	46
Figure 31: Plants of the M ₃ -generation were grown under long day (A) and short day (B) conditions for 39 days.....	46
Figure 32 Analysis of the M ₃ -generation.....	47
Figure 33: Marker distribution with a high frequency of Col-0 fragments in line 21.H ..	48
Figure 34: <i>ssadh</i> mutant plants develop callus on ½ MS	49
Figure 35: Rate of callus formation in Arabidopsis wild type plants is dependent on the SSA concentration in the media.	50
Figure 36: Phenotype of <i>ssadh</i> seeds germinated on ½ MS containing SSA.....	51
Figure 37: Whole plants can be regenerated from SSA-induced callus	51
Figure 38: Callus formation is not dependent on the auxin to cytokinin ratio	52
Figure 39: Influence of inhibitors of auxin transport or activity on SSA-induced callus formation.....	53
Figure 40: GUS-staining of SSA-induced calli	54
Figure 41: Callus formation rate in auxin-related mutants	54
Figure 42: Assay for auxin activity in Arabidopsis	55
Figure 43: Cluster Analysis of <i>ssadh</i> suppressor lines	103
Figure 44: Map of the AtGHBDH-1-GFP fusion construct	119
Figure 45: Map of the AtGHBDH-2-GFP fusion construct	119
Table 1: Recombination frequencies in F ₂ plants obtained by a cross of <i>ssadh</i> suppressor line 4.D to <i>Ler</i> wild types	42
Table 2: Recombination frequencies in F ₂ plants <i>Ler/17.J</i>	45
Table 3: Recombination frequencies in F ₂ plants obtained by a cross of <i>ssadh</i> suppressor line 4.D to <i>Ler</i> wild types	47
Table 4: Analysis of M ₃ plants	99
Table 5: M ₄ plants grown under long day conditions.....	100
Table 6: M ₄ plants grown under short day conditions.....	101

Abstract

The four-carbon, non-protein amino acid γ -amino butyric acid (GABA) is found in all species, where it is involved in various signaling processes. GABA is best characterized as the main inhibitory neurotransmitter in mammalia. On the contrary, work in plants focused mainly on a metabolic role; just some recent findings indicate GABA having a possible signaling function in plants as well.

In *Arabidopsis thaliana*, mutants of both catabolic genes (*GABA transaminase (GABA-T)* and *succinic semialdehyde dehydrogenase (SSADH)*) display phenotypic deviations to wild type; the former grow vegetatively like wild type, but are less fertile due to a misguidance of pollen tubes. The latter are severely affected in growth and development, probably induced by the accumulation of GABA-shunt metabolites and/or reactive oxygen intermediates. The *ssadh* phenotype can be suppressed by interrupting the GABA-shunt upstream of the SSADH function. Based on this, two topics should be covered in this thesis. First, the substance causing the *ssadh* phenotype should be identified; hence, wild type along with GABA-shunt single and double mutants were grown on media containing GABA-shunt intermediates, and plant growth as well as metabolite content in leaf extracts was examined. Second, further genes involved in regulation or function of the GABA-shunt or in sensing of GABA-shunt related metabolites should be identified. Therefore, a population of mutagenized *ssadh* plants was screened for suppressors; among several stable, non-segregating lines, two new *gaba-t* alleles were isolated.

All GABA-shunt intermediates influence plant growth and development. First, GABA enhances plant growth by inducing expression of nitrate uptake transporters, only very high cellular concentrations have an inhibitory effect on plant growth. Second, succinic semialdehyde (SSA) considerably reduces plant growth when applied with the growth media, and higher concentrations (0.8mM and more in the media) induce dedifferentiation mainly of hypocotyl cells in a yet unknown manner. Finally, the enzymatic reduction of SSA produces γ -hydroxybutyric acid (GHB), which leads to reduced root growth in *Arabidopsis* without major effects on rosette size when accumulating in plant tissues.

Zusammenfassung

Die nicht proteinogene Aminosäure γ -Aminobuttersäure (GABA) wurde in allen auf ein Vorkommen hin untersuchten Arten nachgewiesen. Im Zentralnervensystem der Säugetiere wirkt GABA als der wichtigste inhibitorische Neurotransmitter, allerdings konnte für GABA auch in Bakterien und Hefen eine Funktion als Signalsubstanz gezeigt werden. Im Gegensatz dazu beschränkte sich die Forschung an GABA in Pflanzen lange Jahre einzig auf eine Rolle im Stoffwechsel, erst einige neuere Publikationen lassen auch eine Signalfunktion in Pflanzen möglich erscheinen.

Mutanten der GABA-abbauenden Gene (*GABA-Transaminase (GABA-T)* und *Succinic Semialdehyd Dehydrogenase (SSADH)*) zeigen in *Arabidopsis thaliana* einen vom Wildtyp abweichenden Phänotyp. Pflanzen ohne GABA-T-Aktivität sind in der vegetativen Phase nicht von Wildtypen zu unterscheiden, allerdings sind die Schoten der Pflanzen kleiner und enthalten weniger Samenkörner. Dieser Phänotyp konnte durch einen erhöhten GABA-Gehalt im Fruchtknoten erklärt werden, der ein gezieltes Wachstum der Pollenschläuche zu den Samenanlagen verhindert. *ssadh*-Mutanten bilden bereits im Gewächshaus nekrotische Blätter und zeigen ein deutlich verlangsamtes Wachstum. Die Ursache dieses Phänotyps ist noch nicht vollständig geklärt, allerdings wird ein Zusammenhang mit einer hohen Konzentration von Intermediaten des GABA-Stoffwechsels und der Bildung reaktiver Sauerstoffverbindungen diskutiert. Der *ssadh*-Phänotyp kann durch Inhibierung der GABA-T unterdrückt werden, worauf zwei Fragestellungen basieren. Zum einen soll herausgefunden werden, welche Substanz für den *ssadh*-Phänotyp verantwortlich ist, weshalb Einzel- und Doppelmутanten des GABA-Stoffwechsels auf mit Intermediaten des GABA-Stoffwechsels versetzten Sterilmedien angezogen und Wachstum sowie Metabolitgehalt der Pflanzen analysiert werden. Zum anderen sollen weitere Gene identifiziert werden, die entweder indirekt als Regulatoren oder direkt am GABA-Stoffwechsel beteiligt sind bzw. an einer postulierten Signalkaskade mitwirken. Dazu wurde eine Population EMS-mutagenisierter *ssadh*-Pflanzen mit dem Ziel durchmustert, Pflanzen zu isolieren, welche den *ssadh*-Phänotyp unterdrücken. Mehrere stabile, nicht aufspaltende Linien wurden isoliert, unter denen sich auch zwei Linien befanden, welche auf Grund einer mutierten GABA-T keinen *ssadh*-Phänotyp zeigen.

Für alle im GABA-Stoffwechsel vorkommenden Intermediate konnte ein Einfluss auf Wachstum und Entwicklung von Pflanzen gezeigt werden.

Ein erhöhter GABA-Gehalt in den Zellen induziert die Expression von Genen, welche für Nitrat-importierende Proteine codieren. In Folge der erhöhten Nitrat-Aufnahmekapazität steht den Pflanzen mehr Stickstoff zur Verfügung, welcher ein verbessertes Wachstum ermöglicht. Dieser Effekt wird erst bei deutlich erhöhten zellulären GABA-Konzentrationen ins Gegenteil gekehrt.

Succinic Semialdehyd (SSA) verringert bereits in niedrigen Konzentrationen das Pflanzenwachstum, etwas höhere Konzentrationen (ab 0,8mM SSA im Medium) bewirken eine Dedifferenzierung von Zellen im Hypocotyl der Pflanzen, wobei der zugrunde liegende Mechanismus noch unbekannt ist.

Bei der Reduktion von SSA entsteht γ -Hydroxybuttersäure (GHB), welche ein reduziertes Wurzelwachstum ohne deutlich verringertes Sprosswachstum bewirkt.

1. Introduction

1.1. Function and metabolism of γ -amino butyric acid (GABA)

The non-protein amino acid γ -amino butyric acid (GABA) is conserved from bacteria through yeast to vertebrates. GABA was discovered nearly 60 years ago in plants [165], but research focused on vertebrates following the discovery of high GABA levels in the mammalian central nervous system and the identification of its role as the main inhibitory neurotransmitter (1.5.1). For yeast (*Saccharomyces cerevisiae*), a functional GABA-shunt is essential for oxidative stress tolerance (1.5.3), and in plant pathogenic bacteria like *Agrobacterium tumefaciens*, GABA and GABA-shunt metabolites were identified as repressors of quorum sensing signaling (1.5.2). *Escherichia coli* is dependent on the *Gad* acid resistance system, containing two Glutamate Decarboxylase genes (*GadA* and *GadB*) and the GABA exporter (*GadC*), to survive during acidic conditions [38] and expression of GABA-degrading enzymes was found to be induced under nitrogen limiting conditions [151]. In contrast, research in plants focused primarily on a role for GABA as a metabolite, mainly in the context of stress response, until some recent findings were published indicating a possible signaling function for GABA in plants as well (1.2).

In eukaryotes, the GABA-shunt is compartmentalized (Figure 1); the synthesis takes place in the cytoplasm while the degrading enzymes are localized in the mitochondrial matrix. In the cytoplasm, glutamate is irreversibly decarboxylated by the Glutamate Decarboxylase (GAD); the enzyme activity is regulated posttranslationally either by cofactor binding in mammalia or by Ca^{2+} /CaM-induced dimerisation.

For the catabolic steps of the pathway, GABA is imported into mitochondria, where a transamination to succinic semialdehyde occurs. The GABA-Transaminase (GABA-T) undergoes conformational changes following binding of pyridoxal phosphate near the catalytic domain, influencing enzyme activity [47-49, 51]. In mammals, the GABA-T uses α -ketoglutarate as acceptor for the transferred amino group, whereas the plant GABA-T utilizes pyruvate. A direct interaction between GABA-T and Succinic

Semialdehyde Dehydrogenase (SSADH) was published for the mammalian proteins [82] indicating toward a substrate channeling mechanism that prevents a release of the reactive succinic semialdehyde (SSA) into the mitochondrial matrix. In the GABA-shunt, SSA is oxidized to succinate in the NAD^+ -dependent SSADH reaction; succinate is further metabolized in the citric acid cycle. Another possible alternative for SSA degradation might be the reduction to γ -hydroxybutyric acid (GHB), a second neuroactive substance related to GABA [83].

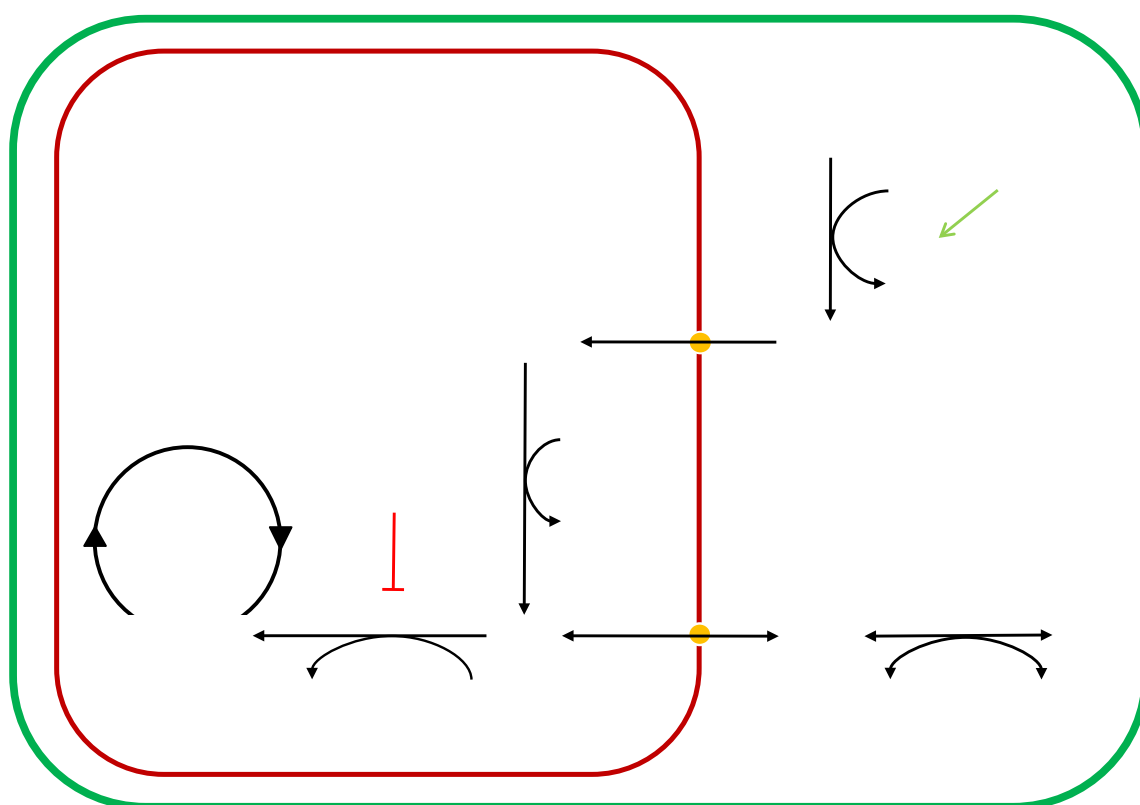


Figure 1: Schematic representation of the GABA-shunt in plants

Enzymes and metabolites of the GABA-shunt are shown in blue; activatory and inhibitory substances in green and red respectively.

GAD – glutamate decarboxylase; GABA – γ -amino butyric acid; GABA-T – GABA transaminase; SSA – succinic semialdehyde; SSADH – SSA dehydrogenase; GHB – γ -hydroxy butyric acid; GHB DH – GHB dehydrogenase; CaM – Calmodulin; TCA – citric acid cycle

1.2. The GABA-shunt in plants

In contrast to vertebrates, the physiological role of GABA in plants remains still unclear. While a rapid GABA accumulation in plants under various stress conditions to very high concentrations is known for many years [38, 56, 62, 63, 96, 118, 151, 184], the GABA-shunt is just recently discussed to possess a signaling function in plants as well [26, 28, 130]. The observed fast increase in the cellular GABA concentration was first discussed as a regulatory mechanism for homeostasis of the cytosolic pH, since GABA synthesis is consuming protons [54]. Later, an increase of the cytosolic Ca^{2+} -concentration preceding the elevated GABA synthesis rate was reported, linking GABA synthesis to stress signaling [50].

Some data indicate toward a possible function of GABA in various processes like pH regulation [41], temporary nitrogen storage [97, 148, 149] or pathogen resistance. An increased expression of GABA-shunt genes and accumulation of GABA in the millimolar range was found upon plant infection with different pathogenic fungi [88, 163, 187] or in response to attack by herbivorous larvae [30, 109, 116], where GABA is discussed to interfere with signaling in the nervous system of the insects or to induce transition between larval and juvenile stages [30, 121, 154, 156].

Exogenously applied GABA affects the expression of a subset of 14-3-3 protein family members in a Ca^{2+} , abscisic acid (ABA) and ethylene-dependent manner [103]. A possible relation between phytohormones and GABA was assumed since exogenous GABA activates ACC synthase transcription [89, 90] as well as GABA synthesis is induced by phytohormones [68, 143]. Additionally, GABA is suggested to be involved in several plant development processes including senescence [7, 114], fertilization [130, 168, 188], and regulation of nitrate uptake by increasing expression of nitrate transporters [22].

For the functionality of the whole pathway, the existence of a GABA-uptake mechanism into the mitochondria is necessary. Therefore, the existence of a yet unknown mitochondrial GABA-Transporter must be supposed.

If GABA or GABA-shunt metabolites are acting directly as a signaling substances *in planta*, then the existence of transporters regulating import or export of the signal molecule from cells and of receptors triggering a signal is essential.

Both high and low affinity GABA transporters localized in the plasma membrane are known. Three low affinity transporters (ProT) with different expression patterns were identified in Arabidopsis [79] allowing the plants to grow on GABA as the sole nitrogen source. In studies with GABA-uptake deficient yeast, heterologous expression of these transporters was sufficient to restore yeast growth, and GABA uptake could be inhibited by proline and quaternary ammonium compounds [33]. A tomato homolog is highly expressed in pollen, where it is necessary for the uptake of compatible solutes during pollen desiccation and germination [152]. Recently, a high-affinity, plasma-membrane localized GABA transporter in Arabidopsis (AtGAT1) was isolated, displaying no sequence similarity to previously described non-plant GABA transporters. In Arabidopsis, the highest gene expression was found in flowers and under conditions inducing GABA accumulation [119].

In plants, no homologs of mammalian or bacterial GABA receptors can be identified by sequence analysis. Although GABA binding sites on the surface of living tobacco protoplasts were detected [190] and a potential modulation of ion transport in *Lemna minor* by GABA was reported [95], but no corresponding genes have been cloned thus far. Both findings indicate toward the existence of GABA-like receptor in plants. Additionally, plant glutamate receptors (GLRs) are discussed to act potentially as GABA receptors in plants [29, 45, 69, 102, 176], but experimental evidence is still lacking.

1.2.1. Glutamate Decarboxylase (GAD)

The first reaction of the GABA-shunt is the pyridoxal phosphate-dependent α -decarboxylation of L-glutamate, catalyzed by the cytosolic Glutamate Decarboxylase (GAD, EC 4.1.1.15).

In plants, the *GAD* genes are differentially expressed in a developmentally controlled manner. They contain a Calmodulin-(CaM)-binding domain in the C-terminal region, allowing a fast regulation of protein activity upon increase of the cytosolic Ca^{2+} concentration [15, 32, 42, 193]. *In vitro*, an enhanced GAD activity in response to the addition of Ca^{2+} /CaM was published for different plant species like soy bean, petunia or tobacco [8, 161, 189]. Interestingly, this stimulation of GAD activity by CaM binding could *in vitro* only be detected at neutral pH (7.0 to 7.5), whereas GAD activity is unaffected by Ca^{2+} /CaM at acidic pH conditions, where a sharp pH optimum at 5.8 was detected. Binding of Ca^{2+} /CaM or a specific monoclonal antibody induces dimerisation *in vitro*, which is essential for the activation of GADs [162, 191]. In tobacco, the overexpression of a truncated GAD without the CaM-binding domain results in plants with reduced growth due to cortex parenchyma cells fail to elongate, as well as very high GABA and low glutamate levels in plant extracts. Hence, the CaM-binding domain is discussed to possess an autoinhibitory effect on GAD activity that is relieved by addition of Ca^{2+} ; the expression of a truncated GAD therefore leads to constitutive activity [16]. This autoinhibition was also observed in rice (*Oryza sativa*), where OsGAD1 contains the CaM binding domain in contrast to OsGAD2 [2]. The former is regulated in a Ca^{2+} -dependent manner, and truncation of the C-terminal extension resulted in a constitutively active enzyme [3] whereas the latter has a very low activity either in presence or absence of CaM/ Ca^{2+} .

The regulation of GAD activity in response to cytosolic Ca^{2+} -levels allow plant cells a very fast response to various stress situations by initiating GABA synthesis, indicating that GABA or the GABA-shunt is involved in plant stress signaling.

In the model plant *Arabidopsis thaliana*, five GAD isoforms exist, among them two have been biochemically characterized, whereas the three additional genes were identified as GADs based on sequence homologies [155, 175]. *AtGAD1* (At5g17330) is expressed exclusively in roots and is essential for sustaining GABA levels in roots whereas the second highly expressed isoform, *AtGAD2* (At1g65960), is expressed in all tissues [27, 175]. Analysis of *AtGAD3* and *AtGAD4* (At2g02000 and At2g02010) reveals a very high sequence identity, most probably due to a recent gene duplication. In northern blots or microarray experiments transcripts are detected in generative organs, even if both genes are indistinguishable due to cross hybridizations. For the last isoform, *AtGAD5* (At3g17760), a weak expression is detected in isolated pollen (<http://www.bar.utoronto.ca/efp/cgi-bin/efpWeb.cgi>).

1.2.2. GABA-Transaminase (GABA-T)

The second step of the GABA-shunt is the pyridoxal phosphate-dependent transfer of the amino group from GABA to pyruvate, yielding SSA and alanine, catalyzed by the GABA-Transaminase (GABA-T, EC 2.6.1.19). Following cell fractionation of soybean tissue, the GABA-T activity could be assigned to the mitochondrial fraction [32]. Evidence for a published α -ketoglutarate dependent GABA-T activity [177, 178] exists only from biochemical data, but thus far no corresponding gene has been cloned.

In *Arabidopsis thaliana*, one *GABA-T* isoform exists (At3g22200), and T-DNA insertion plants are indistinguishable from wild types during vegetative growth. Subsequent transition to the generative phase, *gaba-t* mutant plants reveal a reduced fertility compared to wild type, developing smaller siliques. The high number of unfertilized ovules is due to the accumulation of high GABA concentrations in the transmitting tissue of the ovary [130, 188]. In ovules of *Arabidopsis* wild type plants a GABA gradient is formed, reaching from the stigma to the micropyle, guiding the pollen tube along this gradient to fertilize the egg, which then might stop the production of attractants, e.g. GABA [85, 157].

In response to herbivore attack, plants produce a wide range of volatile organic compounds, among them C6-volatiles (six-carbon alcohols, aldehydes, and esters). When exposed to these compounds, even undamaged plants induce defense-regulated pathways. To elucidate the underlying mechanisms, *Arabidopsis* mutants with altered responses to the C6-volatile E-2-hexenal were isolated, among them a *gaba-t* mutant, termed *her1* [120]. Here, GABA seems to play a key role in E-2-hexenal detoxification; however, the underlying mechanisms are not yet fully understood.

1.2.3. Succinic Semialdehyde Dehydrogenase (SSADH)

The final step of the GABA-shunt is the NAD⁺-dependent oxidation of SSA to succinate in the mitochondrial matrix [32]. The reaction is catalyzed by succinic semialdehyde dehydrogenase (SSADH, EC 1.2.1.16), an enzyme active as homotetramer that is inhibited *in vitro* by high NAD⁺- and adenine nucleotide concentrations [34].

In *Arabidopsis thaliana*, the *SSADH* is a single copy gene (At1g79440), *ssadh* mutant plants display a severe phenotype; they are retarded in growth and less fertile than wild type (Figure 3). The occurrence of necrotic lesions already in the greenhouse, but especially when grown under high light conditions, is discussed in relation to the disruption of the whole GABA-shunt and/or the accumulation of reactive oxygen species [26, 66].

In contrast to the assumption of an intact GABA-shunt being essential for normal plant growth, which was discussed after the isolation of *ssadh* mutants, vegetative growth of *ssadh* mutant plants is improved by inhibiting GABA-T activity. Either, *gaba-t/ssadh* double mutant plants are generated [107] or the structural GABA analog Vigabatrin (γ -vinyl-GABA) is used [66] Vigabatrin can not be metabolized by GABA-T, but interacts with the enzyme and thus irreversibly blocks GABA-T function [174]; in mammalia, it is used as therapeutic in some cases of epileptic disorders.

1.2.4. GHB-Dehydrogenase (GHBDH)

Alternative to the oxidation of SSA by the mitochondrial SSADH, SSA can be reduced to γ -hydroxybutyric acid (GHB) via the GHB-dehydrogenase (GHBDH), also named as succinic semialdehyde reductase (SSR). The GHBDH is localized in the cytosol of animal cells, possibly in plants as well. In mammals, GHB is known to be a neuroactive substance [160], whereas its role in plants is still unknown.

A gene encoding a *GHBDH* (At3g25530) in Arabidopsis was identified by the complementation of an *ssadh*-deficient yeast strain with an Arabidopsis cDNA-library [31]. GHBDH activity is discussed to be regulated by redox balance or the cellular SSA concentrations, probably complementary with SSADH activity. Sequence analysis revealed a homologous gene in Arabidopsis (At1g17650); both genes are upregulated under stress conditions like drought, salinity or oxygen deficiency [4, 5]. *In silico* analysis of the second identified GHBDH predicts the existence of a transit peptide, but the localization of the protein remains ambiguous. *In vitro* activity assays with purified recombinant enzymes revealed a high affinity for glyoxylate and, to a lesser extent, for SSA [86, 87, 158]. Therefore, both enzymes are discussed to be involved in aldehyde detoxification and in regulation of cellular redox homeostasis.

1.3. Auxin related genes in *Arabidopsis thaliana*

The phytohormone auxin is critical for plant growth and regulates several developmental processes. Many bioassays are described to test substances for their auxin function: curvature of decapitated pea shoots, elongation of wheat coleoptiles or inhibition of root elongation and induction of lateral root emergence in *Arabidopsis* [182, 194]. Corresponding to these assays, mutants overproducing auxins tend to have shorter roots and abundant lateral roots. At neutral pH, all known substances with auxin activity contain a strong, negative charge at the carboxyl group and a weaker, positive charge in the aromatic ring in a distance of 0.5nm, which is a key feature of their function [171].

In plants, auxins can be synthesized in several tryptophan-dependent and -independent pathways; the tryptophan-dependent pathways are generally named according to major intermediates. Since the number of genes involved in synthesis, transport, degradation or perception of auxins is very high [139, 186], here, only those genes will be covered, where loss-of-function mutants or GUS-expressing lines are used in this work.

The nitrilase proteins belong to a family with four members in *Arabidopsis*. While NIT1, NIT2, and NIT3 catalyze the hydrolysis of indol-3-acetonitril (IAN) to indol-3-acetic acid (IAA) and are supposed to contribute to the maintenance of IAA homeostasis [127, 132, 138, 181, 183]. In *Arabidopsis*, NIT1 is the highest expressed isoform that aggregates rapidly in response to wounding as early marker of cell death [13, 55]. *nit1* mutants are insensitive to IAN and lack obvious low-auxin phenotypes, indicating that the NIT1 function in auxin synthesis is redundant [127]. NIT2 usually has a basal expression, but induction by pathogens, leaf senescence, and exogenous IAN was reported. This induction correlates with the decreased IAN and increased IAA levels observed under these conditions [13, 80, 141]. Regarding the NIT3 gene, induced expression under sulfur starvation was published [101]. In contrast to the other family members, NIT4 is involved in cyanide detoxification, but not in auxin biosynthesis [137].

To remove the free active auxin, IAA can be conjugated to amino acids or glucose [36, 153, 164]; thus, the overexpression of the microbial IAA-conjugating enzyme IAA-L in *Arabidopsis* reduces the content of free IAA [192].

Auxin is mainly produced in shoot apical regions, its transport is highly regulated and necessary for various processes involving the establishment of the embryonic axis, phyllotaxis, development of vasculature and lateral root formation [11, 57, 71-73]. Both, auxin import and export from the cells are regulated processes, the former controlled by AUX1 (Auxin) and the LAX proteins, the latter by PIN and MDR (multidrug-resistance like) proteins, members of the PGP (P-glycoprotein) family can be involved in either uptake or export of auxin [12, 93, 94, 100]. Proteins of the AUX/LAX family are localized asymmetrically in the plasma membrane, facilitating polar auxin transport and root gravitropism, and are involved in lateral root emergence [19, 60, 111, 169]. The auxin transporters PGP and MDR directly bind the auxin transport inhibitor N-1-naphthylphthalamic Acid (NPA) [122, 126, 173]. The polar localization of PINs is highly dynamic and responds to signal from the serin-threonin kinase PINOID [18]. PIN-mediated auxin transport can be inhibited by 2,3,5-triiodobenzoic acid (TIBA), that prevents the rapid cycling of the PIN proteins between the plasma membrane and a yet unidentified endosomal compartment by vesicle trafficking [61, 76, 91, 135].

Expression of auxin-regulated genes occurs within minutes of auxin application without a requirement for protein synthesis [1], since the promoter regions of these genes contain auxin responsive elements (AuxRE). These elements are recognized by activating transcription factors, the auxin responsive factors (ARFs) forming heterodimers with Aux/IAA proteins, which act as repressors, and prevent expression of auxin-related genes under low auxin conditions [81, 106]. Free IAA binds to a receptor, the F-box protein TIR1, an E3-ubiquitin ligase that is a member of the SCF complex. In response to auxin binding, TIR1 mediates the ubiquitination of Aux/IAA proteins, targeting them to proteosomal degradation, thus allowing the ARF proteins to initiate transcription of auxin-related genes [10, 59, 92, 133, 140].

1.4. Callus formation in *Arabidopsis thaliana*

To ensure coordinated tissue growth during plant development, events like cell division, growth, and differentiation need to be tightly controlled. Therefore, only meristems and surrounding tissues possess mitotic activity. A loss of control results in ectopic cell division and eventually in the development of tumors, i.e. unorganized growing tissue.

Dedifferentiation is in many cases due to an imbalance of the phytohormones auxin and cytokinin, this imbalance often results in tumors growing *in vitro* on media without added hormones as callus. But callus formation can not only be induced by an altered hormone content caused by an increased synthesis or a reduced degradation or inactivation. Alternatively, mutations might render the plants more sensitive toward hormones or influence signaling pathways downstream of hormone perception, which then changes gene expression or controls cell division.

The analysis of *Arabidopsis* cell lines obtained by X-ray mutagenesis revealed three different kinds of cell lines: the first formed shoot-like structures (shooty callus), the second formed roots (rooty callus), and the third grew without organ formation (callus). The first cell lines had low auxin and high cytokinin contents, in contrast to the second lines with high auxin and low cytokinin levels [37, 70]. Growth and differentiation of callus can be influenced by the auxin to cytokinin ratio; a low ratio leads to formation of shoots, whereas a high ratio induces root development [159, 171]. This effect is widely used in plant molecular genetics to regenerate whole plants from explants *in vitro*, e.g. to generate transgenic plant lines.

1.5. GABA acts as signal molecule in various organisms

1.5.1. GABA signaling in the central nervous system of vertebrates

GABA is commonly known as the main inhibitory neurotransmitter in the central nervous system of vertebrates. Excitation of GABAergic neurons results in the release of GABA from vesicles of the presynaptic neuron via Ca^{2+} -dependent exocytosis. By GABA binding to different GABA receptors on the membrane of the postsynaptic cell, a response is triggered; either opening of ion channels or induction of a signaling cascade. To terminate the signal, GABA is imported into the neurons or in neighboring glia cells for degradation.

GABA-mediated signaling is found to be involved in the regulation of many developmental steps from cell proliferation to synaptogenesis and circuit formation in the immature brain. Compared to adult neurons, immature cells have relatively high internal Cl^- concentrations, opening of GABA-gated Cl^- -channels therefore results in membrane depolarization. In invertebrates, a growth-promoting effect through GABA-induced membrane depolarization was found. Taken this into account, already in ancient organisms, a GABA signaling pathway might have existed, where GABA was involved in trophic responses [129].

In vertebrates, two GAD isoforms are known, termed GAD65 and GAD67 that are differentially expressed among brain regions. In contrast to plants, short-term regulation of GAD activity in the mammalian brain is controlled by binding of the cofactor pyridoxal phosphate [25, 113], not by Ca^{2+} -induced dimerisation as in plants. GAD65 is localized more toward the nerve terminals, and is found in the brain in high amounts in the inactive form, suggesting it to be involved in response to short-term changes in demand for GABA. In contrast, GAD67 is found throughout the cell and its transcription is repressed by GABA, maintaining cellular GABA homeostasis [67, 144]

GABA degradation is catalyzed by the single copy genes *GABA-T* [128, 131, 136] and *SSADH* [150]. Malfunctions in GABA catabolism lead to severe mental disorders, caused by inborn gene defects. GABA-T deficiency is a rare disease, resulting in symptoms like psychomotor retardation, lethargy or electroencephalographic abnormalities [117]. Regarding human patients, a nonfunctional SSADH is more common than a mutated GABA-T. SSADH deficiency in human patients results in a disorder termed γ -hydroxybutyric aciduria, which is associated with high extracellular GABA and GHB concentrations. Again, the symptoms are behavioral disturbances and psychosis [64, 77, 134].

The short-chain fatty acid GHB occurs naturally in the mammalian brain and is formed from SSA via the succinic semialdehyde reductase (SSR or GHBDH). Additionally, this enzyme is involved in detoxification of xenobiotic carbonyl compounds [125, 150, 179]. *In vitro*, a conversion of GHB via SSA to GABA was detected by the use of ^3H -labeled GHB as substrate, in contrast to the *in vivo* situation, where the substrate concentrations might be too low to allow this reaction. The distribution of GHB synthesizing enzymes in the cells and high-affinity GHB binding sites in the brain suggest GHB to act as neurotransmitter or modulator of neural activity [84, 110]. The binding sites were identified as GHB receptors located in the presynaptic cells that act via initiation of G-protein coupled signal cascades [160].

GABA uptake in presynaptic neurons is catalyzed by a well-characterized GABA-Transporter, GAT1. To regulate GABAergic neurotransmission, GAT1 distribution, activity and turnover rate must be tightly controlled. Several classes of neurons are shown to express different levels of GAT1, and GFP-labeled protein is visible in different intracellular densities in the synapses. The cytosolic N-terminal domain is reported to interact with syntaxin 1A, a SNARE protein involved in neurotransmitter release and modulation of Ca^{2+} -and Cl^- -channels. Additionally, GAT1 activity is modulated by signaling pathways and protein-protein interactions; tyrosine-phosphorylation directs the protein to the plasma membrane, while unphosphorylated GAT1 remains cytosolic [44, 58, 104, 115].

In vertebrates, three classes of GABA-receptors with different characteristics are known, termed GABA_A-, GABA_B- and GABA_C- receptors [24].

The ionotropic GABA_A-receptors are heteropentameric Cl⁻-channels with two GABA binding sites found in all regions of the central nervous system. The subunits are derived from several related genes or gene families, providing a very high number of potential subunit combinations; however, certain subunit combinations seem to be preferred. Each subunit comprises four transmembrane domains with an intracellular loop between TM3 and TM4, containing a consensus site for phosphorylation by protein kinases. Several chemicals acting antagonistically or modulatory on receptor transport activity are known and are used as therapeutics.

The metabotropic GABA_B-receptors comprise seven transmembrane helices, existing in two isoforms (R1a and R1b). Recently, evidence was found, that functional native receptors are heterodimers composed of one of the R1 isoforms and a newly identified R2 subunit. Binding of GABA results in a conformational change of the receptor, coupling activity to Ca²⁺-and K⁺-channels via heterotrimeric G-proteins and second messenger systems, initiating a signal cascade in the target cell [75].

Although being ionotropic, GABA_C-receptors differ from GABA_A-receptors in several aspects. The general membrane topology is comparable to GABA_A-receptors; they are homo- or heteropentameric Cl⁻-channels, but are insensitive to GABA_A-receptor antagonists and modulators. GABA_C-receptors are mainly expressed in the vertebrate retina. Their slower activation and inactivation curves probably reflect the presence of five ligand-binding sites.

1.5.2. GABA metabolism in *Saccharomyces cerevisiae*

Yeast is often used as a model organism to study the function of mammalian enzymes. The role of GABA in intercellular signaling is intensely studied, whereas only little is known about its intracellular functions. In *Saccharomyces cerevisiae*, several genes are involved in GABA metabolism. GABA transport is mediated via the UGA4 gene, encoding a GABA and δ -aminolevulinic permease [20, 21], which is transcriptionally regulated in response to the available amount and quality of carbon and nitrogen sources [6, 108, 172].

In a search for yeast strains altered in GABA metabolism, an *ssadh*-deficient strain was isolated, that has a reduced growth rate compared to wild type strains and accumulates SSA. Biochemical characterization of the identified enzyme reveals a very high affinity for SSA. As conclusion, a toxicity of SSA seems to be most likely for the observed phenotypes [142].

Overexpression of GAD1 increases the resistance against different oxidants as long as the GABA catabolism remains intact, whereas a loss of either UGA1 (GABA-T) or UGA5 (SSADH) reduces oxidative stress tolerance. Additionally, the expression of UGA5 is induced by exposure to H₂O₂, implying a function of the GABA metabolism in buffering redox changes in yeast [53]. Oxidant resistance seems to be proportional to the gene dosage of GAD1, probably due to either the synthesis of GABA, which is involved in cellular stress response, or the production of the antioxidant NADPH during GABA degradation.

1.5.3. Repression of quorum sensing in *Agrobacterium tumefaciens*

Quorum sensing (QS) is a mechanism of bacterial cell-cell communication during times of high cell density, mediated through small, diffusible signal molecules. If the population grows, then more signal molecules are produced than lost by diffusion or inactivation, this leads to an accumulation of the signal to a threshold level. This results in the activation of receptor proteins and the initialization of complex regulatory cascades inducing coordinated changes in gene expression in individual members of the whole population. In plant pathogenic bacteria, QS mechanisms are often involved in the regulation of colonization and infection of host plants, e.g. by producing cell wall degrading enzymes, altering Ti plasmid transfer, and motility of the cells. This requirement of QS regulatory systems for pathogenicity may offer an option to control bacterial diseases of plants by interfering with the QS system [14, 180].

The activity of the QS system is controlled by two systems, *tra* and *att*. TraR is an N-acyl-homoserine lactone (AHL) receptor that activates transcription of two linked *tra* operons, a *trb* and the *rep* operon [105]. The *rep* operon is necessary for replication of the Ti plasmid in response to AHL binding, and the *tra* and *trb* operons encode structural components for conjugal transfer of the Ti plasmid [74]. AHL-bound TraR enables expression of TraI, which synthesizes AHLs, and of the TraR-repressor TraM, which regulates the activity of TraR at high AHL concentrations [170].

The *att* system is involved in QS signal decay. During the *Agrobacterium* growth phase, the *ALDH* gene – a succinic semialdehyde dehydrogenase – is transcribed, and the transcription of the *attKLM* operon is repressed by attJ. When the stationary phase is reached, a stress signal – ppGpp – interferes with the function of *Agrobacterium* RNA polymerase and *ALDH* is no longer expressed. Thus, SSA can accumulate in the cytosol, bind to attJ, and thereby release the repression of the *attKLM* operon. This operon contains three genes, a lactonase (attM), a homolog to NAD⁺-dependent alcohol dehydrogenases (attL) and a succinic semialdehyde dehydrogenase (attK). The first protein cleaves the γ -butyrolactone ring of AHL and, together with attL, inactivates the

QS signal; whereas the third enzyme removes excessive SSA, gradually disabling the QS signal decay [39, 40, 185].

Exogenous GABA or GABA degradation products from *Agrobacterium* host plants, like SSA, γ -hydroxybutyric acid (GHB) and γ -butyrolactone (GBL), have been reported to bind to attJ and to interfere with bacterial QS. GABA, accumulating in wounded plant tissues and acting as signal between eukaryotes and bacteria, might offer a possibility for the development of defense strategies against bacterial pathogens [43].

1.6. Aims of this thesis

During this work, three main topics should be covered; first, the analysis of *Arabidopsis thaliana* GABA-shunt mutants and the effect of GABA-shunt metabolites on plant growth; second, how is succinic semialdehyde (SSA) linked to callus formation and does a connection between the GABA-shunt and phytohormones exist; and third, the identification of yet unknown genes involved in regulation or function of the GABA-shunt or in GABA sensing.

To assay the effect of GABA-shunt metabolites on plant growth and development, *Arabidopsis* wild type and several GABA-shunt mutants are grown on ½ MS media supplemented with SSA, GHB, GABA, or glutamate. Growth is monitored, and the metabolite contents – with special attention on substances related to GABA – are determined by GC-MS analytics.

To characterize isolated T-DNA insertion lines, their growth under various conditions is observed, and the intracellular localization is analyzed by the expression of fusion proteins tagged with fluorescent markers.

To identify further genes related to GABA-metabolism, a population of EMS-mutagenized *ssadh* plants is screened for suppressor lines, and the corresponding mutations will be identified by map-based cloning.

To test whether a linkage between SSA and phytohormones exists, the callus formation rate in response to combinations of SSA and phytohormones or phytohormone antagonists is determined. Additionally, a possible effect of SSA on the expression of phytohormone related genes is assayed using promoter::GUS lines.

2. Results

2.1. Influence of the GABA-shunt on Arabidopsis plant growth

GABA and GABA-shunt metabolites are known neurotransmitters in mammals, and deficiencies in GABA-degrading enzymes lead to neurodegenerative disorders in patients. To test whether GABA has effects on plant growth and development, knock-out plants were isolated and in comparison to wild types analyzed for their response to exogenously applied GABA-shunt metabolites.

2.1.1. Examination of GABA-shunt mutants

The smaller siliques along with the reduced fertility observed in *gaba-t* mutant plants (Figure 2) was explained by an accumulation of GABA in the transmitting tissue of the ovary, leading to a misguidance of pollen tubes [130]. An increased GABA accumulation was found not only in the flowers of *gaba-t* mutant plants but also in vegetative tissues.

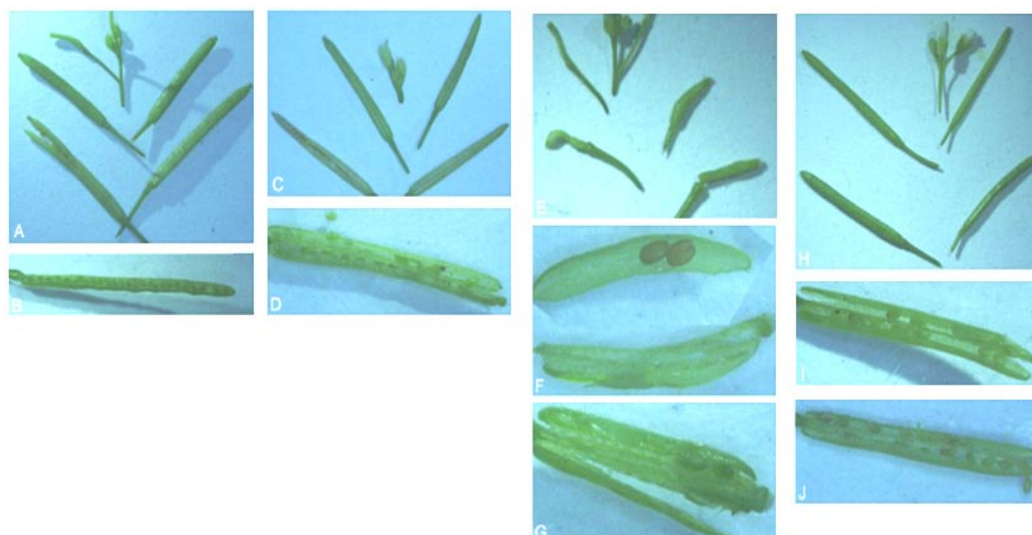


Figure 2: Comparison of Arabidopsis wild type and *gaba-t* mutant siliques

A to D: wild type siliques from main (A, B), and side (C, D) inflorescences

E to J: *gaba-t* mutant siliques from main (E, G), and side (H, J) inflorescences

The developmental retardation observed in *ssadh* mutant plants (Figure 3) was first discussed as a result of the disrupted GABA-shunt. Later, an interruption of the pathway at an earlier reaction was found to be sufficient to suppress the *ssadh* phenotype [66, 107]. This interruption prevents the accumulation of a toxic substance in *ssadh* mutant plants.



Figure 3:
Comparison of Arabidopsis wild type and *ssadh* mutant plants

All plants were grown under greenhouse conditions; the pictures have the same magnification
A: 3-week-old wild type plants
B to H: 21-week-old *ssadh* mutant plants; mutants are dwarfish plants with a retarded development, they have a reduced fertility and necrotic lesions

To further analyze the mutants, the metabolite content in leaf extracts was measured, revealing about 6-fold higher GABA levels in *gaba-t* and *gaba-t/ssadh* mutant plants compared to wild type plants of the same age (Figure 4A). In *ssadh* mutants, GABA levels even accumulated to approximately 16 fold of the wild type levels.

In extracts of wild type and *gaba-t* mutant plants, the GHB levels were at or below the detection limits of the GC-MS system used; these plants did not accumulate large amounts of GHB; in extracts of *gaba-t/ssadh* mutants no major increases in GHB content were measured, levels reached about 8 fold of wild type levels. Compared to the other lines, leaf extracts of *ssadh* mutants, contained vast amounts of GHB; levels were increased 160 fold compared to wild type (Figure 4B). However, the GHB levels do not necessarily reflect the SSA levels in plants, since the GHBDH reaction might be a limiting step *in vivo*. Furthermore, these values should be handled with care, since the *ssadh* plants were about three times older than the other plants when harvested for extraction.

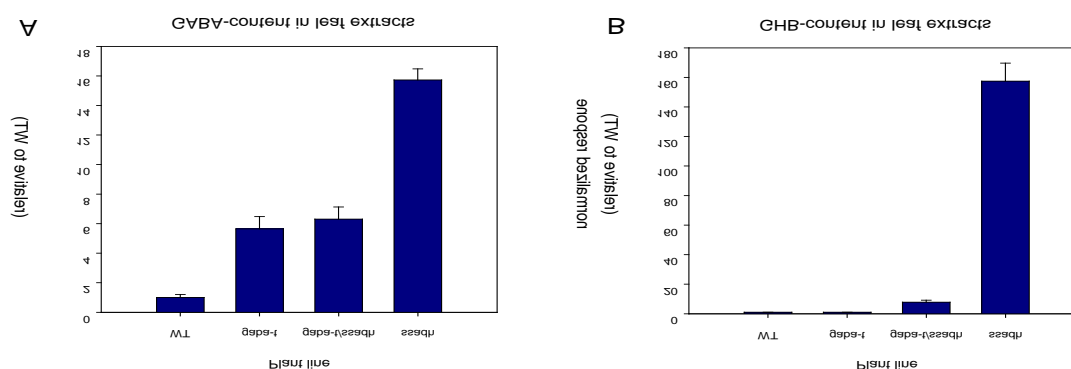


Figure 4: Metabolite measurement of GABA and GHB in GABA-shunt mutants

(A) GABA contents in rosette leaves of wild type, *gaba-t*, *gaba-t/ssadh*, and *ssadh* plants.

(B) GHB contents in rosette leaves of wild type, *gaba-t*, *gaba-t/ssadh*, and *ssadh* plants. The *ssadh* mutants accumulated very high amounts of GHB, whereas for the other lines GHB levels were near the detection limits.

Wild type, *gaba-t*, and *gaba-t/ssadh* plants were grown for 22 days and *ssadh* plants for 75 days on soil under greenhouse conditions. The experiment was repeated twice with six biological replicates analyzed, the bars represent the standard deviation

2.1.2. Effect of GABA-shunt metabolites on plant growth

To assay whether GABA-shunt metabolites have an effect on plant growth, wild type plants of different ecotypes (Columbia-0 – Col-0; Landsberg *erecta* – *Ler*; and Wassilewskija – Ws-2) were grown on ½ MS supplemented with various amounts of GABA, GHB, and SSA respectively, and analyzed for root and shoot development (Figure 5).

GABA was found to induce only minor effects on Arabidopsis wild type plants, whereas SSA and GHB both reduced the growth rate in a concentration dependent manner. The shorter roots and yellowish leaves observed on media containing higher GABA concentrations might be a side effect of nitrogen availability. SSA induced an increased formation of lateral roots, and reduced the length of the main root; along with the shorter root, the rosette size decreased. Further increase of SSA concentrations in the media induced lesions in the leaves. Wild type plants grown on GHB displayed only minor effects on shoot growth, but the roots were notably shorter with a slightly increased number of lateral roots.

Arabidopsis wild type plants were able to grow on GABA as the sole nitrogen source, in contrast to *gaba-t* mutants that grew worse on GABA-containing media than on media without any available nitrogen (Figure 6). Compared to wild type plants, *gaba-t* mutant plants growing on ½ MS displayed a tendency toward an enhanced biomass production. The same effect could be achieved in wild type plants by replacing some inorganic nitrogen (KNO_3 / NH_4NO_3) with GABA. On nitrogen-free media, growth of both wild type and *gaba-t* mutants was reduced and the leaves were yellowish, probably due to nitrogen limitations. On media containing 20mM GABA as the sole nitrogen source, wild type plants still displayed indications of nitrogen limitation and were smaller than on control ½ MS media, but *gaba-t* mutant plants grew even worse on media containing GABA as the sole nitrogen source compared to plants grown on nitrogen-free media.

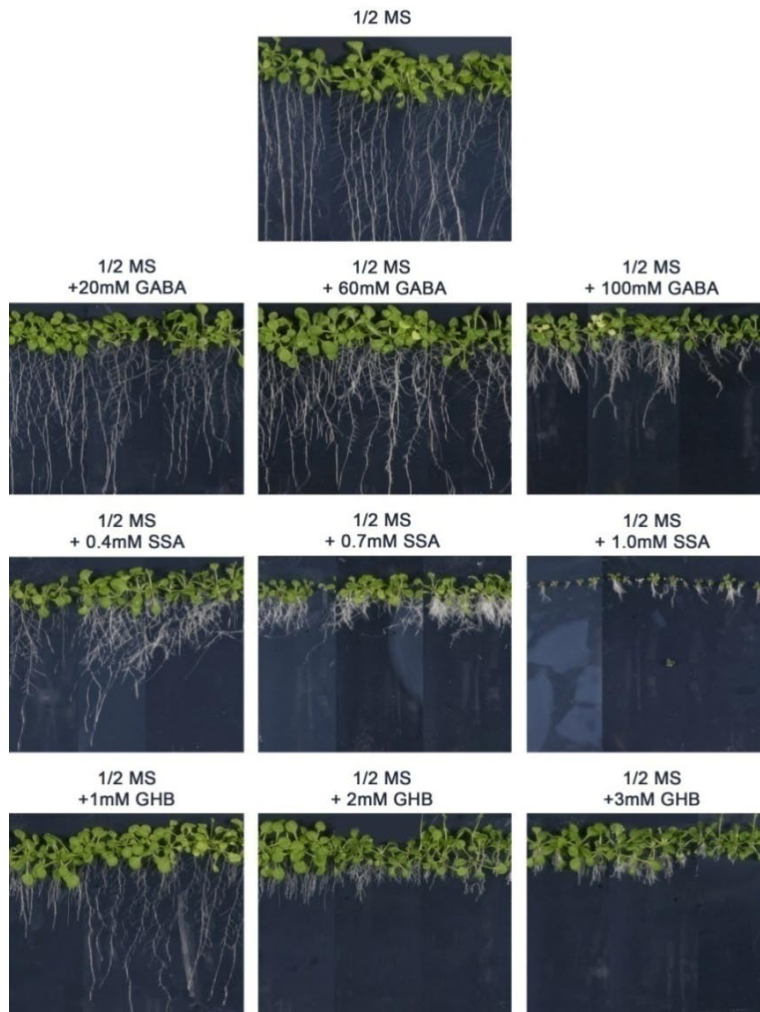


Figure 5: Growth of various Arabidopsis ecotypes on $\frac{1}{2}$ MS supplemented with different concentrations of GABA, SSA, or GHB

Three Arabidopsis ecotypes (left: Col-0, middle: Ler, right: Ws-2) were grown for 16 days on $\frac{1}{2}$ MS supplemented with increasing concentrations of GABA, SSA or GHB and analyzed for effects on plant development.

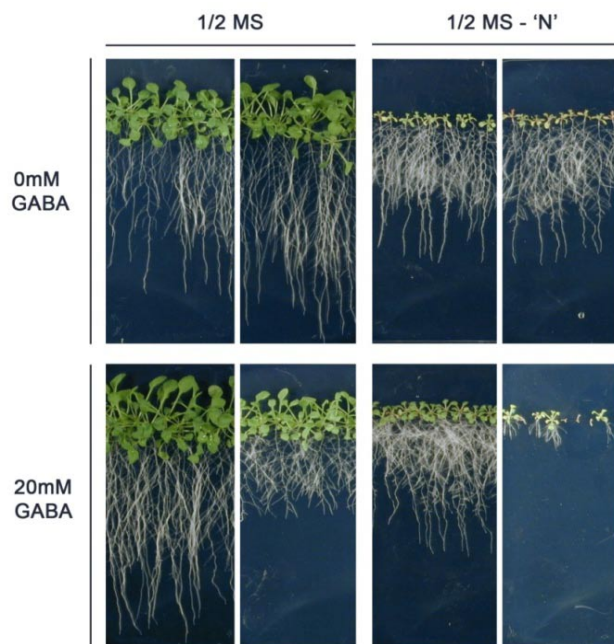


Figure 6: Growth of wild type and *gaba-t* mutant plants on different media

Wild type (left) and *gaba-t* (right) seedlings were grown for 14 days on $\frac{1}{2}$ MS or $\frac{1}{2}$ MS without inorganic nitrogen and either without GABA or supplemented with 20mM GABA. Presence of GABA in the media considerably reduced growth of *gaba-t* plants, whereas growth of wild type plants was increased by GABA. GABA as sole nitrogen source almost inhibited growth of *gaba-t* mutant plants completely.

To examine whether the inhibitory effect of GABA on *gaba-t* mutants is induced by high GABA concentration during germination, *gaba-t* and *gaba-t/ssadh* seedlings were germinated on ½ MS and transferred onto various media five days later. Neither were differences visible compared to seedlings remaining on the plates nor between wild type and *gaba-t* or *gaba-t/ssadh* mutant plants when shifted to ½ MS. Transfer of seedlings to media containing 10mM GABA improved growth of wild type plants whereas in *gaba-t* and *gaba-t/ssadh* mutants, the main root was shorter with a higher number of lateral roots, and the rosette size was slightly reduced compared to control plants.

On GABA as sole nitrogen source, *gaba-t* and *gaba-t/ssadh* plants did not develop much further; some lateral roots were initiated, but did not grow substantially. Furthermore, the leaves turned yellowish and newly formed leaves remained small. In contrast, wild type plants formed a high number of lateral roots, and both root length and rosette size were not much reduced compared to control plants (Figure 7). Germinating seeds on ½ MS supplemented with 10mM GABA for 7 days resulted in the known reduction of *gaba-t* or *gaba-t/ssadh* growth; the plants were then transferred to ½ MS and 14 days later no differences between wild type and *gaba-t* or *gaba-t/ssadh* mutants were visible any more (not shown).



Figure 7: Growth of wild type, *gaba-t*, and *gaba-t/ssadh* mutant plants

Wild type (left), *gaba-t* (middle) and *gaba-t/ssadh* (right) seedlings were grown on ½ MS for 5 days, followed by transfer to the indicated media. Pictures were taken 12 days after transfer.

Both, SSA and GHB affect growth of Arabidopsis wild type plants. To identify the substance responsible for the *ssadh* phenotype, the effect of the metabolites on wild type, *gaba-t*, and *gaba-t/ssadh* plants was assayed. Wild type and *gaba-t* plants were equally affected; no major differences regarding growth or metabolite content were detected. In contrast, *gaba-t/ssadh* mutant plants were highly sensitive toward SSA and GHB, small amounts of either of the substances substantially inhibited growth rates (Figure 8).

On ½ MS, no obvious growth differences were visible among the three lines. In leaf extracts of wild types and *gaba-t* mutants, GHB levels were at the detection limit, whereas levels increased up to 30-fold in *gaba-t/ssadh* mutants compared to wild types. The higher GHB levels in *gaba-t/ssadh* mutant plants in this experiment compared to the data in Figure 4 might be due to different growth conditions (½ MS vs. soil) and plant age.

Low SSA-concentrations in the media induced the formation of lateral roots in wild type and *gaba-t* mutants, but overall growth was not reduced. GC-MS measurements revealed only a minor increase in leaf GHB contents. In contrast, *gaba-t/ssadh* mutants grown under these conditions displayed a considerably reduced growth as well as increased leaf GHB contents compared to wild type. A further increase of the SSA concentrations impaired wild type and *gaba-t* mutants; the plants were smaller and accumulated higher amounts of GHB in the leaves. Growth of *gaba-t/ssadh* mutants was strongly inhibited, and an increase of GHB levels in leaf extracts up to 5000 fold of wild type levels under standard conditions was detected.

The addition of GHB to the media did not influence shoot growth of wild type and *gaba-t* mutants, although increasing the GHB concentration in the media reduced the main root length and induced lateral root formation. Growth of *gaba-t/ssadh* mutants on GHB-containing media was already strongly inhibited by low GHB concentrations. In leaf extracts of plants grown on GHB-containing media, GHB accumulation could be determined; extracts of wild type and *gaba-t* mutants contained roughly equal amounts of GHB, whereas *gaba-t/ssadh* mutants once more accumulated vast amounts of GHB.

Taken together, plant growth and GHB content in plant extracts are not necessarily linked to each other. GHB levels in plants extracts still allowing wild type and *gaba-t* mutant plants to grow fairly unaffected were sufficient to highly impair growth of *gaba-t/ssadh* mutants plants (Figure 8).

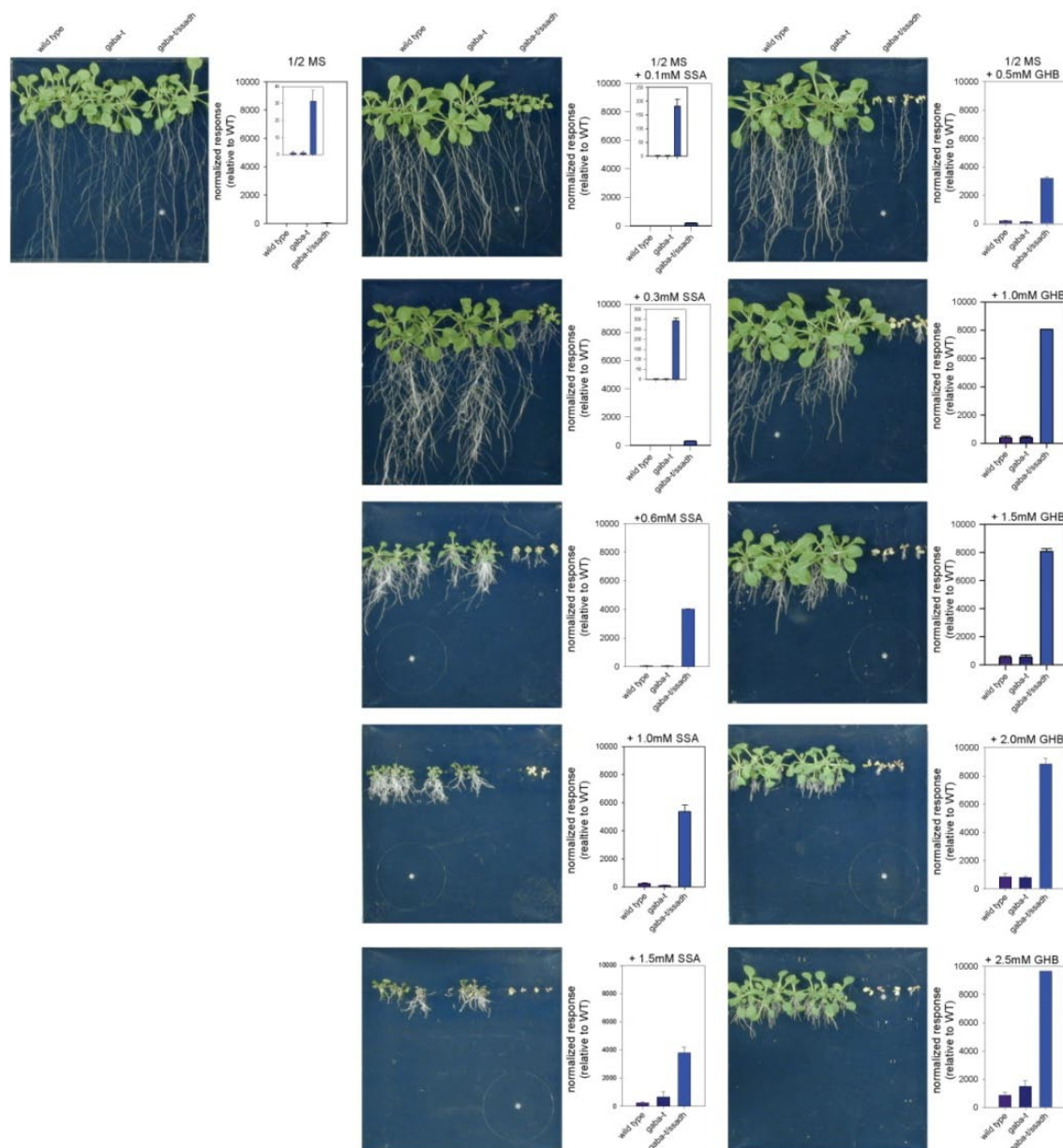


Figure 8: Growth of wild type, *gaba-t*, and *gaba-t/ssadh* plants on $\frac{1}{2}$ MS supplemented with either SSA or GHB in different concentrations

Wild type (left), *gaba-t* (middle) and *gaba-t/ssadh* (right) plants were grown on the indicated media for 15 days until sampling for GC-MS analyses. Pictures of the plates and the determined GHB-contents relative to wild type are presented next to each other. The experiment was repeated three times and 5 biological replicates were analyzed each, with the exception of *gaba-t/ssadh* mutant plants, where the rosette weight of plants grown on higher SSA or GHB concentrations were sufficient only for three samples, the bars represent the standard deviation

2.1.3. Analysis of the Arabidopsis GHBDH-genes

To address the question whether SSA or GHB causes the severe growth phenotype of *ssadh* mutant plants, *ghbdh* mutant plants were isolated and tested for their sensitivity against SSA or GHB.

An Arabidopsis cDNA encoding a GHB-Dehydrogenase was cloned a few years ago [31], and the corresponding gene (At3g25530) was identified by sequence comparison. The genomic sequence did not contain any target information; so the protein was predicted to be cytosolic. Co-localizations of AtGHBDH-1-GFP and a plasma membrane RFP marker [123] displayed a partially overlapping fluorescence (Figure 9), proving the enzyme to be cytosolic as predicted *in silico*.

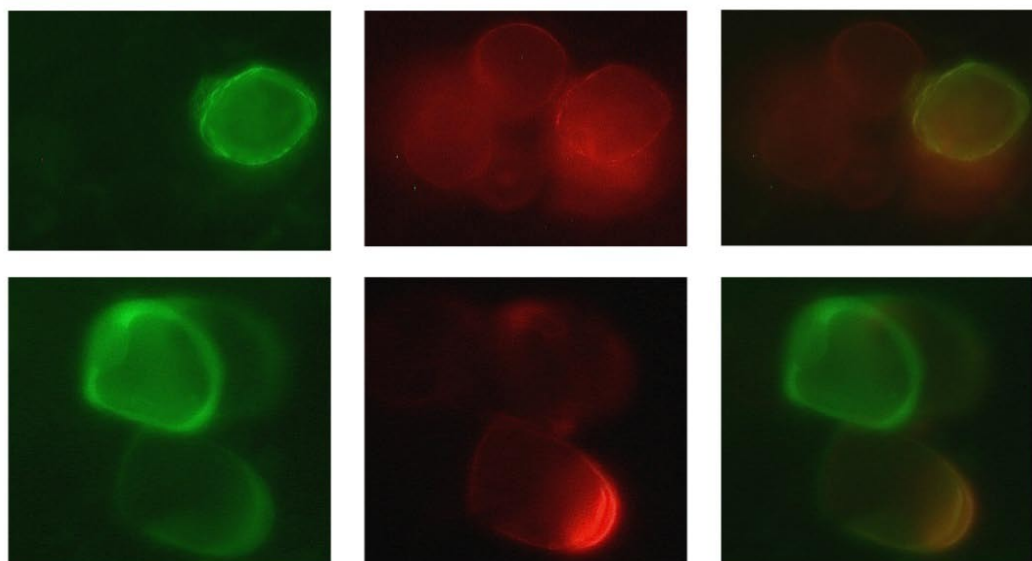


Figure 9: Co-localization of AtGHBDH-1-GFP with a plasma membrane marker

Arabidopsis thaliana cell cultures were transformed with both AtGHBDH-1-GFP and a plasma membrane RFP marker and analyzed three days later by fluorescence microscopy (4.2.1.8). A partially overlapping fluorescence was observed that corresponds to the predicted cytosolic localization of AtGHBDH-1.

Left: GFP-fluorescence, middle: RFP-fluorescence, right: merged

For *GHBDH-1*, two independent T-DNA insertion lines (GabiKat_316D05 and SALK_057410) were isolated, identified as null-mutants by RT-PCR, and no phenotypic differences compared to wild type plants were visible under greenhouse conditions.

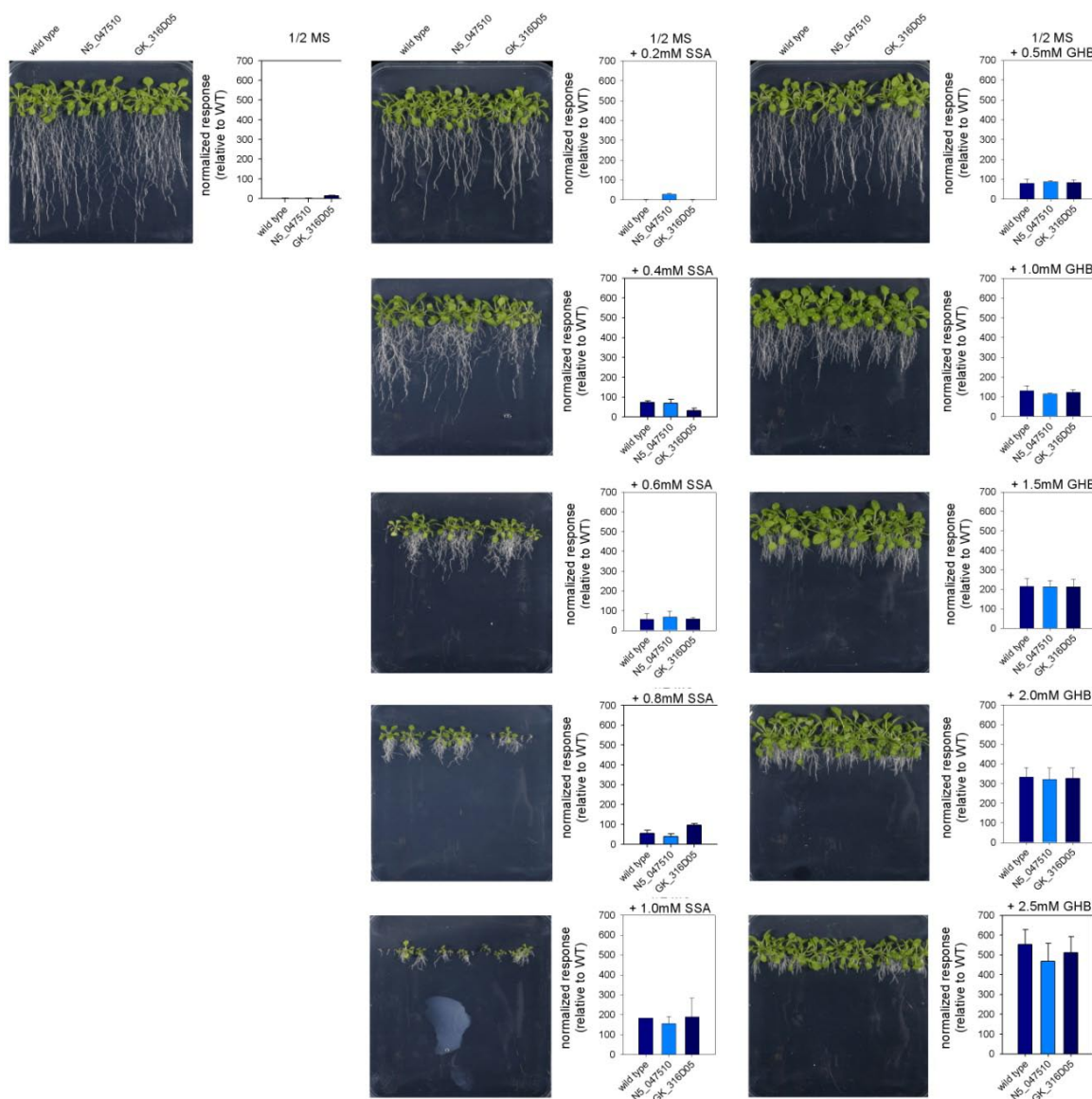


Figure 10: Growth of wild type and two independent *ghbdh-1* lines on 1/2 MS supplemented with SSA or GHB

Plants were grown on the indicated media for 15 days, and then samples for GC-MS analyses were taken. Pictures of the plates and the determined GHB-contents relative to wild type are presented next to each other. The experiment was repeated twice and 6 biological replicates were analyzed each, the bars represent the standard deviation.

Since SSA and GHB can be converted into each other by a dehydrogenase, a block of this reaction was supposed to trigger a difference in response to the substances. Under control conditions (1/2 MS), no differences occurred between wild type and *ghbdh-1* mutant plants. GHB levels were near detection limits of the GC-MS system used. When grown on 1/2 MS + SSA, both wild type and the different *ghbdh-1* mutant lines displayed a reduced root length with an increasing number of lateral roots forming and a smaller

shoot size, with slightly paler leaves compared to control plants. GC-MS analysis revealed the presence of equal amount of GHB in wild type and *ghbdh-1* mutants.

Both wild type and *ghbdh-1* mutant plants grown on ½ MS containing GHB displayed a shortened root length and an almost unchanged shoot growth. Increasing GHB-concentrations further decreased root length. No difference in GHB-content was measured in wild type and *ghbdh-1* mutant plants (Figure 10).

In contrast to the expectation, no differences between wild type and *ghbdh-1* mutant plants occurred in growth experiments on ½ MS supplemented with either SSA or GHB. Additionally, GHB was detectable in plant extracts upon SSA feeding, indicating a second enzyme capable of catalyzing the SSA-GHB conversion exists.

To identify this predicted homologous enzyme in Arabidopsis, a BLAST search with the GHBDH-1 protein sequence was performed, the similar sequences were aligned using ClustalW (<http://www.ebi.ac.uk/Tools/clustalw2/index.html>), and a phylogenetic tree was generated (Figure 11).

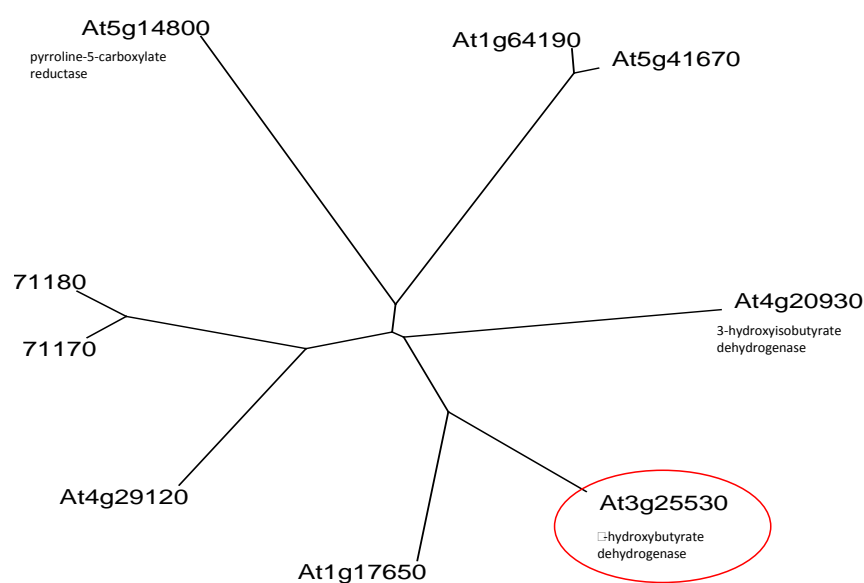


Figure 11: Phylogenetic tree of GHBDH-homologous sequences

Results of a BLAST search with the Arabidopsis GHBDH protein. One of the identified proteins (At1g17650) clusters together with the Arabidopsis *ghbdh* (At3g25530). Protein sequences were annotated as “phosphogluconate dehydrogenase” when not labeled otherwise.

One of the proteins clustered together with GHBDH-1, and a detailed sequence analysis revealed a high identity on protein level. The new identified GHBDH-2 contained an N-terminal presequence, probably being an intracellular targeting sequence (Figure 12).

```

At3g25530 -----MEVGFLGLG 9
At1g17650 MALCSICPRIPLRFRPKPISPFLSKPQICLAYRVYSSLQSTTPSTRDELGTVSIGFLGMG 60
                                         :.:*****:

At3g25530 IMGKAMSMNLLKNGFKVTVWNRTLSKCDELVEHGASVCESPAEVIKKCKYTIAMSDPCA 69
At1g17650 IMGSPMAQNLIKAGCDVTVWNRTKSKCDPLVGLGAKYKSSPEEVTATCDLTFAMLADPES 120
***.:*: **: * .***** ** * ** . ** * .*. *:*****:

At3g25530 ALSVVFDKGGVLEQICEGKGYIDMSTVDAETSLKINEAITGKGGRFVEGPVSGSKKPAED 129
At1g17650 AIDVACKNGAIFGISSGKGYVDVSTVDVASSILISKQIKDTGALFLEAPVSGSKKPAED 180
*.:* .*. *: .*. *****:*****. **: *.: *...*. *:*. *****

At3g25530 GQLIILAAGDKALFEESIPAFDVLGKRSFYLGQVNGAKMKLIVNMIMGSMNAFSEGLV 189
At1g17650 GQLIFLTAGDKPLYEKAAPFLDIMGKSFYLGEVNGAAMKLVVNMIMGSMMASFAEGIL 240
*****:*****. *:***: * :*:*** .*****:***** ***:***** *:*****:

At3g25530 LADKSGLSSDTLLDILDLGAMTNPFKGKGPSMNKSSYPAFPLKHQQKDMRLALALGDE 249
At1g17650 LSQKVGLDPNVLVEVVSQGAINAPMYSLKGPSMIKSVYPTAFLKHQQKDMRLALGLAES 300
*.:* ** .*. *:***: . ***: . ***: . ***** ** ** .*****:*****. *.:.

At3g25530 NAVSMPVAAAANEAFKKARSLGLGDLDFSAVIEAVKFSRE--- 289
At1g17650 VSQSTPIAAAANELYKVAKSYGLSDEDFSAVIEALKAAKSRE 343
: * *:***** :* *: * **.* *****:* :.:

```

Figure 12: Alignment of the two GHBDH protein sequences

An alignment of protein sequences revealed a high similarity on amino acid level (identical residues in red) between AtGHBDH-1 and the new classified AtGHBDH-2. A remarkable difference between both proteins is the N-terminal presequence of At1g17650, probably directing the protein into an organelle.

The N-terminal sequence of the second gene was identified as a targeting signal but predictions regarding the intracellular localization remained ambiguous. In contrast to the published plastidial localization in tobacco BY2-cells [158], transient transformation of leek by particle bombardment or transformation of Arabidopsis cells with AtGHBDH-2-GFP and a RFP-fused plastid marker [123] showed no clear plastidic localization of the GFP-fusion protein (Figure 13 and Figure 14). In contrast, co-transformation of Arabidopsis cells with AtGHBDH-2-GFP and a RFP-fused mitochondrial marker [123] or staining of AtGHBDH-2-GFP transformed cells with Mitotracker Red resulted in overlapping fluorescence, suggesting a mitochondrial localization (Figure 15).

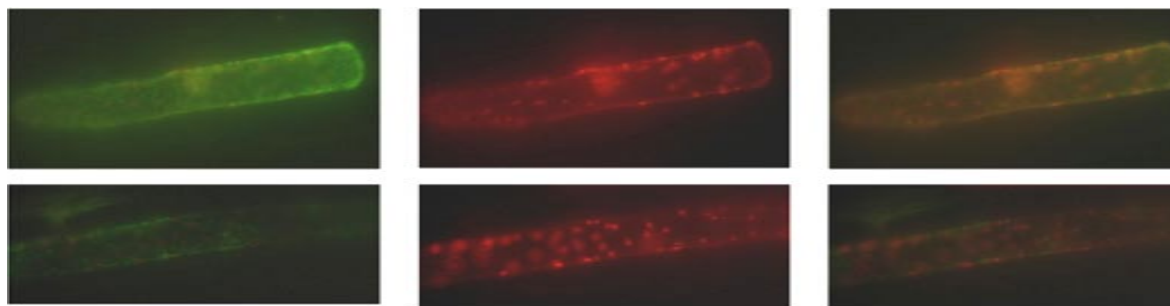


Figure 13: AtGHBDH-2-GFP co-transformation with plastid-localized RFP

Leek epidermal peels were transiently transformed with AtGHBDH-2-GFP and a plastid-localized RFP fusion [123] by particle bombardment (4.2.1.9) and were analyzed by fluorescence microscopy 24 hours later (4.2.1.7). GFP and RFP signals in co-transformed leek cells did not yield overlapping fluorescence patterns.

Left: GFP, middle: RFP, right: merged

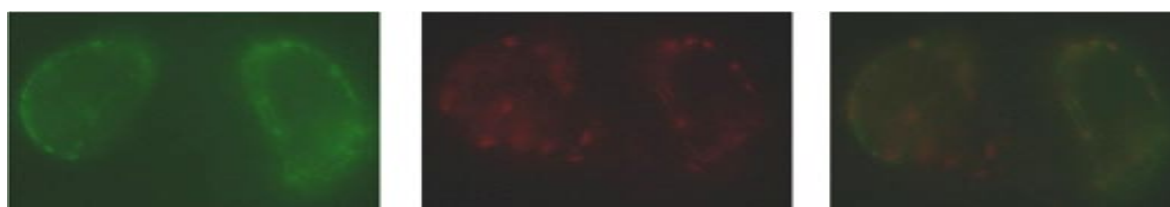


Figure 14: AtGHBDH-2-GFP co-transformation with plastid-localized RFP

Arabidopsis thaliana cell cultures were co-transformed with AtGHBDH-2-GFP and a plastid-localized RFP marker [123] and analyzed three days later by fluorescence microscopy. GFP and RFP signals in co-transformed *Arabidopsis* cells did not yield overlapping fluorescence patterns.

Left: GFP, middle: RFP, right: merged



Figure 15: AtGHBDH-2-GFP co-transformation with mitochondrial-localized RFP

Arabidopsis thaliana cell cultures were co-transformed with AtGHBDH-2-GFP and a mitochondria-localized RFP [123] marker and analyzed three days later by fluorescence microscopy. The GFP and RFP signals in co-transformed *Arabidopsis thaliana* cells had overlapping fluorescence patterns suggesting a mitochondrial localization.

Left: GFP, middle: RFP, right: merged

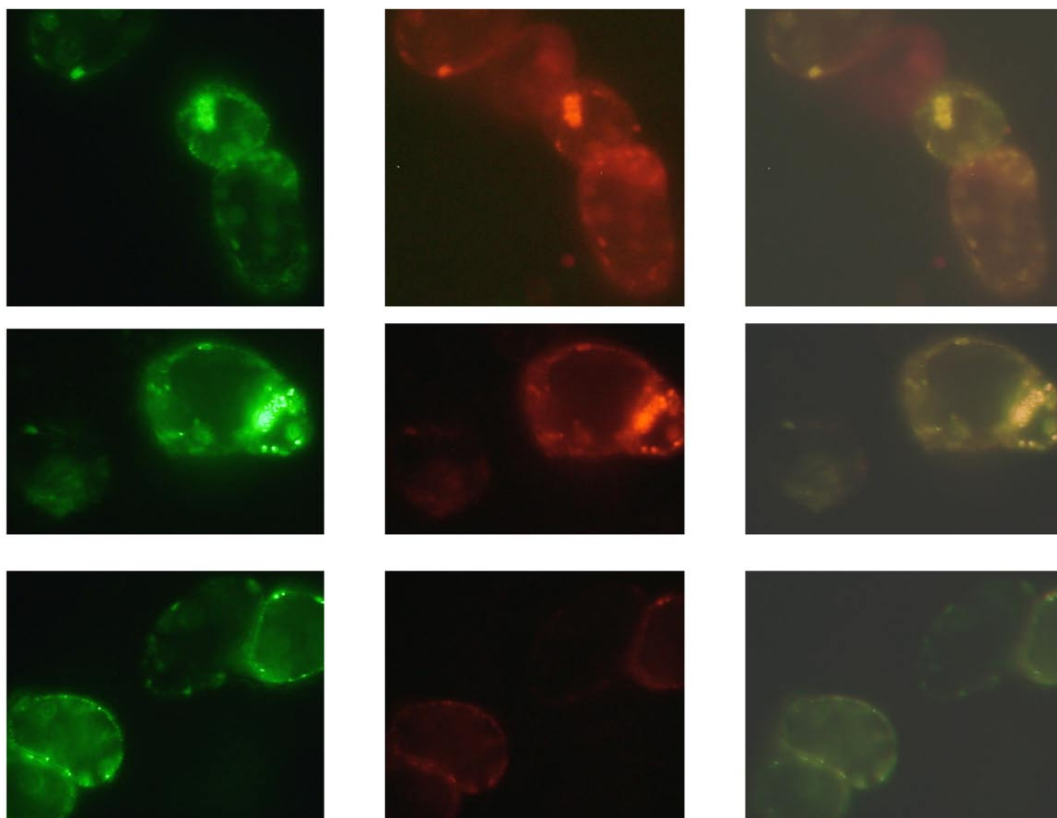


Figure 16: AtGHBDH-2-GFP co-localization with Mitotracker Red

Arabidopsis cells were transformed with AtGHBDH-2-GFP, incubated in the dark for 4 days, then stained with Mitotracker Red for 10min, and analyzed by fluorescence microscopy. The GFP and Mitotracker signals in transformed and stained Arabidopsis cells had overlapping fluorescence patterns, implying a mitochondrial localization of AtGHBDH-2.

Left: GFP, middle: Mitotracker Red, right: merged

An isolated T-DNA insertion line (GabiKat_933D03) for AtGHBDH-2 (At1g17650), displayed no phenotypic differences to wild type plants under greenhouse conditions. To obtain plants without GHBDH activity, *ghbdh-2* mutants were crossed to both *ghbdh-1* alleles. The resulting double homozygous lines displayed no phenotypic discrepancies to wild type plants under greenhouse conditions.

To further address the question whether SSA or GHB triggers the *ssadh* phenotype, wild type along with both *ghbdh-1/ghbdh-2* lines were grown on ½ MS supplemented with either SSA or GHB (Figure 17). Plant sizes as well as GHB levels in leaf extracts were comparable for *ghbdh-1/ghbdh-2* and wild type plants grown on ½ MS.

Addition of SSA to the media resulted in reduced root length and rosette size for wild type and mutant plants, but no growth differences between wild type and *ghbdh-1/ghbdh-2* plants were visible. In contrast to equal growth, metabolite analysis by GC-MS revealed a tendency for *ghbdh-1/ghbdh-2* mutant plants to accumulate less GHB than wild types.

No phenotypic differences were visible between wild type and *ghbdh-1/ghbdh-2* mutant plants grown on 1/2 MS containing GHB, all plants had a reduced root length without a substantial decrease in rosette size. GHB levels in leaf extracts from plants grown on lower GHB-concentrations were not varying among wild type and *ghbdh-1/ghbdh-2* mutant plants. Interestingly, increasing the GHB amount in the media to 5mM resulted in a minor increase of GHB levels in mutant plant extracts.

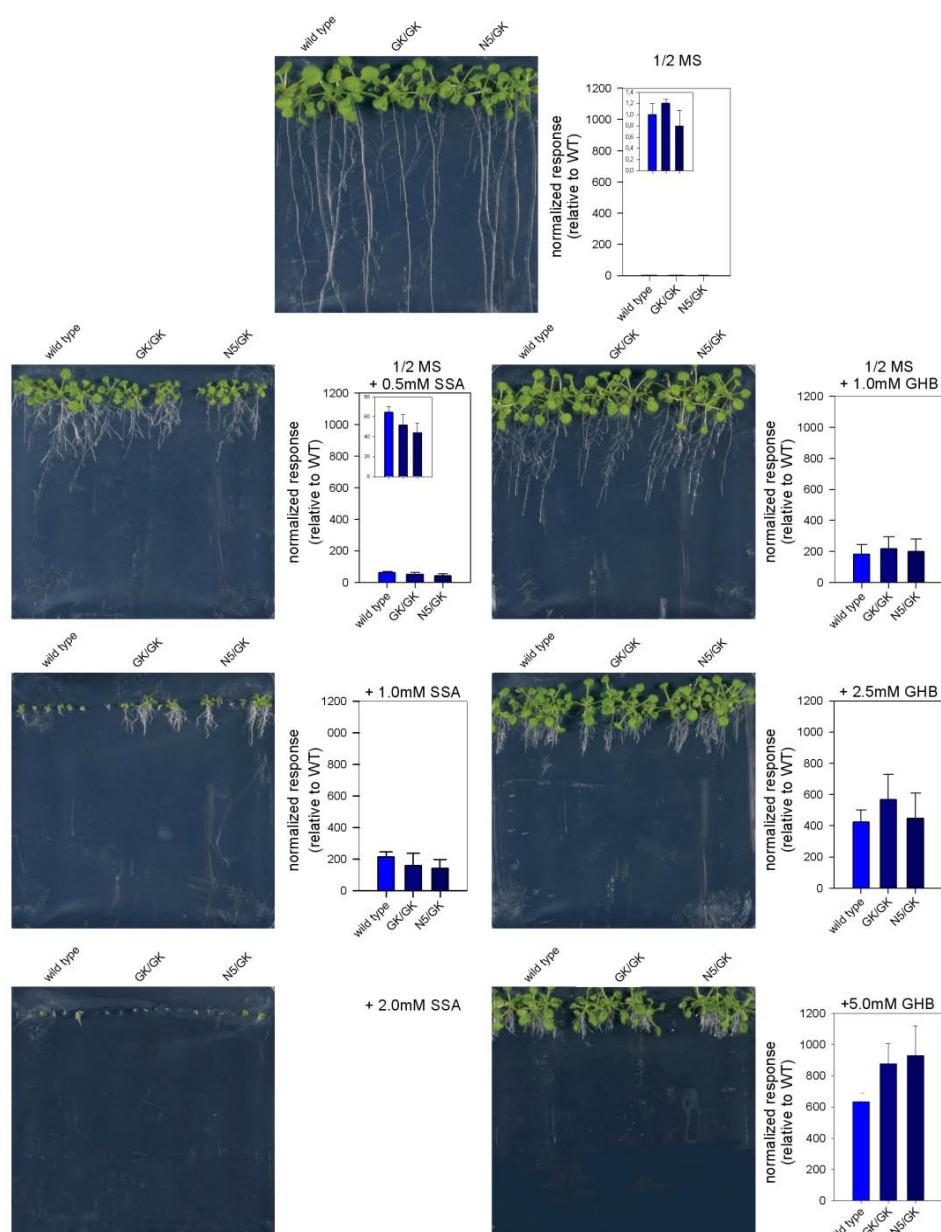


Figure 17: Growth of wild type and two *ghbdh-1/ghbdh-2* lines on 1/2 MS supplemented with SSA or GHB

Plants were grown on the indicated media for 13 days, and then samples for GC-MS analysis were taken. Pictures of the plates and the determined GHB-contents relative to wild type are given next to each other. The experiment was repeated three times and with the exception of plants grown on 1/2 MS + 2mM SSA 6 biological replicates were analyzed, the bars represent the standard deviation.

GK/GK: GabiKat_316D05/ GabiKat_933D03; N5/GK: SALK_057410/ GabiKat_933D03

2.2. Identification of other genes involved in GABA-metabolism

The severe growth phenotype of *ssadh* mutant plants could be repressed by simultaneously inhibiting GABA-T activity, either genetically by generating *gaba-t/ssadh* double mutant plants or biochemically by applying the GABA structural analog Vigabatrin [66] which can not be metabolized and irreversibly blocks GABA-T function. These findings allow the identification of yet unknown genes involved in GABA-metabolism by searching for additional *ssadh* suppressor lines.

2.2.1. Screening of *ssadh* suppressor lines

To identify further genes involved in GABA metabolism or in a putative GABA signaling pathway in plants, additional *ssadh* suppressor mutants should be identified.

Therefore, homozygous *ssadh* seeds were mutagenized using EMS (performed by Lehle Seeds; <http://www.arabidopsis.com>) and screened for plants with improved growth compared to the parental line. In the M₁ generation, out of approximately 30 000 plants, none had a considerably enhanced growth, i.e. no dominant suppressor mutation of the *ssadh* phenotype was detected. Out of approximately 60 000 M₂ plants, 282 *ssadh* suppressor lines displaying different phenotypes (examples in Figure 18) were initially isolated and identified as homozygous *ssadh* knock-out lines by PCR. 198 suppressor lines were rejected following maturation since the lines were not fertile or, even though they grew better their phenotypes still resembled too much the *ssadh* phenotype.



Figure 18: Phenotypes of several independent *ssadh* suppressor mutants

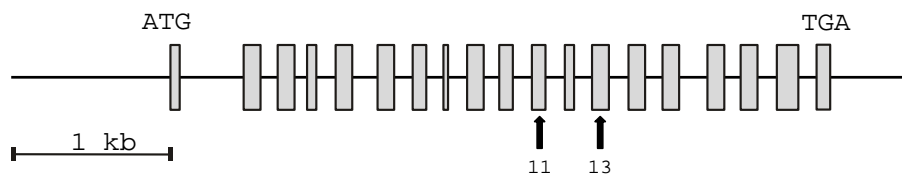
The remaining 84 lines were grown as M₃ generation; lines with segregating multiple EMS-induced mutations were excluded from further analysis. To identify probably allelic lines among the remaining 53 lines, plants were grown on soil under long day and short day conditions, the values recorded included rosette size, flowering time and GHB and GABA levels. Additionally, growth on ½ MS, either unchanged or supplemented with GABA or glutamate, was tested (for detailed values and pictures of plants under various growth conditions, see 6.1). Lines displaying similar developmental characteristics and metabolite contents (6.1.2) were assayed for allelic mutations; thus, plants were crossed, and growth of the offspring was examined. If the EMS induced mutations are located in the same gene, i.e. are allelic, then the F₁ generation should not display the *ssadh* phenotype. For two different lines, 18.B and 19.B, mutations in the same gene could be identified. The three lines chosen for mapping were tested and found not to be allelic to each other

2.2.2. Identification of new *gaba-t* alleles

As a proof-of-concept for the effectiveness of the screening, the identification of new *gaba-t* alleles was essential. For that reason, the *GABA-T* gene including 1kb upstream and 0.5 kb downstream genomic regions was sequenced in eight suppressor lines phenotypically resembling *gaba-t/ssadh* double mutants. Two of the lines contained mutations in the coding sequence (Figure 19).

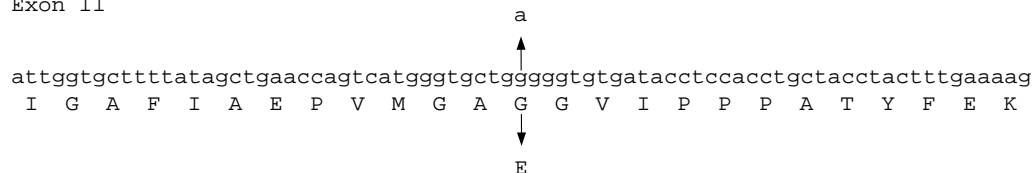
In line 37.B, a single nucleotide exchange from G to A was identified in exon 11, on amino acid level resulting in a replacement of glycine with glutamate. In line 31.A, another G-A transition was found, this time leading to the exchange of glycine by aspartate in exon 13.

A



B

Exon 11



C

Exon 13

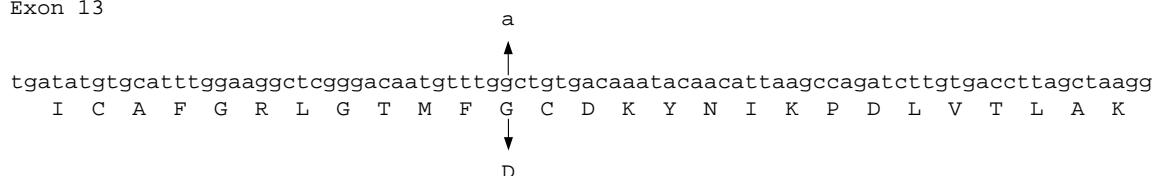


Figure 19: Location of the EMS induced mutations in the *gaba-t* genomic sequence

(A) Gene structure of the sequenced genomic region of At3g22200 including the regions 1kb upstream of the start and 0.5kb downstream of the stop codon. The arrows indicate the position of the identified mutations.

(B) The mutation in line 37.B was mapped to exon 11, leading to an amino acid exchange at position 271 from Gly to Glu.

(C) The mutation in line 32.A is found in exon 13; the Gly at position 312 is exchanged by Asp.

In both cases, glycine is replaced by a larger, charged amino acid, possibly leading to sterical hindrances. By comparison with crystal structures available in public databases, the mutated amino acids were located near the active site in 3D models. Additionally, the mutation in line 37.B is found in a highly conserved region. Alignments of protein sequences from species of all kingdoms revealed at this position in 97% glycine and 3% alanine, the next amino acid (glycine) was completely conserved in all species. Altogether, the mutations will most probably interfere with proper protein folding, cofactor binding, and thus protein activity (Figure 20).

A.t. 31.A	MVVINSLRRLARTTQVHLHSHKYATCMMSGNSTSRRIFTTEAAPEKKNTVGSKGDHMLAPFT	60
A.t. 37.B	MVVINSLRRLARTTQVHLHSHKYATCMMSGNSTSRRIFTTEAAPEKKNTVGSKGDHMLAPFT	60
GABA-T pig	-----SQAAAKVDVEFDYDGPLMKTEVPGPRSRRELMKQLN	35
A.t. 31.A	AGWQSADLDPLVIAK-SEGSYVYDDTGKKYLDLWCTALGGNEPRLVSAAVEQLNTL	119
A.t. 37.B	AGWQSADLDPLVIAK-SEGSYVYDDTGKKYLDLWCTALGGNEPRLVSAAVEQLNTL	119
GABA-T pig	IIQNAAEVHFFFCNYEESRGNLVDVDGNRMLDLYSQISSIPIGYSHPALVKLVQQPQNVS	95
	▲	
A.t. 31.A	PFYHSFWNRRTTKPSLDLAKVLLLEMTAN--KMAKAFFTSGGSDANDTQVK--LVWYYNNA	175
A.t. 37.B	PFYHSFWNRRTTKPSLDLAKVLLLEMTAN--KMAKAFFTSGGSDANDTQVK--LVWYYNNA	175
GABA-T pig	TFINRPALGILPPENFVEKLRRESLLSVAPKGMSQLITMACGSCSNENAFKTIIFMWYRSKE	155
A.t. 31.A	LGRPEKKK-----FIARKKSYHGSTLISASLSGLPPLHQNFDPAPF	217
A.t. 37.B	LGRPEKKK-----FIARKKSYHGSTLISASLSGLPPLHQNFDPAPF	217
GABA-T pig	RGQSAFSSKEELETMINQAPGCPDYSILSFMGAFHGRTMGCLATHSKAIHKIDIPDFDW	215
	▲▲▲	
A.t. 31.A	VLHTDCPHYWRFHLPGETEEEFSTRLAKNLEDLIIK--EGPETIGAFIAEPVMGAGGVIP	275
A.t. 37.B	VLHTDCPHYWRFHLPGETEEEFSTRLAKNLEDLIIK--EGPETIGAFIAEPVMGAGGVIP	275
GABA-T pig	PIAPFRLKYPLEEFVKENQEQEEARCLEEVEDLIVKYRKKKKTVAGIIVEPIQSEGGDNH	275
	▲	
A.t. 31.A	PPATYFEKVQAVVKKYDILFIADEVICAFGRLGTMFDCKYNIKP--DLVTLAKALSSAY	333
A.t. 37.B	PPATYFEKVQAVVKKYDILFIADEVICAFGRLGTMFGCDKYNIKP--DLVTLAKALSSAY	333
GABA-T pig	ASDDFFRKLRLDISRKHGCAFLVDEVQTTGGGSGTKFVAHEHWGLDDPADVMTFSKMMTGG	335
	▲▲▲	
	△	
A.t. 31.A	MPIGAILMSQEVADVINSHSSKLGVSFGHTYSGHPVSCAVAIEALKIYKERNIPEYVAK	393
A.t. 37.B	MPIGAILMSQEVADVINSHSSKLGVSFGHTYSGHPVSCAVAIEALKIYKERNIPEYVAK	393
GABA-T pig	FFHKEEFRPNAPYRIFN-----TWLGDPSKNLLLAEVINIKREDLLSNAAH	382
	▲	
A.t. 31.A	VAPRFQDGVKAFASGSP-IIGETRGTGLILGTEFVDNKSPNEPFPPEWGVGAFFGAECQI	452
A.t. 37.B	VAPRFQDGVKAFASGSP-IIGETRGTGLILGTEFVDNKSPNEPFPPEWGVGAFFGAECQI	452
GABA-T pig	AGKVLLTGLLDLQARYPQFISRVGRGTFCSFDPDESIRNKLSIARNKGVMLGGCGDK	442
A.t. 31.A	SPEEIDESIYG-KALKATEEKVKELKAQHKK	482
A.t. 37.B	SPEEIDESIYG-KALKATEEKVKELKAQHKK	482
GABA-T pig	SIRFRPTLVFRDHHHLFLNIFSDILADFK-	472
	▲▲	

Figure 20: Alignment of protein sequences from Arabidopsis and pig

Alignment of the protein sequences from the two new *gaba-t* alleles in Arabidopsis and the GABA-T sequence from pig, used for crystal structure analysis [166]. In both *gaba-t* alleles, glycine residues near the active site are replaced with a larger, charged amino acid that is most probably interfering with proper protein folding and enzyme activity.

Black triangles indicate active site residues, the white triangle the pyridoxal phosphate-binding site, the mutated residues in the Arabidopsis sequences are underlined.

2.2.3. Map-based cloning of three *ssadh* suppressor lines

To rule out the possibility of an EMS-induced mutation in known GABA-shunt related genes in the three lines analyzed, the genes encoding *GABA-T*, *GHBDH-1*, *GHBDH-2*, and the putative GABA-Transporters, including 1kb upstream of the start codon, the coding region with exon and introns, and 0.5kb downstream of the stop codon, were sequenced, but no mutations were identified.

Three non-allelic lines were chosen for mapping. Using the following SSLP markers (Figure 21), the EMS mutations could be mapped down to the chromosome arm.

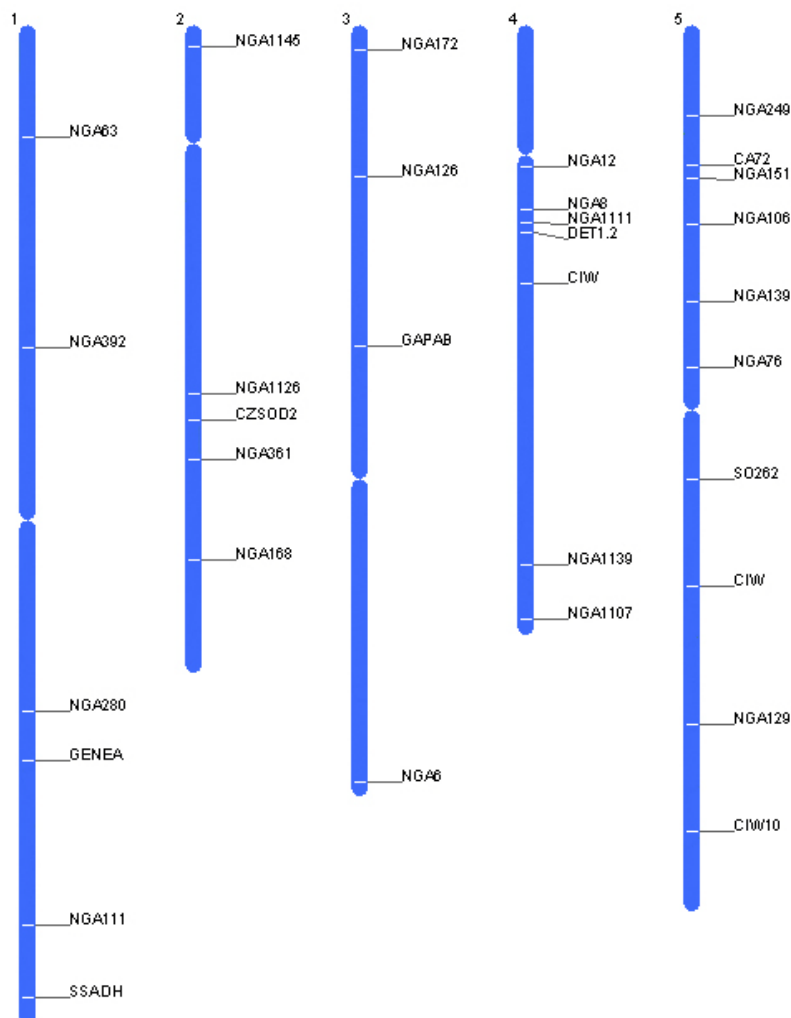


Figure 21: Distribution of the used SSLP markers in the Arabidopsis genome

For all markers, primer sequences and fragment sizes are given in 6.4.5.1. The marker NGA111 exhibits linkage with the *SSADH* gene.

2.2.3.1. Line 4.D

This plant was isolated in the M₂ generation in pool number 4, transferred to single pots, and grown under greenhouse conditions until maturation (Figure 22). The plant had a rather small rosette and flower buds appeared after 36 days.

In the M₃ generation, growth of plants under long and short day conditions and on ½ MS supplemented with GABA or Glutamate was monitored. Plants grown under long day conditions resembled the phenotype of the parental plants, whereas all leaves developing under short day conditions were very small, wrinkled and displayed a pale green color (Figure 23). Determination of the GHB and GABA content in leaf extracts of plants grown under greenhouse conditions by GC-MS revealed 324-fold increased GHB-, and 19-fold increased GABA-levels compared to wild types. This line contained the highest GHB levels in leaf extracts among all *ssadh* suppressor lines.

To further obtain information about plant characteristics, M₃-seeds were germinated on ½ MS supplemented with either GABA or glutamate (Figure 31). Plants grown on ½ MS had very short roots and a reduced rosette size, germination on GABA or glutamate-containing media further reduced the rosette size.



Figure 22: Phenotype of 4.D M₂ plant grown under greenhouse conditions for 44 days.



Figure 23: Plants of the M₃-generation were grown under long day (A) and short day (B) conditions for 39 days

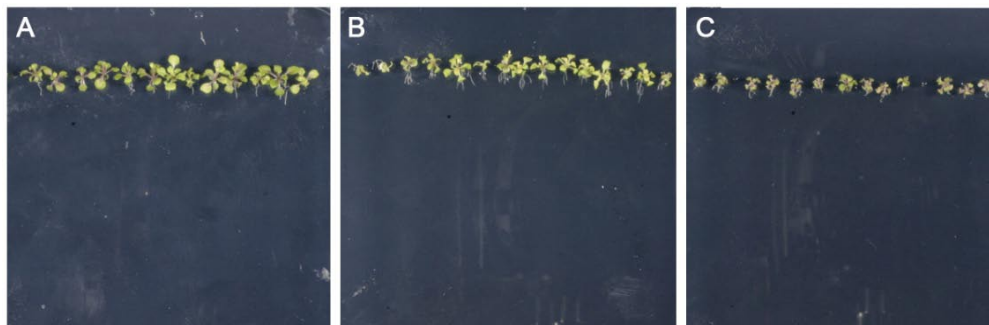


Figure 24: Analysis of the M₃-generation

Plants were grown on (A) $\frac{1}{2}$ MS, (B) $\frac{1}{2}$ MS + 5mM GABA, or (C) $\frac{1}{2}$ MS + 5mM glutamate for 16 days under long day conditions.

To identify the chromosome carrying the mutation, the F₂-population resulting from a cross to *Ler* was screened for double homozygous plants. These plants had yellowish, slightly rounder rosette leaves compared to wild type, allowing for a phenotype-based selection. The SSLP-markers (Figure 21) were used, and the resulting recombination rates were obtained (Table 1). The mutation could be mapped to the upper half of chromosome 4 and by using additional CAPS-markers (6.4.5.2.1); the following recombination rates (Figure 25) were obtained.

Table 1: Recombination frequencies in F₂ plants obtained by a cross of *ssadh* suppressor line 4.D to Ler wild types

Chromosome	Marker	Number of plants	% Col-0	% Ler
1	NGA 392	67	55,2	44,8
	NGA 280	71	86,6	13,4
	NGA 111	74	99,3	0,7
2	NGA 168	56	51,8	48,2
3	NGA 172	75	52,7	47,3
4	NGA 12	20	72,1	27,9
	NGA 8	67	85,1	14,9
	NGA 1111	77	53,2	46,8
	DET1.2	56	67,9	32,1
	NGA 1139	77	48,7	51,3
	NGA 1107	77	48,1	51,9
	CIW	77	67,9	32,1
5	NGA106	74	60,1	39,9
	NGA139	77	66,9	33,1

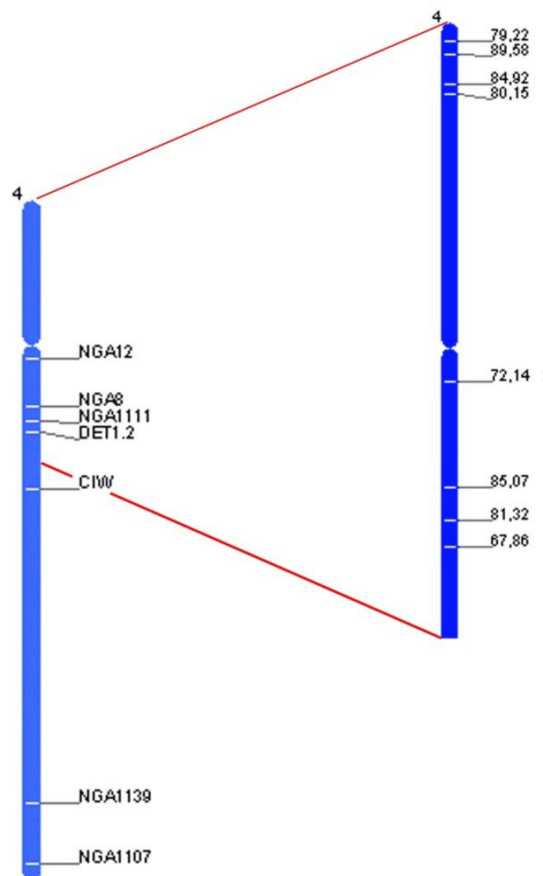


Figure 25: Marker distribution with a high frequency of Col-0 fragments in line 4.D

2.2.3.2. Line 17.J

This plant was isolated from the M₂ generation in pool number 17, transferred to single pots and grown under greenhouse conditions until maturation (Figure 26). Compared to wild type plants, no major differences were visible.

In the M₃ generation, growth of plants under long and short day conditions and on ½ MS supplemented with GABA or Glutamate was monitored. Plants grown under long day conditions resembled the phenotype of the parental plants, whereas all leaves developing under short day conditions were reduced in size and displayed a pale green color (Figure 27). Analyzing the GHB and GABA content in leaf extracts of plants grown under greenhouse conditions using GC-MS revealed 80-fold increased GHB-, and 5-fold increased GABA-levels compared to wild type.

To gain additional knowledge about plant characteristics, seeds were germinated on ½ MS supplemented with either GABA or glutamate (Figure 28). Plants grown on ½ MS displayed no altered root architecture, and some rosette leaves were pale green. Germination on GABA or glutamate-containing media clearly reduced rosette size and root length, plants grown on GABA-containing media were slightly smaller compared to those grown on glutamate.



Figure 26: Phenotype of 17.J M₂ plant grown under greenhouse conditions for 44 days.

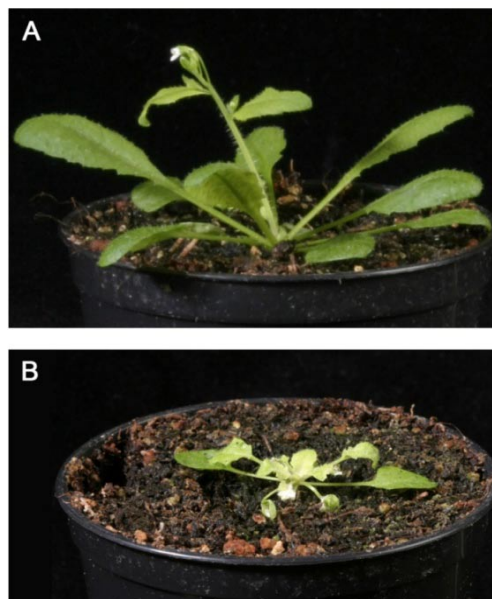


Figure 27: Plants of the M₃-generation were grown under long day (A) and short day (B) conditions for 39 days

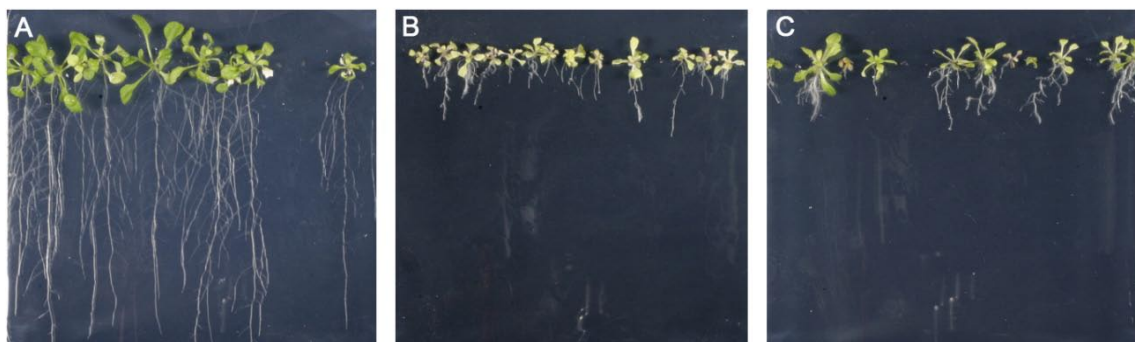


Figure 28: Analysis of the M₃-generation

Plants were grown on $\frac{1}{2}$ MS (A), $\frac{1}{2}$ MS + 5mM GABA (B), or $\frac{1}{2}$ MS + 5mM glutamate (C) for 16 days under long day conditions.

To identify the chromosome carrying the mutation, the F₂-population resulting from a cross to *Ler* was screened for double homozygous plants. These plants were phenotypically indistinguishable from wild types, with the exception of a paler petiole in young, developing leaves. Therefore, all F₂ plants had to be screened by PCR. The SSLP-markers (Figure 21) were used, and the resulting recombination rates were obtained (Table 2). The mutation could be mapped to chromosome 5. Additional CAPS-markers (6.4.5.2.2) were selected to further narrow down the region containing the EMS mutation, and the following recombination rates (Figure 29) were identified.

Table 2: Recombination frequencies in F₂ plants Ler/17.J

Chromosome	Marker	Number of plants	% Col-0	% Ler
1	NGA 392	35	44,3	55,7
2	NGA 1145	38	59,2	40,8
	NGA361	49	57,1	42,9
3	GAPAB	39	56,4	43,6
4	NGA 8	40	52,5	47,5
5	NGA 151	38	60,5	39,5
	NGA106	40	62,5	37,5
	CDPK9	39	65,4	34,6
	NGA76	37	80,0	20,0
	SO262	38	72,4	27,6
	NGA129	35	80,0	20,0
	CIW10	42	82,1	17,9

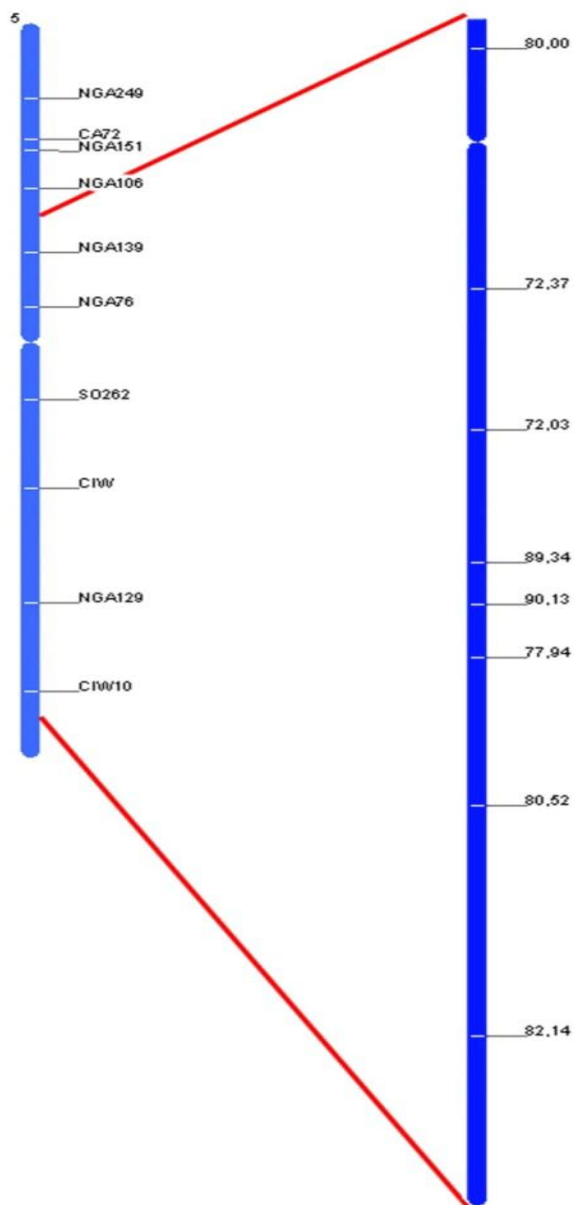


Figure 29: Marker distribution with a high frequency of Col-0 fragments in line 17.J

2.2.3.3. Line 21.H

This plant was isolated in the M₂-generation in pool number 4, transferred to single pots, and grown under greenhouse conditions until maturation (Figure 30). The plant had slightly smaller, pale green rosette leaves, and first flower buds appeared after 41 days.

In the M₃-generation, growth of plants under long and short day conditions and on ½ MS supplemented with GABA or Glutamate was monitored. Plants grown under long day conditions resembled the phenotype of the parental plants whereas plants grown under short day conditions were highly affected, new developing leaves remained very small (Figure 31). Determining the GHB and GABA content in leaf extracts of plants grown under greenhouse conditions by GC-MS revealed 230-fold increased GHB-, and 8-fold increased GABA-levels compared to wild type.

To obtain additional information about plant features, seeds were germinated on ½ MS supplemented with either GABA or glutamate (Figure 32). Plants grown on ½ MS had no altered root morphology, but pale green rosette leaves, germination on GABA or glutamate-containing media, the plant size was plainly reduced.



Figure 30: Phenotype of 21.H M₂ plant grown under greenhouse conditions for 44 days.



Figure 31: Plants of the M₃-generation were grown under long day (A) and short day (B) conditions for 39 days

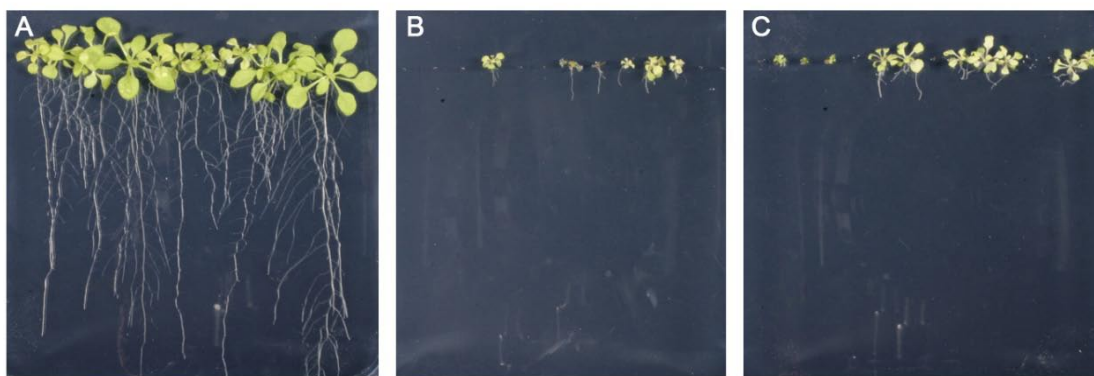


Figure 32 Analysis of the M₃-generation

Plants were grown on $\frac{1}{2}$ MS (A), $\frac{1}{2}$ MS + 5mM GABA (B), or $\frac{1}{2}$ MS + 5mM glutamate (C) for 16 days under long day conditions.

To identify the chromosome carrying the mutation, the F₂-population resulting from a cross to *Ler* was screened for double homozygous plants. These plants had yellowish, slightly smaller rosette leaves compared to wild type, allowing for a phenotype-based selection. Using the SSLP-markers (Figure 21), the mutation could be mapped to the lower arm of chromosome 2 (Table 3). By using additional CAPS-markers (6.4.5.2.3), the region carrying the mutation could be further narrowed (Figure 33).

Table 3: Recombination frequencies in F₂ plants obtained by a cross of *ssadh* suppressor line 4.D to *Ler* wild types

Chromosome	Marker	Number of plants	% Col-0	% Ler
1	NGA 280	26	63,5	36,5
2	CZSOD 2	19	63,2	36,8
	NGA361	31	59,7	40,3
	NGA 168	20	90	10
3	NGA 172	22	59,1	40,9
	NGA126	21	61,9	38,1
4	NGA 8	27	59,3	40,7
5	NGA139	28	58,9	41,1

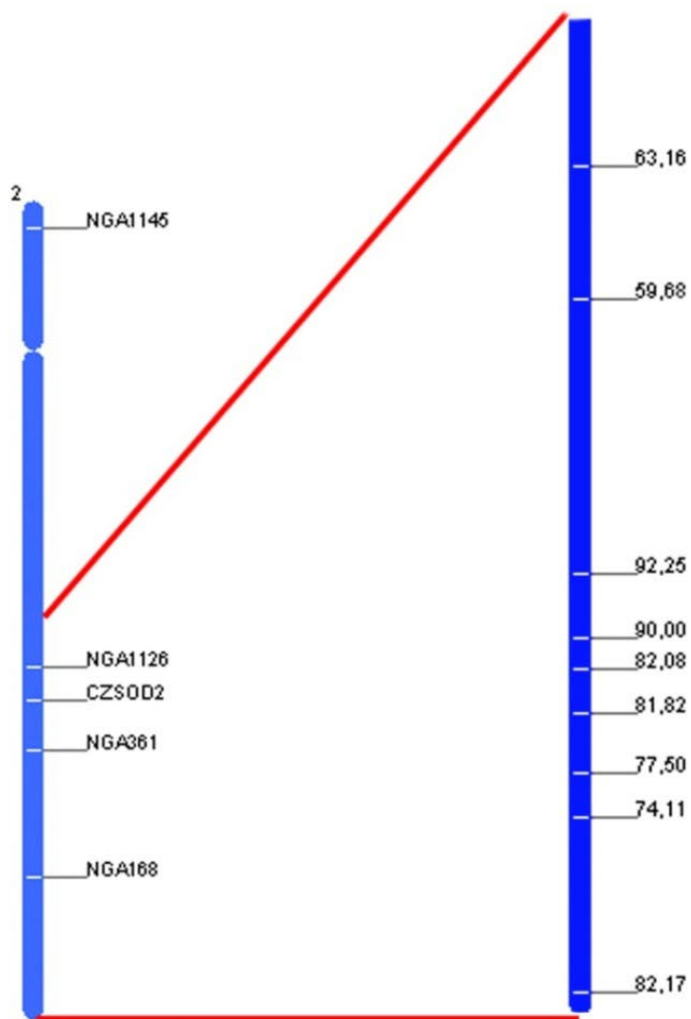


Figure 33: Marker distribution with a high frequency of Col-0 fragments in line 21.H

To further map down the mutations to a smaller chromosomal region, a larger mapping population has to be isolated and more markers have to be available.

2.3. SSA induces callus formation in Arabidopsis

To enhance the survival rates of *ssadh* mutant plants, seeds were germinated on $\frac{1}{2}$ MS and transferred to soil into the greenhouse about eight weeks later. At this time point, the occurrence of dedifferentiated tissue at the hypocotyls of some *ssadh* seedlings was visible (Figure 34). Whether the hypocotyl dedifferentiated or not did not influence overall plant growth. In contrast to Col-0 wild types that formed no dedifferentiated tissue when germinated on $\frac{1}{2}$ MS, 128 out of 1000 *ssadh* mutant plants developed callus under the same conditions.



Figure 34: *ssadh* mutant plants develop callus on $\frac{1}{2}$ MS

(A) Col-0 wild type plants 10 days after germination, none with callus

(B) *ssadh* mutant plants 9 weeks after germination, several plants developed dedifferentiated tissues (C-E) close-up view on dedifferentiated cells

2.3.1. Callus formation is dependent on the SSA concentration

To test whether dedifferentiation is dependent on the cellular SSA concentration, wild type seeds of three different Arabidopsis ecotypes (Col-0, *Ler*, and *Ws-2*) were germinated on $\frac{1}{2}$ MS supplemented with SSA. In all ecotypes analyzed, callus formed at the hypocotyl in a linear response to the SSA concentration in the media; only minor variations appeared among the ecotypes (Figure 35). Notably, the callus formation rate of *ssadh* mutant plants on $\frac{1}{2}$ MS and of wild types on $\frac{1}{2}$ MS + 0.8mM or 1.0mM SSA are comparable.

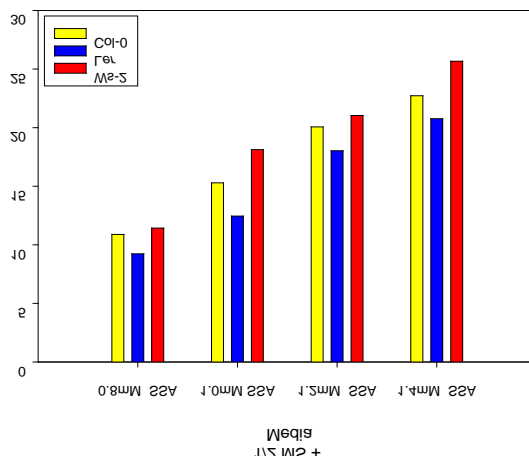


Figure 35: Rate of callus formation in Arabidopsis wild type plants is dependent on the SSA concentration in the media.

Three Arabidopsis ecotypes (Col-0, Ler, and Ws-2) were grown on $\frac{1}{2}$ MS containing different amounts of SSA for 36 days, and among the germinated seeds the number of plants developing dedifferentiated tissue was determined. The experiment was repeated once, each with approximately 300 plants per ecotype analyzed. The given values are the average of both experiments.

Comparing the rate of callus formation among seeds germinating on SSA-containing media with or without added sucrose, no big differences arose. Interestingly, when growing wild type plants on $\frac{1}{2}$ MS + SSA in darkness, no dedifferentiation occurred, probably being an indication toward an underlying light-dependent process.

When *ssadh* mutant seeds were germinated on $\frac{1}{2}$ MS + SSA, all plants developed dedifferentiated tissue, but without restriction to the hypocotyl (Figure 36). Again, growth in darkness prevented callus formation.

To test whether the dedifferentiated cells can be used for regeneration of whole plants, the dedifferentiated cells were isolated and transferred first on shoot-, then on root-induction media; the former containing a lower, the latter a higher auxin-to-cytokinin ratio (Figure 37). The resulting plants were paler than normal wild type plants, but produced seeds in the greenhouse; and their offspring presented no differences to other wild type plants.

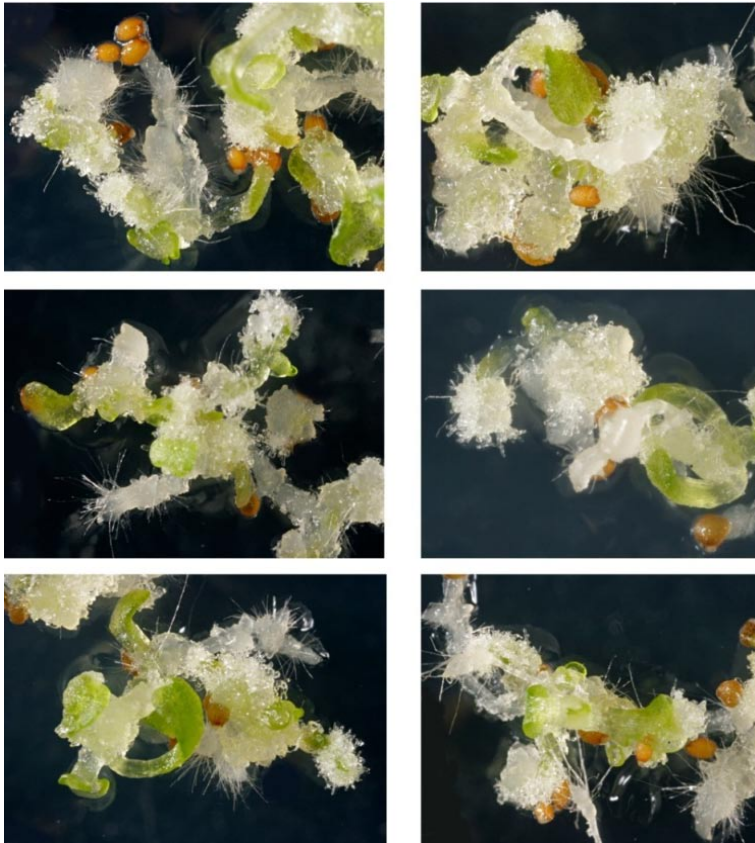


Figure 36: Phenotype of *ssadh* seeds germinated on 1/2 MS containing SSA

ssadh mutant seeds were germinated on 1/2 MS+1.4mM SSA and grown for 28 days. The seedlings developed dedifferentiated tissue not only localized to the hypocotyl. The nature of the root hair like structures emerging from the calli remains unclear.

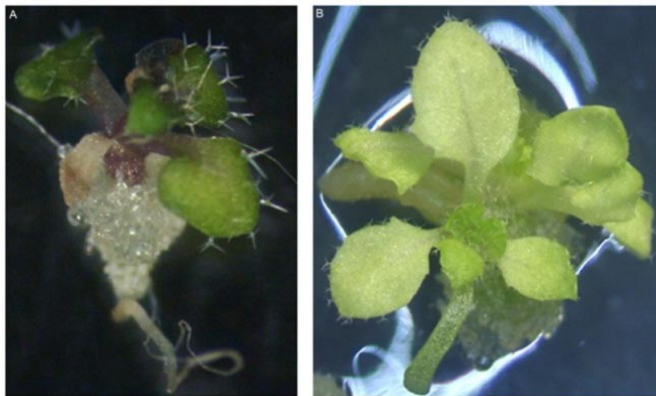


Figure 37: Whole plants can be regenerated from SSA-induced callus

(A) Col-0 wild type developed callus from the hypocotyl after 4 weeks on 1/2 MS + 1.4mM SSA.

(B) Shoots were regenerated from isolated callous cells on media containing a low auxin to cytokinin ratio. The picture was taken 22 days after transfer to shoot-regeneration media.

2.3.2. Does a linkage between SSA-induced callus formation and phytohormones exist?

It has been reported that callus formation occurs dependent on the auxin to cytokinin ratio in tissue and further differentiation can be induced by altering the ratio.

To test whether SSA does influence phytohormone sensitivity in Arabidopsis, the effect of a combination of SSA and auxin or cytokinin on the callus formation rate was assayed. Neither were phenotypic discrepancies visible nor was the callus formation rate altered dramatically between plants grown on the different media (Figure 38).

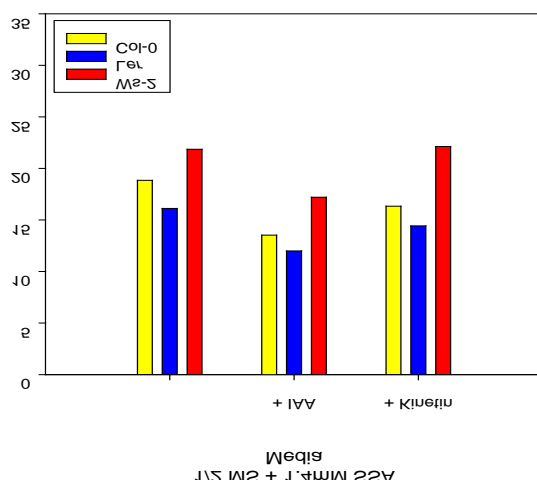


Figure 38: Callus formation is not dependent on the auxin to cytokinin ratio

Three Arabidopsis ecotypes (Col-0, Ler, and Ws-2) were grown on $\frac{1}{2}$ MS containing 1.4mM SSA, or on $\frac{1}{2}$ MS + 1.4mM SSA supplemented with either 10 μ M IAA or 10 μ M kinetin for 36 days. Among the germinated seeds, the number of plants developing dedifferentiated tissue was determined. Addition of IAA and kinetin respectively, did not alter the rate of callus formation much. The experiment was performed two times, each with approximately 300 plants per ecotype analyzed. The given values are the average of both experiments.

Although the addition of IAA or kinetin to $\frac{1}{2}$ MS containing SSA did not notably affect the callus formation rate, the appearance of the calli - especially the phenotype of the *ssadh* calli with root hair like structures emerging from the dedifferentiated cells (Figure 36) - point toward an auxin related mechanism. Therefore, the auxin transport inhibitors NPA and TIBA as well as the antiauxin PCIB [23] were tested regarding their capacity to affect the rate of SSA-induced callus formation. Neither addition of PCIB nor of NPA showed a drastic reduction in callus formation, but the addition of TIBA completely inhibited SSA-induced callus formation (Figure 39).

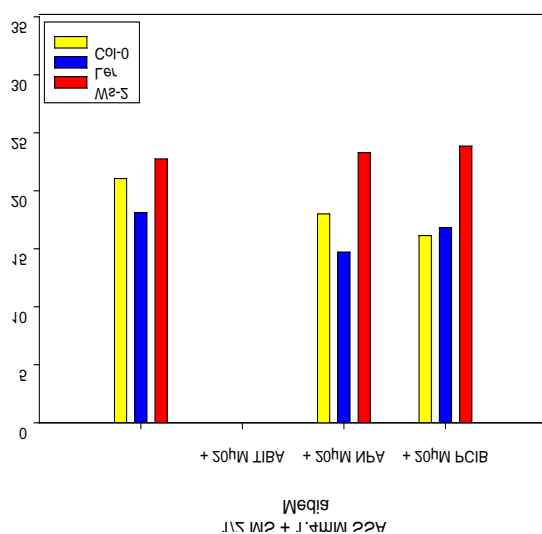


Figure 39: Influence of inhibitors of auxin transport or activity on SSA-induced callus formation

Three Arabidopsis ecotypes (Col-0, Ler and Ws-2) were grown on $\frac{1}{2}$ MS containing 1.4mM SSA and either 20µM TIBA, 20µM NPA or 20µM PCIB for 36 days. Among the germinated seeds, the number of plants developing dedifferentiated tissue was determined. Addition of PCIB or NPA – NPA even in 5-fold higher concentrations - did not alter the rate of callus formation much. In contrast, the auxin-transport inhibitor TIBA completely prevented SSA-induced callus formation. The experiment was repeated once, each with approximately 400 plants per ecotype analyzed, the given values are the average of both experiments.

The TIBA-mediated inhibition of SSA-induced callus formation in Arabidopsis wild type plants refers to auxin-related processes. To assay the expression of various genes related to auxin synthesis, transport, and perception, transgenic Arabidopsis lines expressing GUS under control of auxin-associated promoters were germinated on $\frac{1}{2}$ MS containing SSA, and the calli were stained for GUS activity (Figure 40). A strong signal was detected in plants expressing GUS under control of the NIT1, NIT2, LAX1, and LAX2 promoters. Compared to these lines, plants carrying NIT3::GUS or LAX3::GUS constructs had a weaker expression level. SSA induced promoter activity in plants, visualized by GUS staining for genes involved in import and synthesis of indol-3-acetic acid (IAA). No GUS activity was visible in calli of the other lines tested, which expressed GUS under control of native promoters or the synthetic auxin responsive element DR5, where GUS expression was only detected in root tips of plants grown on media with or without SSA.

In parallel to the promoter-activity assays, the effect of SSA on callus-induction in several auxin-related mutants was assayed (Figure 41). A reduction of callus formation was observed in plant lines deficient in auxin carriers (*aux1*, *lax1*, *lax3*, and *pin3*) or the *arf7/arf19* double mutants and in plants overexpressing an IAA ligase that is involved in removal of active auxin. As control for other phytohormone signaling pathways, plants overexpressing nahG, a bacterial salicylate hydrolase, were assayed, but no difference to the corresponding wild type was detectable.

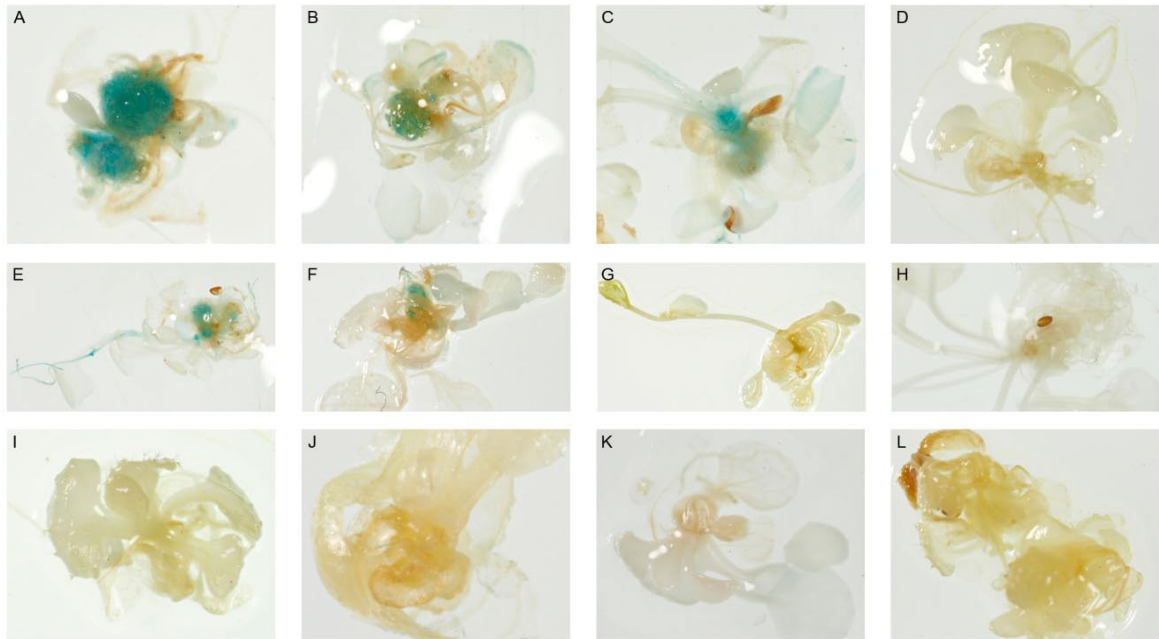


Figure 40: GUS-staining of SSA-induced calli

Plants expressing different Promoter::GUS fusion constructs were germinated on ½ MS + SSA and stained for GUS activity.

Expression was found for NIT1 (A), NIT 2 (B), NIT3 (C), LAX1 (E), LAX2 (F) and very weak for LAX3(G), whereas no staining was visible for NIT4 (D), AXR1 (H), IAA2 (I), PIN1 (J), PIN6 (K) and AUX1 (L)

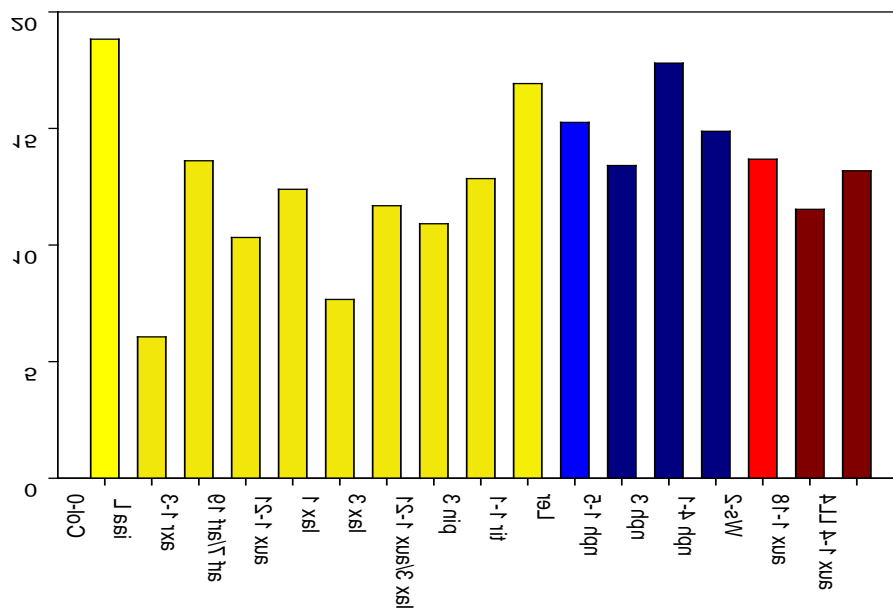


Figure 41

Figure 41: Callus formation rate in auxin-related mutants

Plants mutated in genes involved in different phytohormone pathways were analyzed for their response to SSA. Therefore, the mutants and the corresponding wild type lines were grown for 28 or 31 days on ½ MS + 1.4mM SSA, and the number of plants developing callus was determined. The experiment was repeated twice with 100 to 400 plants analyzed, the given values are the average from all experiments.

2.3.3. Does SSA itself act as auxin?

Several assays are published to test chemicals for their auxin-activity, one among them is the determination of root length in *Arabidopsis* plants [186]. Therefore, *Arabidopsis* wild type seeds from three ecotypes were germinated on media containing either different concentrations of SSA or 2,4-D as positive control for a substance with known auxin activity (Figure 42), and root length was determined 8 days after germination. A reduced root growth was measured for seedlings grown on both SSA and 2,4-D, however the SSA concentrations efficiently inhibiting root growth were about 10000 fold higher than the 2,4-D concentrations.

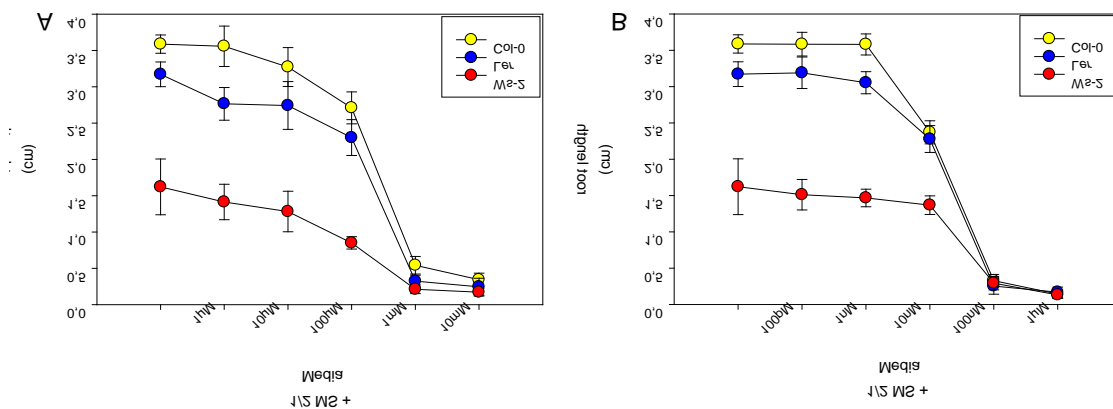


Figure 42: Assay for auxin activity in Arabidopsis

Three *Arabidopsis* ecotypes (Col-0, Ler and Ws-2) were grown on ½ MS supplemented with different concentration SSA (A) or the auxin 2,4-D (B). Root growth of 40 plants each was measured 8 days after germination; the given values are the average and standard deviation.

3. Discussion

3.1. Influence of GABA-shunt metabolites on plant growth

To assay the effect of the GABA-shunt or GABA-related metabolites, growth and development of several GABA-shunt mutants was analyzed in comparison to wild type. Additionally, the effect of exogenously supplied GABA-shunt metabolites on plant growth *in vitro* was examined.

On standard $\frac{1}{2}$ MS media, *gaba-t* mutants display a trend toward an increased shoot growth without an increase in root length. The same effect can be induced in wild type plants by the addition of GABA to the media (Figure 6 and Figure 7). The availability of inorganic nitrogen in the media is essential for plant growth, and nitrate uptake in the roots is a limiting step of nitrate assimilation. In *Brassica napus*, GABA enhances nitrate transporter gene expression, resulting in increased root nitrate uptake capacities [22]. Since *Brassica napus* and *Arabidopsis thaliana* are closely related species, a GABA-induced upregulation of nitrate uptake transporters seems conceivable in Arabidopsis. This regulation would lead to an increased nitrate-uptake capacity and as a result to enhanced growth. Taken together, the endogenous GABA concentrations in *gaba-t* mutant plants might be sufficient to induce expression of nitrate uptake transporters that increases plant growth under standard conditions. In contrast, the cellular GABA concentrations required for the enhanced expression of nitrate uptake transporters might be reached in wild type plants only by the exogenous supply of GABA.

The increasing number of lateral roots forming in wild type plants growing on GABA as sole nitrogen source might be explained in two different ways. GABA – even when available in equal concentrations to inorganic nitrogen in control plates – might be an inappropriate nitrogen source compared to inorganic nitrogen, with limitations regarding GABA-uptake capacities and metabolism. The high affinity GABA transporter GAT1 is very low expressed in the whole plant, with hardly any expression detected in roots. The ProT proteins are low affinity GABA transporters that are not expressed in roots. As conclusion from the expression data (available at <https://www.geneinvestigator.ethz.ch> and <http://www.bar.utoronto.ca/efp>), only minor GABA uptake rates are found in

Arabidopsis roots under physiological conditions. Ammonia can directly be incorporated into amino acids, whereas nitrate has to be reduced in the plastids before being incorporated in α -ketoglutarate, producing glutamate. In contrast, GABA-degradation is localized in the mitochondria and the amino group is transferred to pyruvate, yielding alanine. To obtain all other amino acids starting from GABA, will necessarily include several accessory reactions. Taken together, GABA as sole nitrogen source might induce reduced growth and indications of nitrogen deprivation in plants [112]. The increased number of lateral roots might be required to allow for sufficient GABA uptake capacities. Furthermore, GABA is known to induce ethylene production, a main regulator of root hair and lateral root formation also in Arabidopsis [35, 52, 90].

The impaired growth of *gaba-t* mutant plants on media supplied with GABA could be due to the accumulation of GABA in the plants, initiating a yet unidentified mechanism provoking a developmental inhibition. This effect might argue for GABA acting as signaling molecule in Arabidopsis, where a function in pollen tube guidance and fertilization is known (Figure 2 and [29, 130]); additionally, GABA is long known as signal molecule in several other species (1.5).

The suppression of the *ssadh* phenotype is possible using either a biochemical or a genetic approach to prevent GABA-T function. First, the application of Vigabatrin to *ssadh* mutant plants improves plant growth [66], since Vigabatrin interacts with the GABA-T and irreversibly blocks the protein function. Second, *gaba-t/ssadh* homozygous plants grow like *gaba-t* single mutants under greenhouse conditions, proving *GABA-T* to be epistatic to *SSADH* (2.1.1).

GABA-shunt metabolites can be measured in plant extracts using GC-MS, with the exception of SSA, where - in contrast to human medicine [167] - currently no method is available. To assay whether GABA-shunt metabolites influence plant development, GABA and GHB levels in wild type and several mutant plant lines are determined (2.1.1).

The accumulation of GABA (Figure 4a) in *gaba-t* and *gaba-t/ssadh* mutants is due to GAD activity, while GABA degradation is blocked. In contrast, *ssadh* mutants

accumulate twice as much GABA as the aforementioned lines. In *ssadh* mutants SSA-synthesis from GABA still can occur, resulting in SSA accumulation. In order to remove excess SSA, when a threshold level is reached, an amino group might be transferred from alanine to SSA, thereby producing GABA and further increasing the GABA concentrations; in mammalia, the GABA-T is capable of acting in the reverse direction [179].

GHB levels (Figure 4b) in wild type and *gaba-t* mutants are near the detection limits of the GC-MS system used. Most probably, if GHB is synthesized in the aforementioned plant lines, then it is degraded via SSA to succinate under normal growth conditions, comparable to data published for rat [179]. If GHB-synthesis occurring independently from the GABA-shunt in Arabidopsis is assumed, then the detection of GHB in *gaba-t/ssadh* mutant plants could be explained. The vast amounts of GHB determined in leaf extracts of *ssadh* mutants might be a mechanism comparable to one appearing in human patients with SSA-deficiency, resulting in an accumulation of GHB [77]. Suspecting SSA to be toxic for cells, then GHB synthesis might be an attempt of plants to remove SSA in situations with no or too little functional SSADH protein in the cells. However, the GHBDH would – at least under these conditions - prefer the reduction of SSA to GHB and not the oxidation of GHB to SSA, as known from mammalia.

Given that *ssadh* mutant plants accumulate both SSA and GHB which, either alone or in combination, reduce plant growth and induce the accumulation of reactive oxygen intermediates (ROIs), then the substance causing the *ssadh* phenotype might be identified by the analysis of *gaba-t/ssadh* plants [66, 107]. To address the question whether SSA or GHB has a larger impact on plant growth, *gaba-t*, *gaba-t/ssadh* and wild type plants grown on media containing SSA or GHB were analyzed regarding growth and metabolite content. In these experiments, no differences occurred between wild type and *gaba-t* mutants since both are able to degrade SSA and GHB. In contrast, *gaba-t/ssadh* mutants were highly affected by either SSA or GHB (Figure 8). Interestingly, no correlation was found between GHB content measured in leaf extracts and plant growth observed on the different media. Wild type and *gaba-t* mutant plants are less impaired in growth than *gaba-t/ssadh* plants that contain comparable amounts of GHB in leaf extracts. Additionally, *gaba-t/ssadh* plants with similar GHB amounts in leaf extracts are smaller

when grown on media containing SSA. Several additional findings favoring SSA to be toxic can be stated. First, compared to GHB, lower concentrations of SSA induce severe growth reduction in wild type plants. Second, GHB in the media mainly decreases root length, whereas the rosette size is not altered; supplementation with SSA leads to growth of very small rosettes and a shorter main root with an increased number of lateral roots. Third, in the screening for *ssadh* suppressor lines, several plants lines with improved growth were isolated containing higher GHB amounts in leaf extracts than the *ssadh* mutants (6.1.1). Forth, in *Agrobacterium tumefaciens*, two differentially expressed *SSADH* genes were identified that are probably necessary for SSA detoxification [185], and finally, *SSADH* deficiency in humans lead to neurological disorders, but no reports of *GHBDH* deficiencies are published.

Since SSA and GHB can rapidly be converted into each other, a central point for the identification of the substance causing the *ssadh* phenotype is to inhibit this conversion. In *Arabidopsis*, one gene encoding a *GHBDH* has been published [31] and homozygous T-DNA lines are available. Although these plants were supposed to be unable to catalyze the SSA-GHB conversion and hence growth should vary compared to wild type grown on SSA- or GHB-containing media, surprisingly no differences were observed (Figure 10). The identification of a sequence homologous to the *GHBDH* protein explained this finding, and the analysis of double homozygous plants revealed minor variations in GHB content (Figure 17). Compared to wild type, no growth differences occurred on the different media, but mutant plants accumulate less GHB upon growth on SSA containing media, and more GHB when grown on media supplemented with GHB. These findings indicate a possible SSA or GHB threshold level in plants that must be reached to induce activity of the *GHBDH* proteins *in vivo*. To test this assumption, *GHBDH* activity levels of recombinant and native protein should be assayed. As an alternative hypothesis, the existence of a third protein catalyzing the SSA-GHB conversion can be assumed, probably the more distantly related gene At4g20930, annotated as 3-hydroxyisobutyrate dehydrogenase. So, the isolation of knockout lines for this gene might be helpful in this context.

Taken together, the analysis of a yet not existing *ghbdh* triple mutant or a *gaba-t/ssadh/ghbdh-1/ghbdh-2* quadruple mutant and the development of a method to measure SSA in plant extracts is essential to answer the question which substance is causing the *ssadh* phenotype.

For both GHBDH proteins, the intracellular localization was analyzed using GFP fusion proteins in co-localization studies with RFP-tagged organelle markers [123]. Corresponding to prediction programs, GHBDH-1 localizes to the cytosol (Figure 9). Biochemical analyses of recombinant protein in a published report suggest a preference for SSA as well as for glyoxylate reduction over the corresponding oxidation reactions [86, 87]. If the GHBDH-1 reduces SSA, then the substrate for a cytosolic enzyme can only be present, when SSA export from the mitochondria occurs.

The second protein reveals indifferent localizations when comparing the output of several prediction programs. In contrast to published data, where a plastidial localization is reported [158], neither in Arabidopsis cell culture co-transformed with GHBDH-2-GFP along with a plastidial RFP marker (Figure 14) nor following particle bombardment of leek epidermal peels (Figure 13) co-localization of GHBDH-2-GFP with a plastidial marker is observed. However, since glyoxylate is found predominantly in plastids and peroxisomes, a plastidial localization might be necessary for the enzyme to act *in vivo* as glyoxylate reductase. If SSA reduction is the preferred reaction, then a plastidial localization of the enzyme would not be essential.

In transient transformation of Arabidopsis suspension cells with GHBDH-2-GFP, co-localization is perceived either with a co-transformed mitochondrial RFP marker (Figure 15) or in cells stained with Mitotracker Red (Figure 16). In the mitochondrial matrix, the general reduction potential favors oxidation of substrates, whereas in plastids, substrates are predominantly reduced. This supports the hypothesis that GHB might additionally be produced in a presumed GABA-independent pathway, and is oxidized in the mitochondria via SSA to succinate, comparable to the degradation of the neurotransmitter GHB in the mammalian brain [77, 179].

3.2. Identification of *ssadh* suppressor lines

Since the suppression of the *ssadh* phenotype is possible as presented in 2.1.1 and [66, 107], a population of EMS-mutagenized *ssadh* plants was screened for plants with improved growth, to identify further genes involved in regulation or function of the GABA-shunt. Growth characteristics and metabolite contents of several lines resembled *gaba-t/ssadh* mutants, and among these, two new *gaba-t* alleles were identified by sequencing (2.2.2).

By comparing the Arabidopsis protein sequence to sequences of crystal structures available in public databases, the mutation in line 37.B is identified next to an active site residue, whereas in line 31.A a single residue located both in the recognition site for cofactor binding and near an active site residue is exchanged [166, 174]. These substitutions by larger, negatively charged amino acids will most probably result in an altered protein structure. Minor modifications of the protein structure might result in changed catalytic properties or substrate specificities. In contrast, serious structural modifications will lead to misfolded proteins that are recognized and degraded in ubiquitin-dependent proteolysis [124]. Here, both mutations are supposed to interfere with both the formation of the active site and proper folding of the whole enzyme, thus resulting in protein inactivation and probably even degradation. Therefore, the two *ssadh* suppressor lines most likely contain no functional GABA-T enzyme.

Currently, three other *ssadh* suppressor lines are under investigation to identify the location of the EMS mutation (2.2.3). All available SSLP-markers are used to identify a larger region on the chromosome, where the EMS-mutation might reside. The CAPS-markers proposed by the Marker Tracker (<http://www.bar.utoronto.ca/markertracker/>) are based on the published Col-0 and *Ler* genomic sequences, and are derived from *in silico* analyses, but the sequences were found to produce not necessarily polymorphic fragments following PCR and restriction. To identify a smaller chromosomal region allowing to select a number of possible candidate genes, two points have to be covered: first, more double homozygous F₂ plants need to be isolated and second, more markers – probably also without restriction to PCR-based markers – have to be defined and assayed for polymorphisms.

Plants of line 4.D (2.2.3.1) are those accumulating the highest amounts of GHB in leaf extracts among all *ssadh* suppressor lines analyzed. Corresponding to the metabolite data, growth of the plants on ½ MS plates resemble the phenotype of wild type plants grown on ½ MS supplemented with GHB: the rosette size is not much affected, while the roots are considerably shorter. In comparison to wild types, the reduced rosette size might be due to the *ssadh* mutant background of the plants. A mutation in one of the known *GHBDH* genes could be excluded since the mutation maps to chromosome 4 and the *GHBDH* genes are localized on the chromosomes 2 and 1 respectively. However, the putative third possible GHBDH in Arabidopsis (At4g20930) is located on chromosome 4 within the region possibly containing the EMS-mutation and might induce suppression of the *ssadh* phenotype.

3.3. SSA induces callus formation in *Arabidopsis thaliana*

Arabidopsis ssadh mutant plants growing on ½ MS or wild type plants growing on ½ MS supplemented with SSA develop dedifferentiated tissue in the hypocotyl. The regeneration of whole plants from the isolated dedifferentiated cells is considered as a proof for these cells being callus.

Analyzing the rate of callus formation in wild type plants of three different *Arabidopsis* ecotypes (Figure 35) reveals a positive correlation of callus formation on the SSA concentration in the media. Furthermore, the rate of callus formation was similar in wild type growing on ½ MS supplemented with 0.8mM or 1.0mM SSA and in *ssadh* mutants growing on ½ MS. Probably, a certain cellular SSA concentration is necessary to induce dedifferentiation, which is reached in *ssadh* mutants naturally, whereas in wild type plants this concentration is only accessed upon SSA-feeding. Further arguments supporting callus formation to be a concentration- and light-dependent mechanism are three observations; first, dark grown plants never developed callus; second, increasing the SSA-concentration in the media enhances callus formation in the hypocotyl of wild types; and third, germinating *ssadh* mutants on media containing SSA results in dedifferentiation occurring in several tissues without a restriction to the hypocotyl (Figure 36).

Callus formation in plants is long known to occur in response to the ratio of the phytohormones auxin and cytokinin [37, 159]. However, growing plants on media containing SSA and IAA or SSA and kinetin has no large effect on the rate of callus formation in wild type (Figure 38), indicating that SSA might induce callus formation independent of the auxin or cytokinin supplied in the media. Nevertheless, the phenotype – especially of the *ssadh* calli with emerging root hair like structures (Figure 36) – indicates an auxin-related process.

In contrast to NPA and PCIB – an auxin transport inhibitor and an antiauxin - only the second tested auxin-transport inhibitor TIBA has the ability to prevent SSA-induced callus formation when supplied to the media (Figure 39). TIBA inhibits vesicle

trafficking and thus the recycling of auxin transporters belonging to the AUX/LAX and PIN protein families [61, 98].

In addition to the inhibition of callus formation by preventing cycling of auxin transporters, a considerably reduced rate of callus development was observed in plants with mutations in different auxin transport genes (*aux1*, *lax1*, *lax3*, and *pin3*) as well as in plants overexpressing an IAA ligase (IAA-L plants) that contain lesser amounts of free active auxin (Figure 41). Furthermore, assaying the GUS expression driven by promoters of auxin-related genes reveals SSA-induced promoter activity for the *LAX* genes and for the *NIT1* to *NIT3* genes. The SSA-induced expression of *LAX* genes corresponds to the reduction of callus formation in *lax* mutants, might present evidence for a mechanism related to auxin-transport. The nitrilase proteins 1 to 3 catalyze the hydrolysis of IAN to IAA, increasing the concentration of free, active auxin in the cells. Activation of the *NIT* genes in response to SSA will result in an enhanced IAA production in the dedifferentiated tissue. If SSA-induced callus induction involves an IAA-related mechanism, then expression of the synthetic auxin-responsive promoter DR5 should be detectable in the tissue. Recently published data revealed that DR5 expression is highest in the early stages of callus development and depletes over time. About one week after the transfer to callus induction medium, no DR5 expression was detectable in the calli any more [9, 78]. When assigning this discovery to the SSA-induced callus formation, then DR5 expression should be detectable early during callus development, but this remains to be tested.

In a root elongation assay, a test for auxin activity in Arabidopsis, SSA inhibits root growth, but the required concentrations are much higher than those published for auxins (2.3.3). This supports the hypothesis, that SSA induces the synthesis of auxins in a yet unknown way.

Taken together, the combination of increased IAA synthesis and enhanced transport – especially uptake – might result in the accumulation of free auxin in the cells of the hypocotyl, and as a consequence induce callus.

4. Materials and Methods

4.1. Materials

4.1.1. Chemicals

Chemicals were obtained from the companies:

Biomol (Hamburg, D), Difco (Hamburg, D), Duchefa (Haarlem, NL), Eurobio (Les Ulis Cedex, F), Fluka AG (Buchs, CH), Merck (Darmstadt, D), Roche (Mannheim, D), Roth (Karlsruhe, D), Fisher Scientific GmbH (Schwerte, D), Chromatographie Service GmbH (Langerwehe, D) and Sigma-Aldrich (Deisenhofen, D).

Purity was "research grade" or the highest available.

4.1.2. Enzymes

Enzymes for molecular biology were obtained from the companies:

Invitrogen (Karlsruhe, D), MBI Fermentas (St. Leon-Rot, D), Promega (Mannheim, D), Qiagen (Hilden, D), Roche (Mannheim, D) and Sigma (Deisenhofen, D).

4.1.3. Kits

The following Kits were used following the manufactures protocols:

TRISure (Bioline)

Big Dye ® Terminator Cycle Sequencing Kit v3.1 (Applied Biosystems, Foster City, USA)

CompactPrep Plasmid Midi (Qiagen GmbH, Hilden, D)

QIAquick Gel Extraction Kit (Qiagen GmbH, Hilden, D)

Quantum Prep ® Plasmid Miniprep Kit (BioRad, München, D)

Super Script™ II - Reverse Transcriptase (Bioline)

4.1.4. Antibiotics

The following antibiotics were used:

Antibiotic	stock solution		working concentration
Ampicillin	100 mg/mol	in water	100 µg/mol
Carbenicillin	50 mg/mL	in water	50 µg/mL
Kanamycin	50 mg/mL	in water	50 µg/mL
Gentamycin	25 mg/mL	in water	25 µg/mL
Hygromycin	50 mg/mL	in water	50 µg/mL
Chloramphenicol	75 mg/mL	in ethanol	75µg/mL
Rifampicin	20 mg/mL	in DMSO	100 µg/mL
Rifampicin	30 mg/mL	in DMSO	150 µg/mL

4.1.5. Bacteria

The following bacteria strains were used:

Escherichia coli:

DH5 α

F- supE44 Δ lacU169 (Φ 80, lacZ Δ M15) hsdR17 recA1 endA1 gyrA96 thi-1 relA1
for plasmid amplification

XL10-Blue

F- supE44, hsdR17, recA1, endA1, gyrA46, thi, relA1, lac, F'[proAB+, lacIq, lacZ Δ M15, Tn10(tetr)]
for plasmid amplification

Top10

F- mcrA Δ (mrr-hsdRMS-mcrBC) Φ 80lacZ Δ M15 Δ lacX74 deoR recA1 araD139 Δ (ara-leu)7697 galU galK rpsL (StrR) endA1 nupG
for plasmid amplification

DB3.1

F- gyrA462 endA1 (sr1-recA) mcrB mrr hsdS20(rB-, mB-) supE44 ara-14 galK2 lacY1 proA2 rpsL20(SmR) xyl-5 - leu mtl1
for amplification of plasmids containing the ccdB gene (GATEWAY-cloning)

Agrobacterium tumefaciens:

GV3101 (pMP90)

GV3101 containing the helper plasmid pSoup

SV 0 (super virulent strain for cell culture transformation) *LBA4404.pBBR1MCS virGN54D*

4.1.6. Plant lines

Wild type *Arabidopsis thaliana* plants were of the ecotypes Columbia-0 (Col-0) and Landsberg erecta (Ler). The following T-DNA insertion lines were all in Col-0 background and were obtained from the following sources:

SIGnAL (SALK Institute Genomic Analysis Laboratory, <http://signal.salk.edu>)

MPIZ (http://www.mpiz-koeln.mpg.de/GABI-Kat/GABI-Kat_homepage.html)

FLAG-collection from INRA (<http://www-ijpb.versailles.inra.fr>)

Syngenta (http://www.tmri.org/en/partnership/sail_collection.aspx)

Gene	At number	Line
SSADH	At1g79440	SALK_003223 Gabi-Kat 737E05 SAIL_1278 B12
GABA-T	At3g22200	Gabi-Kat 157D10 SALK_007661 SAIL_1230C03
GAD 1	At5g17330	SALK_017810 SALK_017931
GAD 2	At1g65960	SALK_028819 SALK_033689
GAD 3	At2g02000	SALK_033307
GAD 4	At2g02010	SALK_146398
GAD 5	At3g17760	FLAG_460F07 GABI_326C03
GHBDH-1	At3g25530	Gabi-Kat 316D05 SALK_057410
GHBDH-2	At1g17650	Gabi-Kat 933D03 SALK_047412

4.1.7. Software

Acrobat Reader Version 7.0	
Photoshop Version CS3	Adobe
EndNote Version 9.0	ISI ResearchSoft (USA)
Enhanced Chem Station G1701 CA Dec. 1999	Agilent (USA)
Microsoft Office 2000/2007	
Windows XP	Microsoft
WinNT Version 4.0	
Multi Experiment Viewer 4.2	TIGR
Mozilla Firefox 3.0	Mozilla Foundation
SeqMan II	DNA-Star Inc
Edit Seq	
Sigma Plot Version 10.0	SPSS
Vector NTI Advanced 10.0	Invitrogen

4.1.8. Used Equipment

Autoclave	Sanoklav L 11201	Wolf, Geislingen (D)
Balances	Sartorius FX-40 Sartorius 1264 MP Ohaus GT 4800	Sartorius, Leichlingen Ohaus, Florham Park (USA)
Centrifuges	Eppendorf 5417, 5417 R, 5417 C and 5402	Eppendorf, Hamburg
Clean Bench	Heraeus LaminAir HB 2448	Heraeus, Düsseldorf (D)
Climate Chambers	Percival Scientific CU-36L5 Percival Scientific AR-66L	CLF, Emersacher
Crimper/Decapper	5181-1213 (open) 710-0979 (close)	Agilent (USA)
Dewar		KGW Isotherm
Electroporator	Genepulser II	BioRad, München, D
Freezer	+4 °C, -20 °C -80 °C Hera freeze -80 °C Ultima II	Liebherr Heraeus Revco
GC/MS	Auto Sampler # 7683 Injector # 7683 GC # 6890N MS # 5973N Ionization Gauge Controller # 59864B Forline Pump	Agilent (USA)
Heater	Thermo mixer 5436 Thermostat 5320 HTM-130L	Edwards (Agilent) Eppendorf, Hamburg (D) HLC Bovenden (NL)
Magnetic Stirrer	Ikamag REO or. RET	IKA-Werke, Staufen (D)
NanoDrop	ND 1000	NanoDrop Technologies, Wilmington (USA)
Particle Gun	PDS-1000/He System Macrocarriers 900psi rupture disks Stopping screens 1µm gold microcarriers	BioRad, München, D
PCR Cycler	PTC 100 and PTC 200	MJ Research, distributed by Biozym, (Hess. Oldendorf, D Weilheim
pH-Meter	pH 521 WTW	Pharmacia, Freiburg
Photometer	Pharmacia LKB Novaspec II Pharmacia Ultraspec III	
Pipettes	pipetman Research	Gilson, Lewis Center (USA) Eppendorf, Hamburg (D)
Printer	HP Color Laserjet 3600 HP Laserjet 2300 HP Laserjet 4100	
Shaker	G25	Fa. New Brunswick Scientific GmbH, Nürtingen (D)

Spectrophotometer	SpectraFluor plus SIL	Tecan, Crailsheim
Speedvac	Vacuum Concentrator	Bachofer, Reutlingen (D)
Syringes	Microliter # 705 or. #710 5 or 10 μ L FN 23/42/HP	Hamilton, Bonaduz (CH) Agilent (USA)
TissueLyser		Qiagen, Hilden (D)
Ultrasonic bath	Sonorex-RK255H	Bandelin
Vortexer	Heidolph Reax 2000 Vortex Genie 1 or. 2	Heidolph, Hartenstein Bender & Hobein, Zürich (CH)
Water bath:	Type 1003	Firma GFL, Burgwedel (D)

4.1.9. Consumables

Autoclave tape		3M, Neuss (D)
Adhesive tape for Petri dishes		Servopor Eurofarm (I)
Falcon Tubes	15 mL & 50 mL	Corning Inc. (USA)
fluorescent lamps	Greenhouse: L58W/31-830, L58W/76	Osram
	Climate Chamber: F17T8/TL741 17W, Philips F23T8/TL741, TL70	
Cuvette		Müller Ratiolab, Dreieich (D)
Microtiter Plate		Greiner, Solingen (D)
Para film		Am. National Can, Nenasha (USA)
Pasteur pipettes		Brand, Wertheim (D)
PCR-tubes	8 ^{er} strips 96 ^{er} plates	4titude, (UK)
Petri dishes		Greiner, Solingen (D)
Pipette tips	10 μ L, 200 μ L, 1mL 10 μ L, 5mL	Sarstedt, Nümbrecht (D) Eppendorf, Hamburg (D)
Reaction tubes	1.5mL & 2mL	Sarstedt, Nümbrecht (D)
Scalpels		Braun, Melsungen (D)

Particle Gun

Macrocarriers	165-2335	BioRad (München)
900psi rupture disks	165-2328	
Stopping screens	165-2336	
1 μ m gold microcarriers	165-2263	

GC-MS

Ferule	Injector: 5181-3323 0.4mm ID Vespel, Graphite Interface: 5862-3508, 0.4mm; 200, 250µm	Agilent (USA)
Filament Assembly	50972-60053	Agilent (USA)
GC-Column	HP-50+ L 30m, ID 0.25mm, Film 0.25µm Temp. Limits: 40°C – 280°C	J&W Scientific (USA)
Liner	5183-4711 4 mm ID Split/Split less containing glass wool	Agilent (USA)
Oil	Diffusion Pump: Santovac 5P Ultra Foreline pump: Rough pump oil	Agilent (USA) Edwards (USA)
O-Rings	5180-4182	Agilent (USA)
Septum	5181-3383 1mm prt.	Agilent (USA)
Sample Handling (GC-MS)	Crimp cap and vials Micro inlets G 30/5mm. Screw cap G8 Vial G1 clear	CS-Chromatographie Service GmbH, Langerwehe (D)

4.2. Methods

4.2.1. Work with *Arabidopsis thaliana*

4.2.1.1. Growth conditions

4.2.1.1.1. Greenhouse

Arabidopsis seeds were sown in 9cm plastic pots on a substrate mixture containing three parts soil and one part Vermiculit For vernalization, the pots were kept for a minimum of 48 hours at 4°C in the dark, and then the pots were transferred to the greenhouse for germination. Approximately 2 weeks after germination, the plants were pricked out. In the greenhouse, plants were grown under long day conditions with a light/dark rhythm of 16:8 hours, a temperature of 21°/18°C and a relative humidity of approximately 40%.

4.2.1.1.2. Climate chamber

Arabidopsis thaliana plants were grown on culture plates in a climate chamber (Percival Scientific, Model CU-36L5 or AR-66L_S) with a humidity of 50% and a temperature of 22°C during light period and 18°C during dark period respectively. For growth under long day conditions, the plants were subjected to a day/night rhythm of 16:8 hours, for short day conditions of 8:16 hours.

4.2.1.2. Screening of T-DNA Insertion lines

The genotype of T-DNA insertion lines was determined using PCR-based methods. Therefore, genomic DNA of single plants was isolated and used as template for PCR with two gene specific primers or one gene specific primer and one primer complementary to the flanking sequence of the T-DNA in separate reactions (primer sequences are listed in 6.4.1). Homozygous plants were kept for further analyses.

4.2.1.3. Crossing of *Arabidopsis thaliana* plants

For crossing to other lines, homozygous plants of about 6 weeks age were used with exception of *ssadh* plants, where heterozygous plants were used due to the reduced growth of homozygous plants.

All open flowers and developed siliques were removed from the plants to be pollinated and of the remaining flower buds the three largest buds were opened carefully under the binocular and all organs except the carpels were removed. Stamens of the plants donating pollen were isolated and pollen was transferred onto the carpel of the other line. The flowers used for crossing were labeled, harvested when ripened and were sown on soil. F₁ plants were screened for occurrence of the respective T-DNA inserts in heterozygous state, these were allowed to set seeds, and in the F₂ generation, the offspring was screened in PCR reactions for double homozygous plants.

4.2.1.4. Map-based cloning in *Arabidopsis thaliana*

Sequencing the genome of *Arabidopsis thaliana* ecotypes revealed variations among them: single nucleotide exchanges, a different number of simple sequence repeats or insertions and deletions. For the ecotypes Columbia (Col-0) and Landsberg erecta (Ler), several types of markers have been published [17, 46, 65, 99, 145]. Markers are available via TAIR (<http://www.arabidopsis.org/> > search > markers) or can be designed using Marker Tracker (<http://www.bar.utoronto.ca/markertracker/>). To actually map a single trait to a genomic locus, ssadh suppressor lines were crossed with Ler wild type plants. In the F2 generation, plants without ssadh phenotype were screened for homozygous occurrence of the T-DNA insertion in the ssadh gene. These plants also carry the EMS mutation in homozygous state; otherwise, the plants would display the reduced growth of ssadh plants. The identified double homozygous plants constitute the mapping population.

Since the mapping population was selected was selected for homozygosity of both mutations and both are in Col-0 background, a higher percentage of Col-0 specific fragments will be obtained near the mutations. All distant markers will be equally distributed between Col-0 and Ler specific fragment.

4.2.1.5. GUS Staining

Plants to be tested for promoter activity were vacuum-infiltrated with GUS Staining solution, until plants are completely submerged in the solution and the leaves are slightly translucent. Then, the plants are incubated at 37°C until staining was visible. To enhance visibility of the GUS signal, chlorophyll was extracted by incubating the plants in 80% ethanol at 65°C.

GUS Staining Working Solution	0.1M	NaPO4 pH7
	10mM	EDTA
	0.5mM	K-Ferricyanid
	0.5mM	K-Ferrocyanid
	1mM	X-Gluc
	0,1%	Triton X-100

4.2.1.6. Growth of *Arabidopsis* plants on sterile media

4.2.1.6.1. Surface sterilization of *Arabidopsis* seeds

For growth of *Arabidopsis* plants on sterile media, the seeds were surface sterilized before sowing on plates.

About 100 seeds per line were placed in 1.5mL reaction tubes, which were then placed open in an exsiccator containing a beaker with 100ml sodium hypochlorite. 3mL HCl_{conc.} was added and the lid of the exsiccator was kept closed or approximately 4 hours. Then, the tubes were closed and transferred to the sterile hood, where they were kept open for one hour to allow remaining chlorine gas to evaporate.

4.2.1.6.2. Preparation of MS plates

For plant growth under controlled nutrient conditions *in vitro*, half strength MS media was used, prepared from several stock solutions.

<u>MS Macro I:</u>	21.06mM	NH ₄ NO ₃
	18.8mM	KNO ₃
	1.5mM	MgSO ₄ * 7 H ₂ O
	1.249mM	KH ₂ PO ₄
<u>MS Macro II</u>	2.979mM	CaCl ₂ *2H ₂ O
<u>FeNaEDTA</u>	100μM	FeNaEDTA
<u>MS Micros</u>	100.2μM	H ₃ BO ₃
	70.4μM	MnSO ₄ *H ₂ O
	29.9μM	ZnSO ₄ *7H ₂ O
	1.033μM	Na ₂ MoO ₄ *2H ₂ O
	0.1μM	CuSO ₄ *5H ₂ O
	0.154μM	CoCl ₂
<u>Vitamins (modified MS):</u>	100mg/L	Myo-Inositol
	0.5mg/L	Nicotinic acid
	0.5mg/L	Pyridoxine-HCl
	1.0mg/L	Thiamine-HCl
	2mg/L	Glycine
	0.5g/L	MES
	29.2mM	Sucrose (facultative)

Vitamins were obtained from Duchefa, to prepare the stock solution; 1.038g was dissolved in 10mL H₂O_{bd}.

MS Macro I and II were prepared as 10x stock solution, FeNaEDTA as 100x stock solutions and Vitamins and MS Micros as 1000x stock solution.

For growth experiments with different nitrogen / GABA concentrations, MS Macro I was prepared without NH₄NO₃ and KNO₃. GABA and organic nitrogen (NH₄NO₃ and KNO₃ in the molar ratio of the standard medium) were added to the media from stock solutions. The pH of the solution was set to 5.7 with 1M KOH, for preparation of plates, 0.8_(w/v) Gelrite (Duchefa) was added. The media were autoclaved, and poured in square culture plates (Greiner).

4.2.1.6.3. Sowing of Arabidopsis seeds on sterile media

Surface sterilized (4.2.1.6.1) Arabidopsis seeds were used for growth on sterile MS media. Therefore, dry seeds were spread on autoclaved paper and transferred onto the plates using a sterile toothpick. The seeds were vernalized for 48 hours at 4°C in the dark, and then the plates were transferred in a climate chamber. All plates were sealed using gas permeable adhesive tape.

4.2.1.7. Fluorescence Microscopy

Protein localizations were assayed using the fluorescent proteins GFP of the RFP-derivative mCherry [123]. The optimal excitation and emission wavelengths were 488nm/507nm for GFP and 587nm/610nm for mCherry.

Transformed Arabidopsis cells were pelleted by short centrifugation (5min, 1000rpm) and then spread on a microscope slide, in the case of leek, epidermal peels were prepared and used for microscopy.

4.2.1.8. Arabidopsis thaliana cell culture

4.2.1.8.1. Maintenance of Cell Culture

Arabidopsis thaliana cells were grown in suspension culture in the dark at 18 to 22°C while shaking at about 1560rpm. Once a week, cells were diluted 1:4 with fresh, room temperature media

Approximately every 4 weeks, the cell culture was screened for bacterial contamination and backup plates were prepared. In case of visible bacterial contamination, the diluted cultures were treated with Ticarzidin, before using cells for transformation, they should be diluted twice. For backup plates, 50mL cell culture was centrifuged (15min, 500rpm), the supernatant discarded, the pellet resuspended in some media and spread on plates.

4.3g	Duchefa MS basal salt mixture (M 0221)
4mL	B5 vitamins
400mg	Myo-Inositol
30g	Sucrose
ad 1L	H ₂ O

The pH was set to 5.8 with KOH; for plates, 0.8% Gelrite was added, 0.5mL 2mg/mL 2,4D was added after autoclaving.

4.2.1.8.2. Cell Culture Transformation

For cell culture transformation, *Agrobacterium tumefaciens* strain SV-0 carrying the binary vector and colonies of the antisilencing strain RK19 were picked from fresh plates and were grown for 24h at 28°C in 5mL cultures in YEB containing the appropriate antibiotics (20µg/mL Rifampicin, 75µg/mol Chloramphenicol, 50µg/mL Kanamycin for selection of the binary plasmid). The cells were pelleted by centrifugation (15min, 4000rpm) and resuspended in 1mL Arabidopsis cell culture media.

For coculture, freshly diluted Arabidopsis suspension culture were mixed 50:1 with the different *Agrobacterium* strains, grown for 3 to 5 days in the dark at 25°C, and then screened for expression of the transgene.

4.2.1.9. Biolistic transformation

4.2.1.9.1. Preparation of Microcarriers

For the preparation of the microcarriers, 30mg of 1 μ m gold particles were weighed into a microcentrifuge tube. 1mL 70% EtOH was added, the suspension was vortexed vigorously and then soaked for 15min in 70% EtOH. The gold particles were pelleted by 15 sec centrifugation at 13000rpm and the supernatant was discarded. Then, 1mL H₂O_{dest} was added, the suspension was vortexed and the gold particles pelleted by 10 sec centrifugation at 10000rpm. The supernatant was removed and the washing step was repeated once. Finally, the gold particles were resuspended in 1mL H₂O_{dest} and sonicated for 3sec.

This suspension was divided into 50 μ L aliquots while vortexing and were stored at -80°C.

4.2.1.9.2. DNA Coating of Microcarriers

For each shot, 5 μ L gold suspension (4.2.1.9.1) with a concentration of 30mg/mL was used. To the gold suspension 300ng of each DNA, 10mL 2.5M CaCl₂ and 4 μ L 0.1M spermidine (free base) were added while vortexing. The volume was set to a final volume of 25 μ L with water and the tubes were closed and vortexed for 5 to 10min, during this time, the gold particles were coated with DNA. Then, the gold particles were pelleted by 5sec centrifugation at 10000rpm and the supernatant was discarded. The particles were washed twice, first with 50 μ L 70% EtOH, then with 20 μ L 100% EtOH. Finally the particles were resuspended in 12 μ L 100% EtOH by vortexing. To deagglomerate the particles, the suspension was sonicated for 3sec and the suspension was stored on ice until use.

4.2.1.9.3. Bombardement

For bombardment, the macrocarriers were placed into the macrocarrier holders. 10 μ L of the coated microcarriers were pipetted onto a macrocarrier and spreaded equally. The macrocarriers were dried in vacuum, leaving a dry monolayer of microcarriers.

The conditions for bombardment were: 900psi rupture disk, vacuum 26mm Hg and the sample tray carrying a petri dish with leek epidermis on the third level from the bottom.

Subsequent to the bombardment, the samples were kept in a dark, humid environment at room temperature over night and were analyzed by fluorescence microscopy the following day.

4.2.2. Microbiology

4.2.2.1. Work with *E. coli*

4.2.2.1.1. Media

LB	10g	Trypton
	5g	Yeast Extract
	10g	NaCl
	ad 1L	H ₂ O _{bd}
2YT	16g	Trypton
	10g	Yeast Extract
	5g	NaCl
	ad 1L	H ₂ O _{bd}
SOC	20g	Trypton
	5g	Yeast Extract
	0.585g	NaCl
	0.186g	KCl
	0.953g	MgCl ₂
	1.2g	MgSO ₄ * 7H ₂ O
	36g	Glucose
	ad 1L	H ₂ O _{bd}

For preparation of agar plates, 1.5 %_(w/v) bacto agar was added.

The media were autoclaved and the required antibiotics were added after cooling of the media to about 40°C.

1.1.1.1.1. Growth of *E. coli*

Cells were grown either on agar plates in a 37°C incubator or as liquid cultures in a Shaker.

For liquid cultures, single colonies were picked from LB plates with a sterile toothpick, inoculated in 3mL media and grown over night at 37°C while shaking with 200-250rpm.

For growth of transgenic bacteria, the corresponding antibiotics were added for selection. Bacteria could be kept for several weeks at 4°C on YEB plates or at -80°C as glycerol culture (500µL culture and 500µL 65% Glycerol, 100mM MgSO₄, 25mM Tris-HCl, pH 8.0).

4.2.2.1.2. Preparation of competent cells (*E. coli*)

A 5mL culture was inoculated with a single *E.coli* culture and incubated over night in a 37°C shaker. The next day, 1mL of the overnight culture was used to inoculate a 100mL culture which was grown until an OD₅₅₀ of 0.48 was reached.

The culture was transferred into precooled 50ml tubes, then incubated on ice for 15min and finally the cells were spun down (2000 rpm at 4°C for 10min). All further steps were performed at 4°C. The supernatant was removed; the pellet was resuspended in 15mL TfB1 and incubated on ice for 2 hours. Then, the cells were centrifuged again (2000 rpm at 4°C for 10min) and the supernatant was removed. The cells were resuspended in 4mL TfB2 and transferred in 100µL aliquots into precooled 1.5mL tubes and immediately frozen in liquid nitrogen. The cells were then stored at -80°C until transformation.

To test for transformation efficiency, one aliquot of competent cells was transformed with 10pg PUC19 DNA and the number of grown colonies was determined on the next day.

TfB1	100mM	RbCl ₂
	50mM	MnCl ₂ *4 H ₂ O
	30mM	KAc
	10mM	CaCl ₂
	15% _(v/v)	Glycerin

The pH was adjusted to 7.0 and the media was filter sterilized.

TfB2	10mM	RbCl ₂
	75mM	CaCl ₂
	10mM	MOPS
	15% _(v/v)	Glycerin

The pH was adjusted to 7.0 and the media was filter sterilized.

4.2.2.1.3. *E. coli* transformation

Competent cells were thawed on ice, mixed with plasmid DNA, and incubated on ice for 15min. The cells were then transformed by heat shock (45 to 60 seconds at 42°C). After addition of 1mL SOC, the cells were incubated at 37°C for about 1 hour, and then the cells were plated in different concentrations on selective media and kept at 37°C over night.

4.2.2.2. Work with *Agrobacterium tumefaciens*

4.2.2.2.1. Media

YEB	5g	Bacto Peptone
	5g	Beef Extract
	1g	Yeast Extract
	5g	Sucrose
	0.5g	MgSO ₄ * 7 H ₂ O
	ad 1L	H ₂ O _{bd}
MGL	5g	Bacto Tryptone
	2.5g	Yeast Extract
	5g	NaCl
	5g	Mannitol
	1.16	Na glutamate
	0.25g	KH ₂ PO ₄
	0.1g	MgSO ₄ * 7 H ₂ O
	1mg	Biotin
ad 1L	H ₂ O _{bd}	

The media were autoclaved and the required antibiotics were added after cooling of the media to about 40°C.

4.2.2.2.2. Growth of *Agrobacterium tumefaciens*

For liquid cultures, single colonies were picked from YEB plates with an inoculation loop, inoculated in 3mL media and grown for one to two days at 28°C while shaking with 200-250rpm.

For growth of transgenic bacteria, the corresponding antibiotics were added for selection. Bacteria could be kept for several weeks at 4°C on plates or at -80°C as glycerol culture (500µL culture and 500µL 65% Glycerol, 100mM MgSO₄, 25mM Tris / HCl, pH 8.0).

4.2.2.2.3. Preparation of competent cells (*Agrobacterium tumefaciens*)

A 5mL MGL preculture was inoculated with *Agrobacterium tumefaciens* and grown over night, then the culture was diluted in 100mL MGL and grown until a density of OD600 of about 0.5 was reached. The culture was centrifuged (5min at 4°C and 5000rpm) and the cells were resuspended in 40mL cold buffer (1mM HEPES pH 7.0) followed by another centrifugation step (5min at 4°C and 5000rpm). Then, the cells were washed in 2mL cold buffer (1mM HEPES pH 7.0 containing 10%_(v/v) glycerol) and finally resuspended in 200µL 1mM HEPES pH 7.0 containing 10%_(v/v) glycerol. 50µL aliquots were frozen directly in liquid nitrogen and stored at -80°C.

4.2.2.2.4. Transformation of Agrobacteria

4.2.2.2.4.1. Electroporation

Competent cells were thawed on ice, mixed with about 200ng plasmid DNA, and kept on ice for 2min. Then, the cells were transferred into precooled 0.2cm cuvettes. The electroporation conditions were 25 μ F, 400 Ω , 2.5 kV pulse with a retention time of 8-9msec. Following electroporation, 1mL room temperature YEB containing the antibiotics used for selection was added and the culture was incubated at 28°C whilst shaking with 100-150rpm.

The cells were plated in different concentrations on antibiotics containing YEB plates and were grown at 28°C for two days.

4.2.2.2.4.2. Freeze-Thaw Method

Competent cells were thawed on ice, mixed with about 200ng plasmid DNA, and incubated on ice for 5min, followed by 5min frozen in liquid nitrogen and 5min at 37°C. Then, 1mL YEB containing antibiotics was added and the cells were incubated at 28°C for about 2 hours, then the cells were plated in different concentrations on selective media and kept at 28°C for about 2 days.

4.2.3. Molecular biology techniques

4.2.3.1. Plasmid Preparation

4.2.3.1.1. Mini Preparation

Plasmid DNA from E.coli in Miniprep scale was isolated using the QuantumPrep Kit (BIORAD) following the manufacturer's protocols. A part of the overnight culture could be used for storage as glycerol stock cultures at -80°C.

4.2.3.1.2. Midi Preparation

Plasmid DNA from E.coli in Midiprep scale was isolated using the CompactPrep Plasmid Midi Kit (QIAGEN) following the manufacturer's protocols. A part of the overnight culture could be used for storage as glycerol stock cultures at -80°C.

4.2.3.2. Preparation of *Arabidopsis thaliana* genomic DNA

4.2.3.2.1. Fast Prep – Method a

Plants used for identification of the mapping population were screened by PCR, using genomic DNA isolated from single plants. One leaf from each seedling was harvested into a tube from an 8-tube strip. Then, 300µL extraction buffer and a 5mm stainless steel bead were added. The strips were inserted into the adapters of the tissue lyser and shaken at 30Hz for 90sec. The solution could be stored at -20°C until further use or 1µL was used as template for a 25µL PCR reaction.

Extraction Buffer	50mM	Tris HCl pH 7.2
	300mM	NaCl
	10%	sucrose

The buffer was autoclaved and stored in aliquots.

4.2.3.2.2. Fast Prep – Method b

One leaf from each plant was harvested into a 2mL tube, frozen in liquid nitrogen, and stored at -80°C until preparation. The tissue was pulverized with 400µL extraction buffer. Cell debris was removed by centrifugation and the supernatant was transferred into a new 1.5mL tube. The DNA was precipitated with Isopropanol, pelleted by centrifugation and the supernatant was discarded. The resulting pellet was dried and resuspended in 50-100µL H₂O_{bd} and could be stored at -20°C.

Extraction Buffer	200mM	Tris HCl pH 7.5
	250mM	NaCl
	25mM	EDTA
	0.5%	SDS

4.2.3.2.3. Standard Preparation

For isolation of genomic DNA with a higher purity, tissue (usually flowers and buds) from single plants was harvested into reaction tubes, frozen in liquid nitrogen, and stored at -80°C until preparation.

Samples were pulverized and taken up in $500\mu\text{L}$ extraction buffer. Then, $400\mu\text{L}$ PCI (phenol, chloroform, and isoamyl alcohol in a ratio of 25:24:1) was added and the samples were mixed. The samples were centrifuged for 15min at 3500rpm to remove proteins and plant material from the aqueous phase, which was transferred into a new tube. Following addition of $300\mu\text{L}$ Isopropanol, the samples were incubated at room temperature for 10min, and then DNA was pelleted by centrifugation (20min, 3500rpm). The pellet was washed twice with 70% ethanol, dried, and resuspended in $50\mu\text{L}$ RNase containing water (1:100 RNase dilution).

2x Buffer	0.6M	NaCl
	100mM	Tris HCl pH 7.5
	40mM	EDTA
	4% _(w/v)	Sarkosyl
	1% _(w/v)	SDS
Extraction Buffer	25mL	2x Buffer
	20mL	12M Urea
	2.5mL	Phenol
	2.5mL	H ₂ O

4.2.3.3. Expression Analysis

4.2.3.3.1. RNA-Isolation

For RNA isolation, about 100mg plant tissue was harvested into 1.5mL tubes and directly frozen in liquid nitrogen. The samples were homogenized with 1mL TRIsure reagent and incubated at room temperature for 5min. Then, $200\mu\text{L}$ chloroform was added to the samples, which were kept at room temperature for 2min and then centrifuged at 4°C for 10min at 14000rpm. The supernatant was transferred into a new tube, mixed with $500\mu\text{L}$ Isopropanol, incubated at room temperature for 10min. The RNA was precipitated by centrifugation (4°C , 5min, 7500rpm), washed with 75% ethanol and air dried, then the RNA pellet was resuspended in DEPC-H₂O and the concentration was determined photometrical (4.2.3.4).

4.2.3.3.2. DNase digestion

To avoid false-positive results when testing the expression level of a gene, genomic DNA was removed by DNase digestion prior to cDNA synthesis.

The reaction mix contained $2.5\mu\text{g}$ total RNA, $4\mu\text{L}$ RT-buffer and $1\mu\text{L}$ DNase I (10U) in a total volume of $20\mu\text{L}$. The samples were incubated at 37°C for 20 to 30min. For DNase inactivation, $2\mu\text{L}$ 25mM EDTA was added and the samples were heated to 65°C for 10min.

4.2.3.3.3. Reverse Transcription

For cDNA synthesis, 11µL DNase digestion and 1µL oligo-dT primer were incubated for 5min at 70°C and were then transferred directly into ice. Then, 1µL 10mM dNTP's, 4µL 5xRT-buffer, 2.75µL DEPC-H₂O and 0.25µL BioScript Reverse Transcriptase were added. cDNA synthesis took place at 37°C for about 1hour, then the enzyme was deactivated by heating to 70°C for 10min.

4.2.3.4. Photometric determination of nucleic acid concentrations

To determine the concentration of isolated nucleic acids (4.2.3.2.3 and 4.2.3.3.1), 1µL sample was used for photometric measurement using a nanodrop machine. The concentration of the sample was calculated from the absorption at a wavelength of 260nm.

4.2.3.5. PCR

The PCR is a method to amplify a DNA fragment using complementary oligonucleotides (primers), and a thermo stable DNA polymerase. The annealing temperature is dependent on the primer sequence, the elongation time and temperature on the fragment length and the used polymerase.

<u>Step</u>	<u>Temperature</u>	<u>Time</u>
Denaturing	95°C	5min
Denaturing	95°C	0:30min
Annealing	Primer dependent	0:30min
Elongation	72°C (68°C for <i>Pfx</i>)	1min/kb (2min/kb for <i>Pfu</i>)
Elongation	72°C (68°C for <i>Pfx</i>)	5:00min
	16°C	endless

Commercially available polymerases were used with the buffer supplemented, for the homemade *Taq*; the following final concentrations were applied:

67mM	Tris HCl, pH 8.8
16mM	(NH ₄) ₂ SO ₄
0.1%	Tween
1.5mM	MgCl ₂
0.2mM	dNTP's (each nucleotide)
0.2mM	Primer 1
0.2mM	Primer 2

4.2.3.6. Gel electrophoresis

DNA fragments of different size were separated using agarose gel electrophoresis and visualized by ethidium bromide staining under UV-light (254nm wavelength). Agarose concentration was chosen dependent on the fragment size, smaller fragments were separated using high percentage gels (3-5% agarose in TBE), larger fragments in low percentage gels (0.8-2.5% agarose in TAE).

Agarose was boiled in the corresponding buffer in a microwave and ethidium bromide was added before pouring the gel.

For electrophoresis, size marker (1kb ladder, Invitrogen or 20bp ladder, MBI) and samples mixed with loading dye were pipetted into the gel slots and the gel was run at an amperage of approximately 150mA, corresponding to a voltage between 80 and 130V, dependent on size and percentage of the gel.

50x TAE	2M 1M 50mM	Tris/ Acetic Acid, pH 7.5 Sodium acetate EDTA	
10x TBE	0.89M 0.89M 20mM	Tris/NaOH, pH 8.3 Boric Acid EDTA	
Ethidium bromide	0.5% _(w/v)	Ethidium bromide in methanol	
6x Loading Dye	10mM 60mM 60%	Tris-HCl (pH 7.6) EDTA Glycerol	
Plus one or two of the following dyes	0.15% 0.03% 0.03% 0.03%	Orange G Bromophenol blue Cresol Red Xylene cyanol FF	migrates in 1% gel at: 50-100bp 200-300bp ~3000bp ~4000bp

4.2.3.7. Gateway-Cloning

GATEWAY[®]-Cloning uses the site-specific recombination activity of bacteriophage λ for all steps during cloning.

The sequence of interest is amplified with either gene specific primers containing an *attB1* site 5' of the forward primer and an *attB2* site 5' of the reverse primer or primers containing a 5' CACC-sequence in the forward primer and the unmodified reverse primer. The PCR fragments are then recombined using BP-Clonase into a pDONR vector or via TOPO-Cloning into pENTR/D-TOPO[™]. Positive clones of the *Entry Vectors* are then used for LR-recombination into the selected *Destination Vectors*.

For the TOPO-Cloning, 0.2 μ L Salt Solution, 0.2 μ L TOPO-pENTR[™], 0.1 μ L PCR fragment and 0.7 μ L sterile water were mixed, incubated at room temperature for approximately 30min and then transformed into *E.coli*.

BP reactions were set up as following: 10ng-50ng PCR product, 50ng Entry Vector, 1µl 5xBP-Reaction Buffer and 1µL BP-Clonase and filled up with sterile water to 5µL. LR reactions were set up as following: 10ng-50ng Entry Clone, 50ng Destination Vector, 1µl 5x LR-Reaction Buffer and 1µL LR-Clonase and filled up with sterile water to 5µL. The reaction were incubated at room temperature over night, stopped by addition of 1µL Proteinase K, and then transformed into *E.coli*.

4.2.3.8. Restriction Digestion of Nucleic Acids

Restriction endonucleases recognize stretches of 4 or more nucleotides in a palindrome sequence and introduce double strand breaks specifically at these sites.

A reaction contained DNA, one or several restriction endonucleases, the corresponding reaction buffer, and sterile water in a volume of 10µL to 50µL. The reaction temperature was dependent on the optimal reaction temperature of the enzyme; the reaction time was between 2 hours and 16 hours.

4.2.3.9. Precipitation of Nucleic acids

Nucleic acid can be precipitated from an aqueous solution by addition of alcohol and salts by reducing solubility in water. Therefore, a DNA containing solution was mixed with 2.5 volume 100% ethanol and 0.1volume 3M Sodium acetate pH 5.2. DNA was pelleted by centrifugation (14 000rpm for 30min), washed with 500µL 75% ethanol and air-dried. The dry pellet was dissolved in 25µL H₂O_{bd} and the concentration was determined (4.2.3.4).

4.2.3.10. Sequencing

Sequence reactions were performed using the chain termination method [146, 147], using the Big Dye® Terminator Cycle Sequencing Kit Version 3.1 (Applied Biosystems).

A sequencing reaction contained 100ng to 150ng plasmid DNA or 0.5ng to 25ng PCR product as template, one primer with a final concentration of 1mM and 2µL Big Dye v3.1 in a total volume of 10µL. This mix was filled up with HPLC-H₂O to 20µL after the sequence reaction.

The PCR program used for sequencing consists of the following steps:

Sequence runs were performed at the Institute for Genetics of the University of Cologne and the data was available via network.

<u>Step</u>	<u>Temperature</u>	<u>Time</u>
Denaturing	96°C	0:20min
Denaturing	96°C	0:10min
Annealing	50°C	0:05min
Elongation	60°C	4:00min
Elongation	60°C	5:00min
	16°C	endless

4.2.4. Metabolite Analysis

4.2.4.1. GC-MS measurements

4.2.4.1.1. Extraction

60 to 100mg plant tissue per sample was harvested in 2mL tubes and frozen immediately in liquid nitrogen. For metabolite extraction, the tissue was pulverized and mixed with 300 μ L cold methanol and 30 μ L Ribitol (0,3mg/mL in methanol). Samples were stored on ice during extraction followed by incubation at 70°C for 15min. 200 μ L chloroform was added, then mixed and incubated for 5min at 37°C. Finally 400 μ L HPLC water was added, mixed and centrifugation for 5min at 14.000rpm.

For each aliquot, 160 μ L of the upper polar phase was removed and transferred into 1.5mL glass flasks and vacuum dried in a speed vac for about 90min without heating. Samples could then be stored at -20°C until derivatisation.

4.2.4.1.2. Derivatisation

Derivatisation took place in two steps: first, samples were suspended in 40 μ L Methoxyamine hydrochloride (20mg/mL in pyridine) and kept at 30°C for 90min, then 70 μ L MSTFA was added and samples were incubated at 37°C for 30min. Then, the derivatized extracts were transferred in glass flasks with micro inserts and analyzed.

4.2.4.1.3. Measurement

Measurements were performed using a GS-MS system from Agilent Technologies. As carrier gas, He 5.0 was used. 2 μ L derivatized sample were injected split less onto the column. A run consisted of the following steps: first, the oven temperature was kept at 70°C for 5min, then the temperature was increased with a ramp of 5°C/min up to 280°C, kept there for 7min and finally, the oven was cooled to 70°C and kept there for 5min before injecting the next sample. During the whole runtime, the inlet was kept on 250°C, the mass spectrometer at 280°C.

5. References

1. Abel, S. and Theologis, A., *Early genes and auxin action*. . Plant Physiol, 1996. **111**:9-17.
2. Akama, K., Akihiro, T., Kitagawa, M., and Takaiwa, F., *Rice (Oryza sativa) contains a novel isoform of glutamate decarboxylase that lacks an authentic calmodulin-binding domain at the C-terminus*. Biochim Biophys Acta, 2001. **1522**:143-50.
3. Akama, K. and Takaiwa, F., *C-terminal extension of rice glutamate decarboxylase (OsGAD2) functions as an autoinhibitory domain and overexpression of a truncated mutant results in the accumulation of extremely high levels of GABA in plant cells*. J Exp Bot, 2007. **58**:2699-707.
4. Allan, W.L. and Shelp, B.J., *Fluctuations of g-aminobutyrate, g-hydroxybutyrate, and related amino acids in Arabidopsis leaves as a function of the light-dark cycle, leaf age, and N stress*. Can. J. Bot., 2006. **84**:1339-1346.
5. Allan, W.L., Simpson, J.P., Clark, S.M., and Shelp, B.J., *Gamma-hydroxybutyrate accumulation in Arabidopsis and tobacco plants is a general response to abiotic stress: putative regulation by redox balance and glyoxylate reductase isoforms*. J Exp Bot, 2008. **59**:2555-64.
6. Andre, B., Talibi, D., Soussi Boudekou, S., Hein, C., Vissers, S., and Coornaert, D., *Two mutually exclusive regulatory systems inhibit UASGATA, a cluster of 5'-GAT(A/T)A-3' upstream from the UGA4 gene of Saccharomyces cerevisiae*. Nucleic Acids Res, 1995. **23**:558-64.
7. Ansari, M.I., Lee, R.-H., and Chen, S.-C.G., *A novel senescence-associated gene encoding g-aminobutyric acid (GABA):pyruvate transaminase in upregulated during rice leaf senescence*. Physiologia Plantarum, 2005. **123**:1-8.
8. Arazi, T., Baum, G., Snedden, W.A., Shelp, B.J., and Fromm, H., *Molecular and biochemical analysis of calmodulin interactions with the calmodulin-binding domain of plant glutamate decarboxylase*. Plant Physiol, 1995. **108**:551-61.
9. Atta, R., Laurens, L., Boucheron-Dubuisson, E., Guivarc'h, A., Carnero, E., Giraudat-Pautot, V., Rech, P., and Chriqui, D., *Pluripotency of Arabidopsis xylem pericycle underlies shoot regeneration from root and hypocotyl explants grown in vitro*. The Plant Journal, 2008. **9999**.
10. Badescu, G.O. and Napier, R.M., *Receptors for auxin: will it all end in TIRs?* Trends Plant Sci, 2006. **11**:217-23.
11. Bainbridge, K., Guyomarc'h, S., Bayer, E., Swarup, R., Bennett, M., Mandel, T., and Kuhlemeier, C., *Auxin influx carriers stabilize phyllotactic patterning*. Genes Dev., 2008. **22**:810-823.
12. Bandyopadhyay, A., Blakeslee, J.J., Lee, O.R., Mravec, J., Sauer, M., Titapiwatanakun, B., Makam, S.N., Bouchard, R., Geisler, M., Martinoia, E., Friml, J., Peer, W.A., and Murphy, A.S., *Interactions of PIN and PGP auxin transport mechanisms*. Biochemical Society Transactions, 2007. **035**:137-141.
13. Bartel, B. and Fink, G., *Differential regulation of an auxin-producing nitrilase gene family in Arabidopsis thaliana*. . Proceedings of the National Academy of Sciences, 1994. **91**.
14. Bauer, W.D. and Mathesius, U., *Plant responses to bacterial quorum sensing signals*. Current Opinion in Plant Biology, 2004. **7**:429-433.

15. Baum, G., Chen, Y., Arazi, T., Takatsuji, H., and Fromm, H., *A plant glutamate decarboxylase containing a calmodulin binding domain. Cloning, sequence, and functional analysis.* J Biol Chem, 1993. **268**:19610-7.
16. Baum, G., Lev-Yadun, S., Fridmann, Y., Arazi, T., Katsnelson, H., Zik, M., and Fromm, H., *Calmodulin binding to glutamate decarboxylase is required for regulation of glutamate and GABA metabolism and normal development in plants.* Embo J, 1996. **15**:2988-96.
17. Bell, C.J. and Ecker, J.R., *Assignment of 30 microsatellite loci to the linkage map of Arabidopsis.* Genomics, 1994. **19**:137-44.
18. Benjamins, R., Quint, A., Weijers, D., Hooykaas, P., and Offringa, R., *The PINOID protein kinase regulates organ development in Arabidopsis by enhancing polar auxin transport.* Development, 2001. **128**:4057-4067.
19. Bennett, M., Marchant, A., Green, H., May, S., Ward, S., Millner, P., Walker, A., Schultz, B., and Feldmann, K., *Arabidopsis AUX1 gene: a permease-like regulator of root gravitropism.* Science, 1996. **273**:948-950.
20. Bermudez Moretti, M., Correa Garcia, S., Ramos, E.H., and Batlle, A., *GABA uptake in a Saccharomyces cerevisiae strain.* Cell Mol Biol (Noisy-le-grand), 1995. **41**:843-9.
21. Bermudez Moretti, M., Perullini, A.M., Batlle, A., and Correa Garcia, S., *Expression of the UGA4 gene encoding the delta-aminolevulinic and gamma-aminobutyric acids permease in Saccharomyces cerevisiae is controlled by amino acid-sensing systems.* Arch Microbiol, 2005. **184**:137-40.
22. Beuve, N., Rispaill, N., Lainé, P., Clquet, J.-B., Ourry, A., and Le Deunff, E., *Puative role of γ -aminobutyric acid (GABA) as a long distance signal in up-regulation of nitrate uptake in Brassica napus.* Plant, Cell and Environment, 2004. **27**:1035-1046.
23. Biswas, K.K., Ooura, C., Higuchi, K., Miyazaki, Y., Van Nguyen, V., Rahman, A., Uchimiya, H., Kiyosue, T., Koshiba, T., Tanaka, A., Narumi, I., and Oono, Y., *Genetic Characterization of Mutants Resistant to the Antiauxin p-Chlorophenoxyisobutyric Acid Reveals That AAR3, a Gene Encoding a DCN1-Like Protein, Regulates Responses to the Synthetic Auxin 2,4-Dichlorophenoxyacetic Acid in Arabidopsis Roots.* Plant Physiol., 2007. **145**:773-785.
24. Bormann, J., *The 'ABC' of GABA receptors.* Trends Pharmacol Sci, 2000. **21**:16-9.
25. Bosma, P.T., Blazquez, M., Collins, M.A., Bishop, J.D., Drouin, G., Priede, I.G., Docherty, K., and Trudeau, V.L., *Multiplicity of glutamic acid decarboxylases (GAD) in vertebrates: molecular phylogeny and evidence for a new GAD paralog.* Mol Biol Evol, 1999. **16**:397-404.
26. Bouche, N., Fait, A., Bouchez, D., Moller, S.G., and Fromm, H., *Mitochondrial succinic-semialdehyde dehydrogenase of the gamma-aminobutyrate shunt is required to restrict levels of reactive oxygen intermediates in plants.* Proc Natl Acad Sci U S A, 2003. **100**:6843-8.
27. Bouche, N., Fait, A., Zik, M., and Fromm, H., *The root-specific glutamate decarboxylase (GAD1) is essential for sustaining GABA levels in Arabidopsis.* Plant Mol Biol, 2004. **55**:315-25.
28. Bouche, N. and Fromm, H., *GABA in plants: just a metabolite?* Trends Plant Sci, 2004. **9**:110-5.
29. Bouche, N., Lacombe, B., and Fromm, H., *GABA signaling: a conserved and ubiquitous mechanism.* Trends Cell Biol, 2003. **13**:607-10.

30. Bown, A.W., Hall, D.E., and MacGregor, K.B., *Insect footsteps on leaves stimulate the accumulation of 4-aminobutyrate and can be visualized through increased chlorophyll fluorescence and superoxide production*. *Plant Physiol*, 2002. **129**:1430-4.
31. Breitkreuz, K.E., Allan, W.L., Van Cauwenberghe, O.R., Jakobs, C., Talibi, D., Andre, B., and Shelp, B.J., *A novel gamma-hydroxybutyrate dehydrogenase: identification and expression of an Arabidopsis cDNA and potential role under oxygen deficiency*. *J Biol Chem*, 2003. **278**:41552-6.
32. Breitkreuz, K.E. and Shelp, B.J., *Subcellular Compartmentation of the 4-Aminobutyrate Shunt in Protoplasts from Developing Soybean Cotyledons*. *Plant Physiol*, 1995. **108**:99-103.
33. Breitkreuz, K.E., Shelp, B.J., Fischer, W.N., Schwacke, R., and Rentsch, D., *Identification and characterization of GABA, proline and quaternary ammonium compound transporters from Arabidopsis thaliana*. *FEBS Lett*, 1999. **450**:280-4.
34. Busch, K., Piehler, J., and Fromm, H., *Plant succinic semialdehyde dehydrogenase: dissection of nucleotide binding by surface plasmon resonance and fluorescence spectroscopy*. *Biochemistry*, 2000. **39**:10110-7.
35. Busch, K.B. and Fromm, H., *Plant succinic semialdehyde dehydrogenase. Cloning, purification, localization in mitochondria, and regulation by adenine nucleotides*. *Plant Physiol*, 1999. **121**:589-97.
36. Campanella, J.J., Olajide, A.F., Magnus, V., and Ludwig-Muller, J., *A novel auxin conjugate hydrolase from wheat with substrate specificity for longer side-chain auxin amide conjugates*. *Plant Physiol*, 2004. **135**:2230-40.
37. Campell, B.R. and Town, C.D., *Physiology of Hormone Autonomous Tissue Lines Derived From Radiation-Induced Tumors of Arabidopsis thaliana*. *Plant Physiol.*, 1991. **97**:1166-1173.
38. Capitani, G., De Biase, D., Aurizi, C., Gut, H., Bossa, F., and Grutter, M.G., *Crystal structure and functional analysis of Escherichia coli glutamate decarboxylase*. *Embo J*, 2003. **22**:4027-37.
39. Carlier, A., Chevrot, R., Dessaux, Y., and Faure, D., *The assimilation of gamma-butyrolactone in Agrobacterium tumefaciens C58 interferes with the accumulation of the N-acyl-homoserine lactone signal*. *Mol Plant Microbe Interact*, 2004. **17**:951-7.
40. Carlier, A., Uroz, S., Smadja, B., Fray, R., Latour, X., Dessaux, Y., and Faure, D., *The Ti plasmid of Agrobacterium tumefaciens harbors an attM-paralogous gene, aiiB, also encoding N-Acyl homoserine lactonase activity*. *Appl Environ Microbiol*, 2003. **69**:4989-93.
41. Carroll, A.D., Fox, G.G., Laurie, S., Phillips, R., Ratcliffe, R.G., and Stewart, G.R., *Ammonium Assimilation and the Role of [gamma]-Aminobutyric Acid in pH Homeostasis in Carrot Cell Suspensions*. *Plant Physiol*, 1994. **106**:513-520.
42. Chen, Y., Baum, G., and Fromm, H., *The 58-Kilodalton Calmodulin-Binding Glutamate Decarboxylase Is a Ubiquitous Protein in Petunia Organs and Its Expression Is Developmentally Regulated*. *Plant Physiol*, 1994. **106**:1381-1387.
43. Chevrot, R., Rosen, R., Haudecoeur, E., Cirou, A., Shelp, B.J., Ron, E., and Faure, D., *GABA controls the level of quorum-sensing signal in Agrobacterium tumefaciens*. *Proc Natl Acad Sci U S A*, 2006. **103**:7460-4.
44. Chiu, C., Jensen, K., Sokolova, I., Wang, D., Li, M., Deshpande, P., Davidson, N., Mody, I., Quick, M., Quake, S., and Lester, H., *Number, density, and surface/cytoplasmic distribution of GABA transporters at presynaptic structures*

- of knock-in mice carrying GABA transporter subtype 1-green fluorescent protein fusions.* J.Neurosci., 2002. **22**:10251-10266.
45. Chiu, J.C., Brenner, E.D., DeSalle, R., Nitabach, M.N., Holmes, T.C., and Coruzzi, G.M., *Phylogenetic and Expression Analysis of the Glutamate-Receptor-Like Gene Family in Arabidopsis thaliana.* Mol Biol Evol, 2002. **19**:1066-1082.
 46. Cho, R.J., Mindrinos, M., Richards, D.R., Sapolsky, R.J., Anderson, M., Drenkard, E., Dewdney, J., Reuber, T.L., Stammers, M., Federspiel, N., Theologis, A., Yang, W.H., Hubbell, E., Au, M., Chung, E.Y., Lashkari, D., Lemieux, B., Dean, C., Lipshutz, R.J., Ausubel, F.M., Davis, R.W., and Oefner, P.J., *Genome-wide mapping with biallelic markers in Arabidopsis thaliana.* Nat Genet, 1999. **23**:203-7.
 47. Choi, S.Y., Churchich, D.R., and Churchich, J.E., *Binding of new PLP analogs to the catalytic domain of GABA transaminase.* Biochem Biophys Res Commun, 1985. **127**:346-53.
 48. Choi, S.Y. and Churchich, J.E., *4-Aminobutyrate aminotransferase reaction of sulfhydryl residues connected with catalytic activity.* J Biol Chem, 1985. **260**:993-7.
 49. Choi, S.Y. and Churchich, J.E., *4-Aminobutyrate aminotransferase. Conformational changes induced by reduction of pyridoxal 5-phosphate.* Biochim Biophys Acta, 1985. **830**:120-6.
 50. Cholewa, E., Cholewinski, A.J., Shelp, B.J., Snedden, W.A., and Bown, A.W., *Cold-shock-stimulated γ -aminobutyric acid synthesis is mediated by an increase in cytosolic Ca^{2+} , not by an increase in cytosolic H^+ .* Can. J. Bot., 1997. **75**:375-382.
 51. Churchich, J.E. and Moses, U., *4-Aminobutyrate aminotransferase. The presence of nonequivalent binding sites.* J Biol Chem, 1981. **256**:1101-4.
 52. Clark, D.G., Gubrium, E.K., Barrett, J.E., Nell, T.A., and Klee, H.J., *Root formation in ethylene-insensitive plants.* Plant Physiol, 1999. **121**:53-59.
 53. Coleman, S.T., Fang, T.K., Rovinsky, S.A., Turano, F.J., and Moye-Rowley, W.S., *Expression of a glutamate decarboxylase homologue is required for normal oxidative stress tolerance in Saccharomyces cerevisiae.* J Biol Chem, 2001. **276**:244-50.
 54. Crawford, L.A., Bown, A.W., Breitkreuz, K.E., and Guinel, F.C., *The Synthesis of [γ]-Aminobutyric Acid in Response to Treatments Reducing Cytosolic pH.* Plant Physiol, 1994. **104**:865-871.
 55. Cutler, S. and Somerville, C., *Imaging plant cell death: GFP-Nit1 aggregation marks an early step of wound and herbicide induced cell death.* BMC Plant Biology, 2005. **5**:4.
 56. De Biase, D., Tramonti, A., John, R.A., and Bossa, F., *Isolation, overexpression, and biochemical characterization of the two isoforms of glutamic acid decarboxylase from Escherichia coli.* Protein Expr Purif, 1996. **8**:430-8.
 57. De Smet, I., Tetsumura, T., De Rybel, B., Frey, N.F.d., Laplaze, L., Casimiro, I., Swarup, R., Naudts, M., Vanneste, S., Audenaert, D., Inze, D., Bennett, M.J., and Beeckman, T., *Auxin-dependent regulation of lateral root positioning in the basal meristem of Arabidopsis.* Development, 2007. **134**:681-690.
 58. Deken, S.L., Beckman, M.L., Boos, L., and Quick, M.W., *Transport rates of GABA transporters: regulation by the N-terminal domain and syntaxin 1A.* Nat Neurosci, 2000. **3**:998-1003.
 59. Dharmasiri, N., Dharmasiri, S., and Estelle, M., *The F-box protein TIR1 is an auxin receptor.* Nature, 2005. **435**:441-5.

60. Dharmasiri, S., Swarup, R., Mockaitis, K., Dharmasiri, N., Singh, S.K., Kowalchyk, M., Marchant, A., Mills, S., Sandberg, G., Bennett, M.J., and Estelle, M., *AXR4 is required for localization of the auxin influx facilitator AUX1*. Science, 2006. **312**:1218-20.
61. Dhonukshe, P., Grigoriev, I., Fischer, R., Tominaga, M., Robinson, D.G., Hajek, J., Paciorek, T., Petrůšek, J., Seifertová, D., Tejos, R., Meisel, L.A., Zamalov, E., Gadella, T.W.J., Stierhof, Y.-D., Ueda, T., Oiwa, K., Akhmanova, A., Brock, R., Spang, A., and Friml, J., *Auxin transport inhibitors impair vesicle motility and actin cytoskeleton dynamics in diverse eukaryotes*. Proceedings of the National Academy of Sciences, 2008. **105**:4489-4494.
62. Donnelly, M.I. and Cooper, R.A., *Succinic semialdehyde dehydrogenases of Escherichia coli: their role in the degradation of p-hydroxyphenylacetate and gamma-aminobutyrate*. Eur J Biochem, 1981. **113**:555-61.
63. Donnelly, M.I. and Cooper, R.A., *Two succinic semialdehyde dehydrogenases are induced when Escherichia coli K-12 Is grown on gamma-aminobutyrate*. J Bacteriol, 1981. **145**:1425-7.
64. Drasbek, K.R., Vardya, I., Delenclos, M., Gibson, K.M., and Jensen, K., *SSADH deficiency leads to elevated extracellular GABA levels and increased GABAergic neurotransmission in the mouse cerebral cortex*. J Inher Metab Dis, 2008.
65. Drenkard, E., Richter, B.G., Rozen, S., Stutius, L.M., Angell, N.A., Mindrinos, M., Cho, R.J., Oefner, P.J., Davis, R.W., and Ausubel, F.M., *A simple procedure for the analysis of single nucleotide polymorphisms facilitates map-based cloning in Arabidopsis*. Plant Physiol, 2000. **124**:1483-92.
66. Fait, A., Yellin, A., and Fromm, H., *GABA shunt deficiencies and accumulation of reactive oxygen intermediates: insight from Arabidopsis mutants*. FEBS Lett, 2005. **579**:415-20.
67. Falkenberg, T., Lindefors, N., O'Connor, W.T., Zachrisson, O., Camilli, F., and Ungerstedt, U., *GABA release and GAD67 mRNA expression in rat hippocampus following entorhinal cortex activation*. Brain Res Mol Brain Res, 1997. **48**:413-6.
68. Ford, Y.-Y., Ratcliffe, R.G., and Robins, R.J., *Phytohormone-induced GABA production in transformed root cultures of Datura stramonium: an in vivo ¹⁵N NMR study*. J Exp Bot, 1996. **47**:811-818.
69. Forde, B.G. and Lea, P.J., *Glutamate in plants: metabolism, regulation, and signalling*. J Exp Bot, 2007. **58**:2339-58.
70. Frank, M., Rupp, H.-M., Prinsen, E., Motyka, V., Van Onckelen, H., and Schumling, T., *Hormone Autotrophic Growth and Differentiation Identifies Mutant Lines of Arabidopsis with Altered Cytokinin and Auxin Content or Signaling*. Plant Physiol., 2000. **122**:721-730.
71. Friml, J., Vieten, A., Sauer, M., Weijers, D., Schwarz, H., Hamann, T., Offringa, R., and Jürgens, G., *Efflux-dependent auxin gradients establish the apical-basal axis of Arabidopsis*. Nature 2003. **426**:147-153.
72. Fukaki, H., Okushima, Y., Tasaka, M., and Kwang, W.J., *Auxin-Mediated Lateral Root Formation in Higher Plants*, in *International Review of Cytology*. 2007, Academic Press. p. 111-137.
73. Fukaki, H., Tameda, S., Masuda, H., and Tasaka, M., *Lateral root formation is blocked by a gain-of-function mutation in the SOLITARY-ROOT/IAA14 gene of Arabidopsis*. Plant J, 2002. **29**:153-68.
74. Fuqua, C., Winans, S.C., and Greenberg, E.P., *Census and consensus in bacterial ecosystems: the LuxR-LuxI family of quorum-sensing transcriptional regulators*. Annu Rev Microbiol, 1996. **50**:727-51.

75. Galvez, T., Parmentier, M.-L., Joly, C., Malitschek, B., Kaupmann, K., Kuhn, R., Bittiger, H., Froestl, W., Bettler, B., and Pin, J.-P., *Mutagenesis and Modeling of the GABAB Receptor Extracellular Domain Support a Venus Flytrap Mechanism for Ligand Binding*. J. Biol. Chem., 1999. **274**:13362-13369.
76. Geldner, N., Friml, J., Stierhof, Y.D., Jurgens, G., and Palme, K., *Auxin transport inhibitors block PIN1 cycling and vesicle trafficking*. Nature, 2001. **413**:425-8.
77. Gibson, K.M., Gupta, M., Pearl, P.L., Tuchman, M., Vezina, L.G., Snead, O.C., 3rd, Smit, L.M., and Jakobs, C., *Significant behavioral disturbances in succinic semialdehyde dehydrogenase (SSADH) deficiency (gamma-hydroxybutyric aciduria)*. Biol Psychiatry, 2003. **54**:763-8.
78. Gordon, S.P., Heisler, M.G., Reddy, G.V., Ohno, C., Das, P., and Meyerowitz, E.M., *Pattern formation during de novo assembly of the Arabidopsis shoot meristem*. Development, 2007. **134**:3539-3548.
79. Grallath, S., Weimar, T., Meyer, A., Gumy, C., Suter-Grotemeyer, M., Neuhaus, J.M., and Rentsch, D., *The AtProT family. Compatible solute transporters with similar substrate specificity but differential expression patterns*. Plant Physiol, 2005. **137**:117-26.
80. Grsic-Rausch, S., Kobelt, P., Siemens, J.M., Bischoff, M., and Ludwig-Muller, J., *Expression and Localization of Nitrilase during Symptom Development of the Clubroot Disease in Arabidopsis*. Plant Physiol., 2000. **122**:369-378.
81. Guilfoyle, T.J., Ulmasov, T., and Hagen, G., *The ARF family of transcription factors and their role in plant hormone-responsive transcription*. Cell Mol Life Sci, 1998. **54**:619-27.
82. Hearl, W.G. and Churchich, J.E., *Interactions between 4-aminobutyrate aminotransferase and succinic semialdehyde dehydrogenase, two mitochondrial enzymes*. J Biol Chem, 1984. **259**:11459-63.
83. Hearl, W.G. and Churchich, J.E., *A mitochondrial NADP+-dependent reductase related to the 4-aminobutyrate shunt. Purification, characterization, and mechanism*. J Biol Chem, 1985. **260**:16361-6.
84. Hechler, V., Gobaille, S., and Maitre, M., *Selective distribution pattern of g-hydroxybutyrate receptors in the rat forebrain and midbrain as revealed by quantitative autoradiography*. Brain Res., 1992. **572**:345-348.
85. Higashiyama, T., Yabe, S., Sasaki, N., Nishimura, Y., Miyagishima, S., Kuroiwa, H., and Kuroiwa, T., *Pollen tube attraction by the synergid cell*. Science, 2001. **293**:1480-1483.
86. Hoover, G.J., Prentice, A.G., Merrill, A.R., and Shelp, B.J., *Kinetic mechanism of a recombinant Arabidopsis glyoxylate reductase: studies of initial velocity, dead-end inhibition and product inhibition* Can. J. Bot., 2007. **85**:896-902.
87. Hoover, G.J., Van Cauwenberghe, O.R., Breitzkreuz, K.E., Clark, S.M., Merrill, A.R., and Shelp, B.J., *Characteristics of an Arabidopsis glyoxylate reductase: general biochemical properties and substrate specificity for the recombinant protein, and developmental expression and implications for glyoxylate and succinic semialdehyde metabolism in planta*. Can. J. Bot., 2007. **85**:883-895.
88. Janzen, D.J., Allen, L.J., MacGregor, K.B., and Bown, A.W., *Cytosolic acidification and g-aminobutyric acid synthesis during the oxidative burst in isolated Asparagus sprengeri mesophyll cells*. Can. J. Bot., 2001. **70**:438-443.
89. Kathiresan, A., Miranda, J., Moloney, M.M., Chinnappa, C.C., and Reid, D.M., *g-Aminobutyric acid promotes stem elongation in Stellaria longipes: the role of ethylene*. Plant Growth Regul., 1998. **26**:131-137.

90. Kathiresan, A., Tung, P., Chinnappa, C.C., and Reid, D.M., *gamma-Aminobutyric acid stimulates ethylene biosynthesis in sunflower*. Plant Physiol, 1997. **115**:129-35.
91. Keitt, G.W. and Baker, R.A., *Auxin Activity of Substituted Benzoic Acids and Their Effect on Polar Auxin Transport*. Plant Physiol, 1966. **41**:1561-1569.
92. Kepinski, S. and Leyser, O., *The Arabidopsis F-box protein TIR1 is an auxin receptor*. Nature, 2005. **435**:446-51.
93. Kepinski, S. and Leyser, O., *Plant development: auxin in loops*. Curr Biol, 2005. **15**:R208-10.
94. Kerr, I.D. and Bennett, M.J., *New insight into the biochemical mechanisms regulating auxin transport in plants*. Biochem J, 2007. **401**:613-22.
95. Kinnersley, A.M. and Lin, F., *Receptor modifiers indicate that 4-aminobutyric acid (GABA) is a potential modulator of ion transport in plants*. Plant Growth Regul. , 2000. **32**:65-76.
96. Kinnersley, A.M. and Turano, F.J., *Gamma aminobutyric acid (GABA) and plant responses to stress*. Crit.Rev.Plant.Sci., 2000. **19**:479-509.
97. Kishinami, I., *Accumulation of γ -Aminobutyric Acid due to Ammonium in Various Cultured Plant Cells*. Plant Cell Physiol., 1987. **28**:1459-1464.
98. Kleine-Vehn, J., Dhonukshe, P., Swarup, R., Bennett, M., and Friml, J., *Subcellular Trafficking of the Arabidopsis Auxin Influx Carrier AUX1 Uses a Novel Pathway Distinct from PIN1*. Plant Cell, 2006. **18**:3171-3181.
99. Konieczny, A. and Ausubel, F.M., *A procedure for mapping Arabidopsis mutations using co-dominant ecotype-specific PCR-based markers*. Plant Journal, 1993. **4**:403-410.
100. Kramer, E.M., *PIN and AUX/LAX proteins: their role in auxin accumulation*. Trends in Plant Science, 2004. **9**:578-582.
101. Kutz, A., Müller, A., Kaiser, P.H.W.M., Piotrowski, M., and W., W.E., *A role for nitrilase 3 in the regulation of root morphology in sulphur-starving Arabidopsis thaliana*. The Plant Journal, 2002. **30**:95-106.
102. Lacombe, B., Becker, J.D., Hedrich, R., DeSalle, R., Hollmann, M., Kwak, J.M., Schroeder, J.I., Le Novere, N., Nam, H.G., Spalding, E.P., Tester, M., Turano, F.J., Chiu, J., and Coruzzi, G.M., *The identity of plant glutamate receptors*. Science, 2001. **292**:1486-1487.
103. Lancien, M. and Roberts, M.R., *Regulation of Arabidopsis thaliana 14-3-3 gene expression by γ -aminobutyric acid*. Plant, Cell and Environment, 2006. **29**:1430-1436.
104. Law, R., Stafford, A., and Quick, M., *Functional regulation of gamma-aminobutyric acid transporters by direct tyrosine phosphorylation*. J. Biol. Chem., 2000. **275**:23986-23991.
105. Li, P.L. and Farrand, S.K., *The replicator of the nopaline-type Ti plasmid pTiC58 is a member of the repABC family and is influenced by the TraR-dependent quorum-sensing regulatory system*. J Bacteriol, 2000. **182**:179-88.
106. Liscum, E. and Reed, J.W., *Genetics of Aux/IAA and ARF action in plant growth and development*. Plant Mol Biol, 2002. **49**:387-400.
107. Ludewig, F., Hüser, A., Fromm, H., Beauclair, L., and Bouche, N., *Mutants of GABA transaminase (POP2) suppress the severe phenotype of succinic semialdehyde dehydrogenase (ssadh) mutants in arabidopsis*. PLoS ONE, 2008. **3**:e3383.
108. Luzzani, C., Cardillo, S.B., Bermudez Moretti, M., and Correa Garcia, S., *New insights into the regulation of the Saccharomyces cerevisiae UGA4 gene: two*

- parallel pathways participate in carbon-regulated transcription. Microbiology, 2007. 153:3677-84.*
109. MacGregor, K.B., Shelp, B.J., Peiris, S., and Bown, A.W., *Overexpression of glutamate decarboxylase in transgenic tobacco plants deters feeding by phytophagous insect larvae. J Chem Ecol, 2003. 29:2177-82.*
 110. Maitre, M., *The γ -hydroxybutyrate signalling system in brain: organization and functional implications. . Prog. Neurobiol., 1997. 51:337–361.*
 111. Marchant, A., Kargul, J., May, S., Muller, P., Delbarre, A., Perrot-Rechenmann, C., and Bennett, M., *AUX1 regulates root gravitropism in Arabidopsis by facilitating auxin uptake within root apical tissues. . EMBO Journal, 1999. 18:2066-2073.*
 112. Marschner, H., *Mineral Nutrition of Higher Plants. 2nd ed. 1995.*
 113. Martin, D.L. and Rinvall, K., *Regulation of gamma-aminobutyric acid synthesis in the brain. J Neurochem, 1993. 60:395-407.*
 114. Masclaux, C., Van Cauwenberghe, O.R., Brugière, N., Morot-Gaudry, J.-F., and Hirel, B., *Characterization of the sink/source transition in tobacco (Nicotiana tabacum L.) shoots in relation to nitrogen management and leaf senescence. Planta, 2000. 211:510-518.*
 115. McHugh, E.M., Zhu, W., Milgram, S., and Mager, S., *The GABA transporter GAT1 and the MAGUK protein Pals1: interaction, uptake modulation, and coexpression in the brain. Molecular and Cellular Neuroscience, 2004. 26:406-417.*
 116. McLean, M.D., Yevtushenko, D.P., Deschene, A., Van Cauwenberghe, O.R., Makmoudova, A., Potter, J.W., Bown, A.W., and Shelp, B.J., *Overexpression of glutamate decarboxylase in transgenic tobacco plants confers resistance to the northern root-knot nematode. Molecular Breeding, 2003. 11:277-285.*
 117. Medina-Kauwe, L.K., Tobin, A.J., De Meirleir, L., Jaeken, J., Jakobs, C., Nyhan, W.L., and Gibson, K.M., *4-Aminobutyrate aminotransferase (GABA-transaminase) deficiency. J Inher Metab Dis, 1999. 22:414-27.*
 118. Metzger, E., Levitz, R., and Halpern, Y.S., *Isolation and properties of Escherichia coli K-12 mutants impaired in the utilization of gamma-aminobutyrate. J Bacteriol, 1979. 137:1111-8.*
 119. Meyer, A., Eskandari, S., Grallath, S., and Rentsch, D., *AtGAT1, a high affinity transporter for gamma-aminobutyric acid in Arabidopsis thaliana. J Biol Chem, 2006. 281:7197-204.*
 120. Mirabella, R., Rauwerda, H., Struys, E.A., Jakobs, C., Triantaphylides, C., Haring, M.A., and Schuurink, R.C., *The Arabidopsis her1 mutant implicates GABA in E-2-hexenal responsiveness. Plant J, 2007.*
 121. Morse, D.E., Hooker, N., Duncan, H., and Jensen, L., *γ -Aminobutyric acid, a neurotransmitter, induces planktonic abalone larvae to settle and begin metamorphosis. Science, 1979. 204:407-410.*
 122. Murphy, A.S., Hoogner, K.R., Peer, W.A., and Taiz, L., *Identification, Purification, and Molecular Cloning of N-1-Naphthylphthalmic Acid-Binding Plasma Membrane-Associated Aminopeptidases from Arabidopsis. Plant Physiol., 2002. 128:935-950.*
 123. Nelson, B.K., Cai, X., and Nebenfuhr, A., *A multicolored set of in vivo organelle markers for co-localization studies in Arabidopsis and other plants. Plant J, 2007. 51:1126-36.*
 124. Nelson, D.L. and Cox, M.M., *Lehninger Principles of Biochemistry.*

125. Nirenberg, M.W. and Jakoby, W.B., *Enzymatic utilization of gamma-hydroxybutyric acid*. J Biol Chem, 1960. **235**:954-60.
126. Noh, B., Murphy, A., and Spalding, E., *Multidrug Resistance-like genes of Arabidopsis required for auxin transport and auxin-mediated development*. The Plant Cell, 2001. **13**:2441-2454.
127. Normanly, J., Grisafi, P., Fink, G.R., and Bartel, B., *Arabidopsis Mutants Resistant to the Auxin Effects of Indole-3-Acetonitrile Are Defective in the Nitrilase Encoded by the NIT1 Gene*. Plant Cell, 1997. **9**:1781-1790.
128. Osei, Y.D. and Churchich, J.E., *Screening and sequence determination of a cDNA encoding the human brain 4-aminobutyrate aminotransferase*. Gene, 1995. **155**:185-7.
129. Owens, D.F. and Kriegstein, A.R., *Is there more to GABA than synaptic inhibition?* Nat Rev Neurosci, 2002. **3**:715-27.
130. Palanivelu, R., Brass, L., Edlund, A.F., and Preuss, D., *Pollen tube growth and guidance is regulated by POP2, an Arabidopsis gene that controls GABA levels*. Cell, 2003. **114**:47-59.
131. Park, J., Osei, Y.D., and Churchich, J.E., *Isolation and characterization of recombinant mitochondrial 4-aminobutyrate aminotransferase*. J Biol Chem, 1993. **268**:7636-9.
132. Park, W.J., Kriechbaumer, V., Muller, A., Piotrowski, M., Meeley, R.B., Gierl, A., and Glawischnig, E., *The Nitrilase ZmNIT2 Converts Indole-3-Acetonitrile to Indole-3-Acetic Acid*. Plant Physiol., 2003. **133**:794-802.
133. Parry, G. and Estelle, M., *Auxin receptors: a new role for F-box proteins*. Curr Opin Cell Biol, 2006. **18**:152-6.
134. Pearl, P.L., Capp, P.K., Novotny, E.J., and Gibson, K.M., *Inherited disorders of neurotransmitters in children and adults*. Clinical Biochemistry, 2005. **38**:1051-1058.
135. Petrasek, J., Mravec, J., Bouchard, R., Blakeslee, J.J., Abas, M., Seifertova, D., Wisniewska, J., Tadele, Z., Kubes, M., Covanova, M., Dhonukshe, P., Skupa, P., Benkova, E., Perry, L., Krecek, P., Lee, O.R., Fink, G.R., Geisler, M., Murphy, A.S., Luschnig, C., Zazimalova, E., and Friml, J., *PIN proteins perform a rate-limiting function in cellular auxin efflux*. Science, 2006. **312**:914-8.
136. Petty, F., Fulton, M., Kramer, G.L., Kram, M., Davis, L.L., and Rush, A.J., *Evidence for the segregation of a major gene for human plasma GABA levels*. Mol Psychiatry, 1999. **4**:587-9.
137. Piotrowski, M., Schönfelder, S., and Weiler, E.W., *The Arabidopsis thaliana isogene NIT4 and its orthologs in tobacco encode β -cyano-L-alanine hydratase/nitrilase*. J. Biol. Chem., 2001. **276**:2616 - 2621.
138. Pollmann, S., Muller, A., Piotrowski, M., and Weiler, E.W., *Occurrence and formation of indole-3-acetamide in Arabidopsis thaliana*. Planta, 2002. **216**:155-61.
139. Pollmann, S., Müller, A., and Weiler, E.W., *Many Roads Lead to "Auxin": of Nitrilases, Synthases, and Amidases*. Plant Biology, 2006:326-333.
140. Quint, M. and Gray, W.M., *Auxin signaling*. Curr Opin Plant Biol, 2006. **9**:448-53.
141. Quirino, B., Normanly, J., and Amasino, R., *Diverse range of gene activity during Arabidopsis thaliana leaf senescence includes pathogen-independent induction of defense-related genes*. . Plant Molecular Biology 1999. **40**.

142. Ramos, F., el Guezzar, M., Grenson, M., and Wiame, J.M., *Mutations affecting the enzymes involved in the utilization of 4-aminobutyric acid as nitrogen source by the yeast Saccharomyces cerevisiae*. Eur J Biochem, 1985. **149**:401-4.
143. Reggiani, R., Aurisano, N., Mattana, M., and Bertani, A., *ABA induces 4-Aminobutyrate Accumulation in Wheat Seedlings*. Phytochemistry, 1993. **34**:605-609.
144. Rinvall, K., Sheikh, S.N., and Martin, D.L., *Effects of increased gamma-aminobutyric acid levels on GAD67 protein and mRNA levels in rat cerebral cortex*. J Neurochem, 1993. **60**:714-20.
145. Salathia, N., Lee, H.N., Sangster, T.A., Morneau, K., Landry, C.R., Schellenberg, K., Behere, A.S., Gunderson, K.L., Cavalieri, D., Jander, G., and Queitsch, C., *Indel arrays: an affordable alternative for genotyping*. Plant J, 2007. **51**:727-37.
146. Sanger, F. and Coulson, A.R., *A rapid method for determining sequences in DNA by primed synthesis with DNA polymerase*. J Mol Biol, 1975. **94**:441-8.
147. Sanger, F., Nicklen, S., and Coulson, A.R., *DNA sequencing with chain-terminating inhibitors*. Proc Natl Acad Sci U S A, 1977. **74**:5463-7.
148. Satya Narayan, V. and Nair, P.M., *The 4-Aminobutyrate Shunt in Solanum tuberosum*. Phytochemistry, 1986. **25**:997-1001.
149. Satya Narayan, V. and Nair, P.M., *Metabolism, enzymology and possible roles of 4-aminobutyrate in higher plants*. Phytochemistry, 1990. **29**:367-375.
150. Schaller, M., Schaffhauser, M., Sans, N., and Wermuth, B., *Cloning and expression of succinic semialdehyde reductase from human brain. Identity with aflatoxin B1 aldehyde reductase*. Eur J Biochem, 1999. **265**:1056-60.
151. Schneider, B.L., Ruback, S., Kiupakis, A.K., Kasbarian, H., Pybus, C., and Reitzer, L., *The Escherichia coli gabDTPC operon: specific gamma-aminobutyrate catabolism and nonspecific induction*. J Bacteriol, 2002. **184**:6976-86.
152. Schwacke, R., Grallath, S., Breitzkreuz, K.E., Stransky, E., Stransky, H., Frommer, W.B., and Rentsch, D., *LeProT1, a transporter for proline, glycine betaine, and gamma-amino butyric acid in tomato pollen*. Plant Cell, 1999. **11**:377-92.
153. Seidel, C., Walz, A., Park, S., Cohen, J.D., and Ludwig-Müller, J., *Indole-3-Acetic Acid Protein Conjugates: Novel Players in Auxin Homeostasis*. Plant Biology, 2006:340-345.
154. Shelp, B.J., Bown, A.W., and Faure, D., *Extracellular gamma-aminobutyrate mediates communication between plants and other organisms*. Plant Physiol, 2006. **142**:1350-2.
155. Shelp, B.J., Bown, A.W., and McLean, M.D., *Metabolism and functions of gamma-aminobutyric acid*. Trends Plant Sci, 1999. **4**:446-452.
156. Shelp, B.J., Van Cauwenberghe, O.R., and Bown, A.W., *Gamma aminobutyrate: from intellectual curiosity to practical pest control*. Can. J. Bot., 2003. **81**:1045-1048.
157. Shimizu, K.K. and Okada, K., *Attractive and repulsive interactions between female and male gametophytes in Arabidopsis pollen tube guidance*. Development, 2000. **127**:4511-4518.
158. Simpson, J.P., Di Leo, R., Dhanoa, P.K., Allan, W.L., Makhmoudova, A., Clark, S.M., Hoover, G.J., Mullen, R.T., and Shelp, B.J., *Identification and characterization of a plastid-localized Arabidopsis glyoxylate reductase isoform: comparison with a cytosolic isoform and implications for cellular redox homeostasis and aldehyde detoxification*. J Exp Bot, 2008. **59**:2545-54.

159. Skoog, F. and Miller, C.O., *Chemical regulation of growth and organ formation in plant tissues cultured in vitro*. Symp Soc Exp Biol, 1957. **11**:118-131.
160. Snead, O.C., 3rd, *Evidence for a G protein-coupled gamma-hydroxybutyric acid receptor*. J Neurochem, 2000. **75**:1986-96.
161. Snedden, W.A., Arazi, T., Fromm, H., and Shelp, B.J., *Calcium/Calmodulin Activation of Soybean Glutamate Decarboxylase*. Plant Physiol, 1995. **108**:543-549.
162. Snedden, W.A., Koutsia, N., Baum, G., and Fromm, H., *Activation of a recombinant petunia glutamate decarboxylase by calcium/calmodulin or by a monoclonal antibody which recognizes the calmodulin binding domain*. J Biol Chem, 1996. **271**:4148-53.
163. Solomon, P.S. and Oliver, R.P., *Evidence that gamma-aminobutyric acid is a major nitrogen source during Cladosporium fulvum infection of tomato*. Planta, 2002. **214**:414-20.
164. Staswick, P.E., Serban, B., Rowe, M., Tiryaki, I., Maldonado, M.T., Maldonado, M.C., and Suza, W., *Characterization of an Arabidopsis enzyme family that conjugates amino acids to indole-3-acetic acid*. Plant Cell, 2005. **17**:616-27.
165. Stewart, G.R., *gamma-aminobutyric acid: a constituent of the potato tuber?* Science, 1949. **110**:439-440.
166. Storici, P., Capitani, G., De Biase, D., Moser, M., John, R.A., Jansonius, J.N., and Schirmer, T., *Crystal Structure of GABA-Aminotransferase, a Target for Antiepileptic Drug Therapy*. Biochemistry, 1999. **38**:8628-8634.
167. Struys, E.A., Jansen, E.E., Gibson, K.M., and Jakobs, C., *Determination of the GABA analogue succinic semialdehyde in urine and cerebrospinal fluid by dinitrophenylhydrazine derivatization and liquid chromatography-tandem mass spectrometry: application to SSADH deficiency*. J Inher Metab Dis, 2005. **28**:913-20.
168. Swanson, R., Edlund, A.F., and Preuss, D., *Species specificity in pollen-pistil interactions*. Annu Rev Genet, 2004. **38**:793-818.
169. Swarup, K., Benkova, E., Swarup, R., Casimiro, I., Peret, B., Yang, Y., Parry, G., Nielsen, E., De Smet, I., Vanneste, S., Levesque, M.P., Carrier, D., James, N., Calvo, V., Ljung, K., Kramer, E., Roberts, R., Graham, N., Marillonnet, S., Patel, K., Jones, J.D., Taylor, C.G., Schachtman, D.P., May, S., Sandberg, G., Benfey, P., Friml, J., Kerr, I., Beeckman, T., Laplace, L., and Bennett, M.J., *The auxin influx carrier LAX3 promotes lateral root emergence*. Nat Cell Biol, 2008. **10**:946-54.
170. Swiderska, A., Berndtson, A.K., Cha, M.R., Li, L., Beaudoin, G.M., 3rd, Zhu, J., and Fuqua, C., *Inhibition of the Agrobacterium tumefaciens TraR quorum-sensing regulator. Interactions with the TraM anti-activator*. J Biol Chem, 2001. **276**:49449-58.
171. Taiz, L. and Zeiger, E., *Plant Physiology*. 2nd ed.
172. Talibi, D., Grenson, M., and Andre, B., *Cis- and trans-acting elements determining induction of the genes of the gamma-aminobutyrate (GABA) utilization pathway in Saccharomyces cerevisiae*. Nucleic Acids Res, 1995. **23**:550-7.
173. Terasaka, K., Blakeslee, J.J., Titapiwatanakun, B., Peer, W.A., Bandyopadhyay, A., Makam, S.N., Lee, O.R., Richards, E.L., Murphy, A.S., Sato, F., and Yazaki, K., *PGP4, an ATP binding cassette P-glycoprotein, catalyzes auxin transport in Arabidopsis thaliana roots*. Plant Cell, 2005. **17**:2922-39.

174. Toney, M.D., Pascarella, S., and De Biase, D., *Active site model for gamma-aminobutyrate aminotransferase explains substrate specificity and inhibitor reactivities*. *Protein Sci*, 1995. **4**:2366-74.
175. Turano, F.J. and Fang, T.K., *Characterization of two glutamate decarboxylase cDNA clones from Arabidopsis*. *Plant Physiol*, 1998. **117**:1411-21.
176. Turano, F.J., Panta, G.R., Allard, M.W., and van Berkum, P., *The Putative Glutamate Receptors from Plants Are Related to Two Superfamilies of Animal Neurotransmitter Receptors via Distinct Evolutionary Mechanisms*. *Mol Biol Evol*, 2001. **18**:1417-1420.
177. Van Cauwenberghe, O.R., Makmoudova, A., McLean, M.D., Clark, S.M., and Shelp, B.J., *Plant pyruvate-dependent gamma-aminobutyrate transaminase: identification of an Arabidopsis cDNA and its expression in Escherichia coli*. *Can. J. Bot.*, 2002. **80**:933-941.
178. Van Cauwenberghe, O.R. and Shelp, B.J., *Biochemical characterization of partially purified gaba:pyruvate transaminase from Nicotiana tabacum*. *Phytochemistry*, 1999. **52**:575-581.
179. Vayer, P., Schmitt, M., Bourguignon, J.J., Mandel, P., and Maitre, M., *Evidence for a role of high Km aldehyde reductase in the degradation of endogenous gamma-hydroxybutyrate from rat brain*. *FEBS Lett*, 1985. **190**:55-60.
180. Von Bodman, S.B., Bauer, W.D., and Coplin, D.L., *Quorum sensing in plant-pathogenic bacteria*. *Annu Rev Phytopathol*, 2003. **41**:455-82.
181. Vorwerk, S., Biernacki, S., Hillebrand, H., Janzik, I., Muller, A., Weiler, E.W., and Piotrowski, M., *Enzymatic characterization of the recombinant Arabidopsis thaliana nitrilase subfamily encoded by the NIT2/NIT1/NIT3-gene cluster*. *Planta*, 2001. **212**:508-16.
182. Wain, R. and Wightman, F., *The growth-regulating activity of certain ω -substituted alkyl carboxylic acids in relation to their β -oxidation within the plant*. *Proceedings of the National Academy of Sciences*, 1954. **142** 525-536.
183. Wajant, H. and Effenberger, F., *Characterization and synthetic applications of recombinant AtNIT1 from Arabidopsis thaliana*. *European Journal of Biochemistry*, 2002. **269**:680-687.
184. Wallace, W., Secor, J., and Schrader, L.E., *Rapid Accumulation of γ -Aminobutyric Acid and Alanine in Soybean Leaves in Response to an Abrupt Transfer to Lower Temperature, Darkness or Mechanical Manipulation*. *Plant Physiol*, 1984. **75**:170-175.
185. Wang, C., Zhang, H.B., Wang, L.H., and Zhang, L.H., *Succinic semialdehyde couples stress response to quorum-sensing signal decay in Agrobacterium tumefaciens*. *Mol Microbiol*, 2006. **62**:45-56.
186. Woodward, A.W. and Bartel, B., *Auxin: Regulation, Action, and Interaction*. *Ann Bot*, 2005. **95**:707-735.
187. Wu, C., Zhou, S., Zhang, Q., Zhao, W., and Peng, Y., *Molecular cloning and differential expression of an gamma-aminobutyrate transaminase gene, OsGABA-T, in rice (Oryza sativa) leaves infected with blast fungus*. *J Plant Res*, 2006. **119**:663-9.
188. Yang, Z., *GABA, a new player in the plant mating game*. *Dev Cell*, 2003. **5**:185-6.
189. Yevtushenko, D.P., McLean, M.D., Peiris, S., Van Cauwenberghe, O.R., and Shelp, B.J., *Calcium/calmodulin activation of two divergent glutamate decarboxylases from tobacco*. *J Exp Bot*, 2003. **54**:2001-2.

-
190. Yu, G., Liang, J., He, Z., and Sun, M., *Quantum dot-mediated detection of gamma-aminobutyric acid binding sites on the surface of living pollen protoplasts in tobacco*. Chem Biol, 2006. **13**:723-31.
 191. Yuan, T. and Vogel, H.J., *Calcium-calmodulin-induced dimerization of the carboxyl-terminal domain from petunia glutamate decarboxylase. A novel calmodulin-peptide interaction motif*. J Biol Chem, 1998. **273**:30328-35.
 192. Zhao, Y., Christensen, S., Fankhauser, C., Cashman, J., Cohen, J., Weigel, D., and Chory, J., *A role for flavin monooxygenase-like enzymes in auxin biosynthesis*. Science, 2001. **291**:306-309.
 193. Zik, M., Arazi, T., Snedden, W.A., and Fromm, H., *Two isoforms of glutamate decarboxylase in Arabidopsis are regulated by calcium/calmodulin and differ in organ distribution*. Plant Mol Biol, 1998. **37**:967-75.
 194. Zimmerman, P. and Hitchcock, A., *Substituted phenoxy and benzoic acid growth substances and the relation of structure to physiological activity*. Contributions of the Boyce Thompson Institute, 1942. **12**.

6. Appendix

6.1. Features of selected *ssadh* suppressor lines

6.1.1. Growth characteristics and metabolite contents

Table 4: Analysis of M₃ plants

Rosette diameter conditions and relative GHB- and GABA-contents in leaf extracts from M₃ plants grown under greenhouse from plants conditions

Line	rosette diameter [cm]	GHB-content (relative to WT)	GABA-content (relative to WT)
<i>gaba-t</i>	5.0	1.00	9.43
<i>gaba-t/ssadh</i>	4.9	14.20	10.08
wild type	5.1	1.00	1.00
1F	2.76	113.20	4.64
3C	4.7	95.02	4.47
3F	2.4	86.88	6.46
3L	4.42	132.12	4.85
4B	2.88	62.64	2.84
4D	2.44	323.71	19.32
5E		159.76	4.43
6B	2.22	53.26	6.43
7D	3.69	40.15	1.22
7F	1.74	69.75	2.82
8G	1.98	100.50	5.02
10F	2.88	201.70	7.81
12B		60.13	2.10
12F	3.36	125.50	4.99
13K	3.09	107.22	2.65
13M	2.19	170.62	2.75
13O	3.3	150.23	7.08
15A	4.41	82.09	2.94
17J	4.32	82.25	5.07
18B	5.43	1.94	0.82
18J	1.77	44.33	2.56
18N	1.59	61.78	4.10
19B	7.24		0.84
20H	2.37	99.49	3.80
21H	3.21	231.94	7.77
23F	1.98	257.09	10.52
24E	2.22		0.00
24F	3.36	196.44	11.11
24G		131.12	5.13
26F	1.72	168.66	5.82
29B	3.36	129.13	4.39
29C	2.97	148.82	4.34

30L	3.21	9.54	4.90
30M	2.67	1.00	1.72
31A	2.31	12.48	12.08
32F	2.43		
34D			
34G	2.1		
35A	2.61	99.06	2.50
35D	5.07	20.11	8.55
35F			
35J	3.42		
35K	2.24	119.10	1.53
37H	2.18	119.79	5.15
37J		136.03	4.88
38H	3.1	213.68	2.73
39C	2.31	70.58	2.90
39D	2.49	139.50	2.40
39E	4.35	160.19	1.18
39H	2.1	129.06	2.18

Table 5: M₄ plants grown under long day conditions

Rosette diameter 36 and 47 days after germination, appearance of first flower buds and the number of leaves when flowering for M₄-plants grown under long day conditions.

Line	rosette diameter	rosette diameter	flowering time [days]	number of leaves
	[cm] 36 days	[cm] 47 days		
1F	3.53	5.19	38	13
3C	2.41	4.88	41	13
3F	1.30	4.36	43	12
3L	1.94	1.75	41	15
4B				
4D	2.20	3.86	39	14
5E	2.71	5.89	46	12
6B	2.30	4.69	46	12
7D	3.11	5.56	40	11
7F	2.05	4.69	43	14
8G	2.23	3.00	40	9
10F	1.83	1.18	44	12
12B				
12F	1.79	4.18	37	11
13K				
13M	1.11	1.96	48	13
13O	1.92	3.27	45	13
15A	2.84	4.58	48	13
17J	3.43	6.55	42	14
18B	6.14	10.50	38	17

18J	2.10	4.25	52	17
18N	1.89	4.91	45	16
19B	6.54	9.00	37	17
20H	1.18	1.40	43	11
21H	2.32	3.93	44	13
23F	1.45	2.40	43	14
24E	2.15	4.91	41	13
24F	1.68	2.51	43	12
24G	0.74	1.96		
26F	1.56	3.27	42	11
29B	3.55	4.58	39	14
29C	1.79	5.02	45	16
30L	2.28	4.04	43	14
30M	1.41	2.73	35	10
31A	1.59	2.07	38	9
32F	2.30	2.62	41	13
34D	1.72	2.07	50	18
34G	2.09	3.38	39	11
35A	2.64	4.47	41	11
35D	2.57	3.38	43	16
35F	3.19	5.75	48	15
35J	2.13	5.24	42	14
35K	1.80	3.38	41	14
37H	1.44	2.07		
37J	0.98	2.29		
38H	2.28	4.15	47	17
39C	2.43	4.25	48	18
39D	2.70	3.16	42	11
39E	3.77	8.14	37	14
39H	1.33	1.31	45	12

Table 6: M₄ plants grown under short day conditions

Rosette diameter 36 and 47 days after germination, appearance of first flower buds and the number of leaves when flowering for M₄-plants grown under short day conditions.

Line	rosette diameter	rosette diameter	flowering	number of leaves
	[cm] 36 days	[cm] 47 days	time [days]	
1F			46	14
3C	2.70	1.88	*	
3F			*	
3L	1.41	3.66	*	
4B				
4D			*	

5E	0.55	1.02	*	
6B			*	
7D	0.42	0.90	*	
7F	2.74	3.07	*	
8G			*	
10F	2.08	0.54	*	
12B			*	
12F		3.44	14	47
13K			*	
13M	2.85	1.94	*	
13O	1.82	3.07	*	
15A	1.52	1.83	*	
17J	3.27	0.98	*	
18B	6.78		*	
18J	1.27	1.92	*	
18N	1.01	1.83	*	
19B	6.86		20	46
20H	3.43	1.71	*	
21H	1.92	1.41	*	
23F	2.36	1.64	8	33
24E	3.11	2.40	*	
24F		2.10	*	
24G	1.50	0.74	*	
26F	1.45	1.59	*	
29B	2.14	2.08	*	
29C	2.05	2.44	*	
30L	1.77		*	
30M		2.25	14	47
31A	2.04	1.60	14	50
32F	2.31	1.60	*	
34D	1.87	1.28	*	
34G	1.66	1.35	*	
35A	2.61	3.68	*	
35D	1.75	1.68	*	
35F	3.51	3.02	*	
35J	1.38	1.20	*	
35K	2.82	2.29	14	48
37H	0.97	1.05	*	
37J			*	
38H	1.33		*	
39C	2.74	2.29	*	
39D	1.82	1.55	*	
39E	4.79		*	
39H	2.29	2.95	*	

6.1.2. Cluster analysis

The cluster analysis was performed on growth characteristics and metabolite contents of *ssadh* suppressor lines using the MeV software, available at the TIGR homepage:

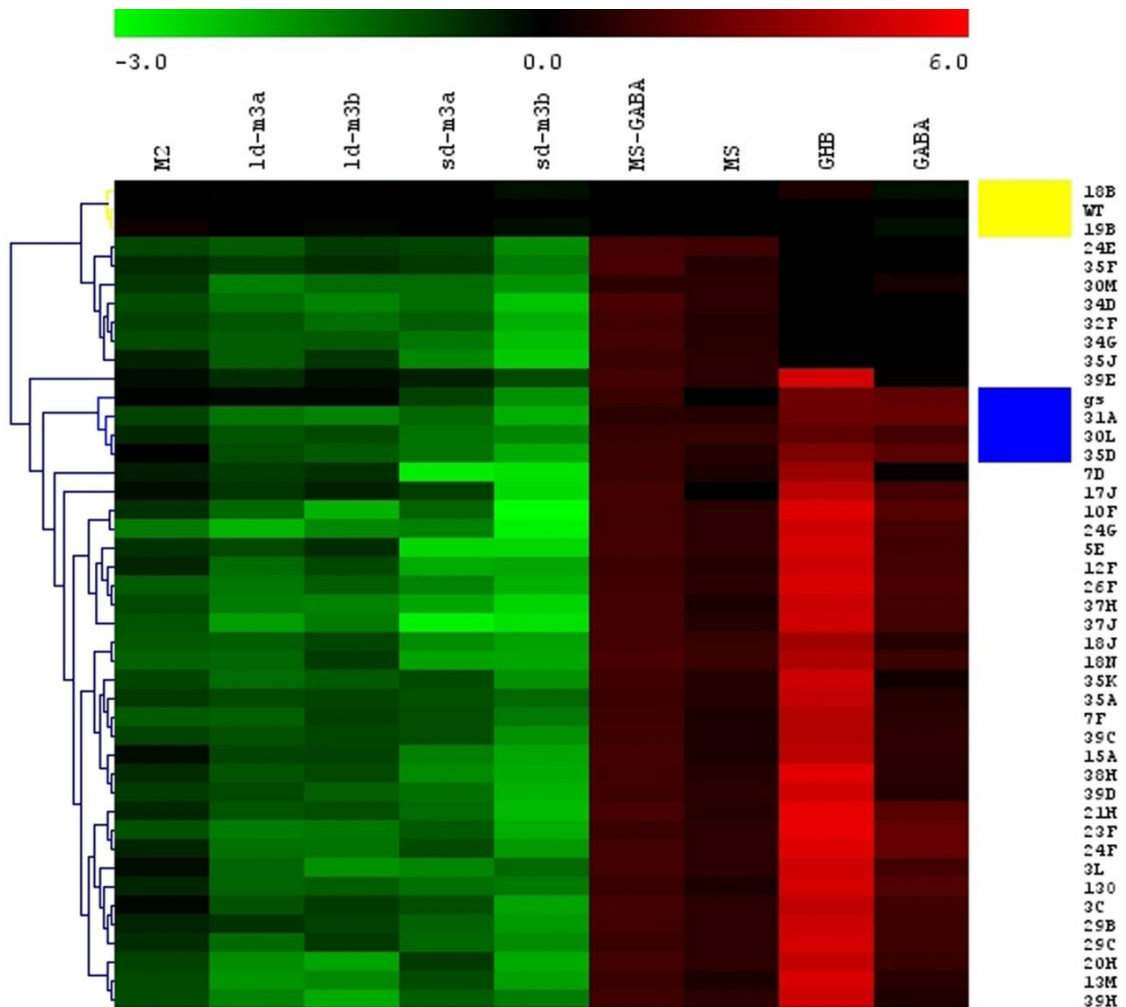


Figure 43: Cluster Analysis of *ssadh* suppressor lines

Plant lines were clustered based on growth characteristics and metabolite content. The values are relative to wild type and logarithmic. The yellow block indicated plants highly similar to wild types; the blue corresponds to *gaba-t/ssadh* comparable plants.

M2: rosette diameter of M₂-plants

ld-m3: rosette diameter of M₃-plants grown under long day conditions for 20 (a) or 39 (b) days

sd-m3: rosette diameter of M₃-plants grown under short day conditions for 20 (a) or 39 (b) days

MS-GABA: plant size of M₃-plants grown on ½ MS supplemented with GABA

MS: plant size of M₃-plants grown on ½ MS

GHB: GHB-content in leaf extracts of M₃-plants grown under greenhouse conditions

GABA: GABA-content in leaf extracts of M₃-plants grown under greenhouse conditions

6.1.3. Phenotypes

For all lines, the pictures provide details on plant growth in the following order:

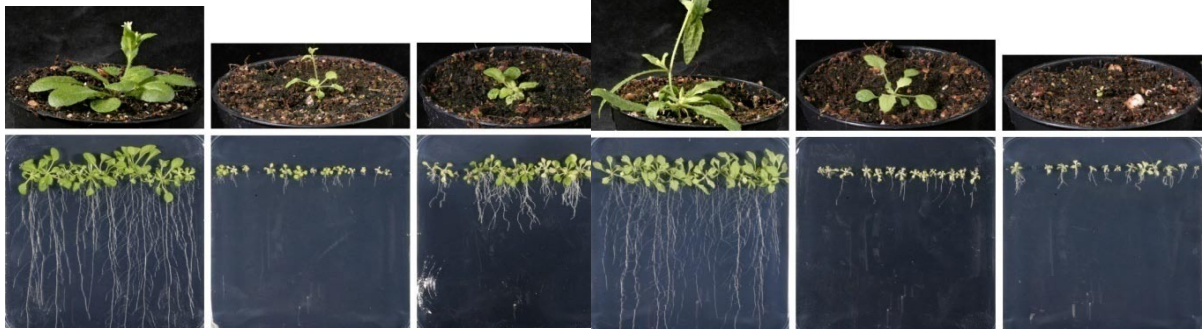
First row: M₂ plant grown under greenhouse conditions for 44 days, a representative M₃ plant grown for 39 days under long day conditions, a characteristic M₃ plant grown under short day conditions for 39 days

Second row: M₃ plants grown for 16 days under long day conditions on the indicated media, ½ MS, ½ MS + 5mM GABA, and ½ MS + 5mM glutamate

1.A



3.C



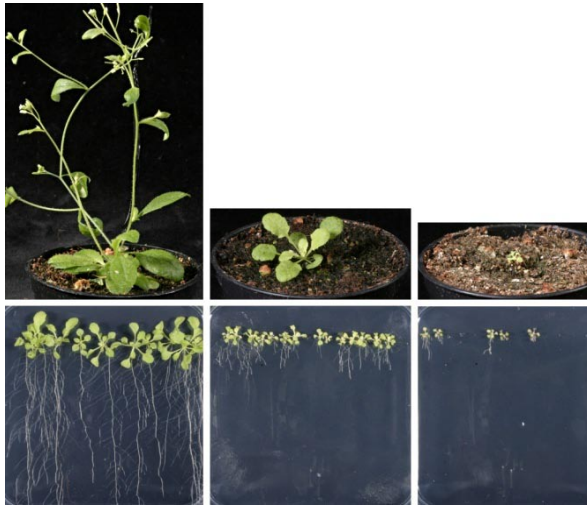
3.L



6.B



7.D



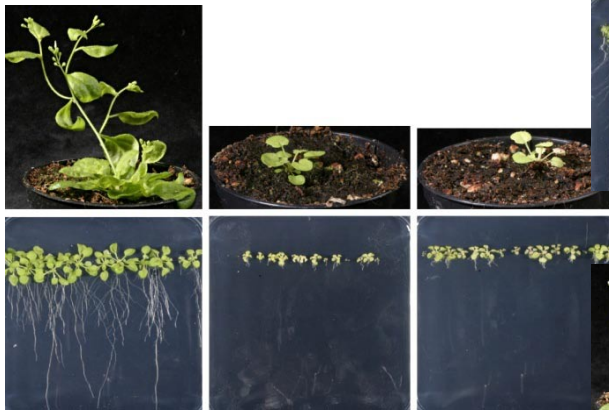
12.F



8.J



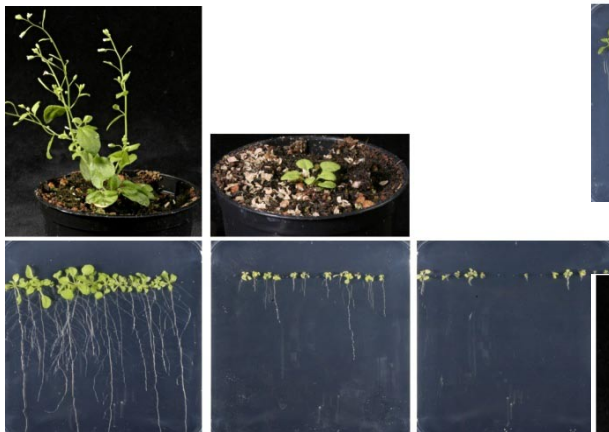
7.F



8.M



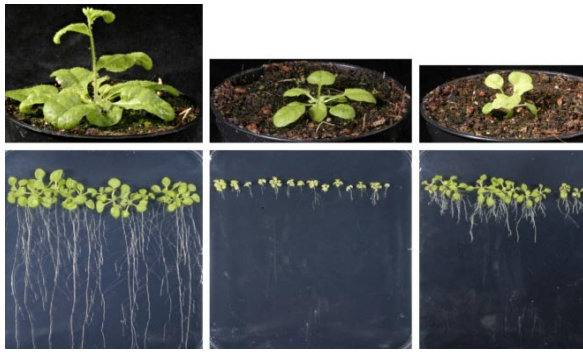
8.G



10.F



15.A



19.B



18.B



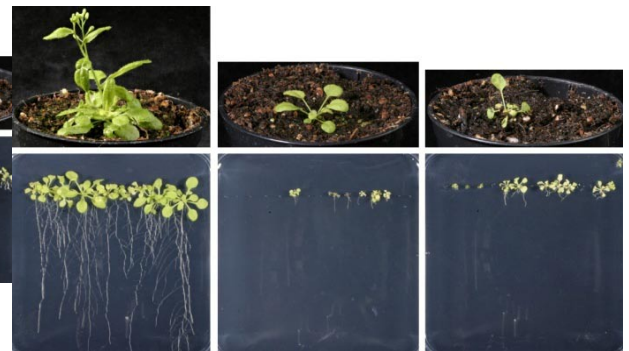
20.H



18.J



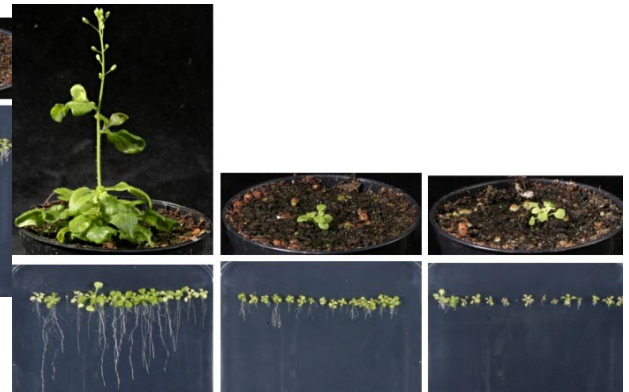
21.H



18.N



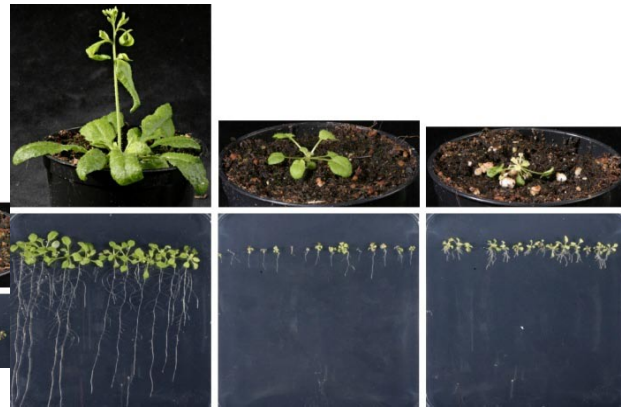
23.F



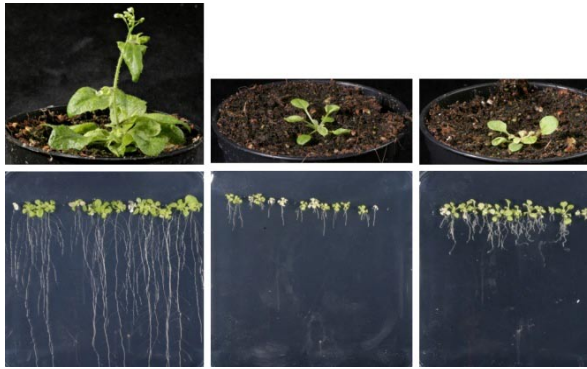
24.E



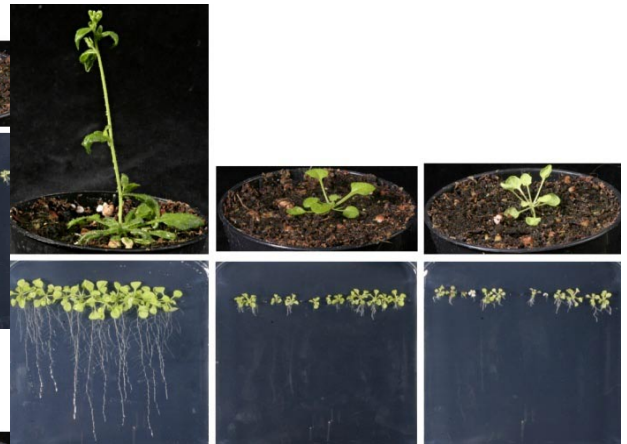
29.B



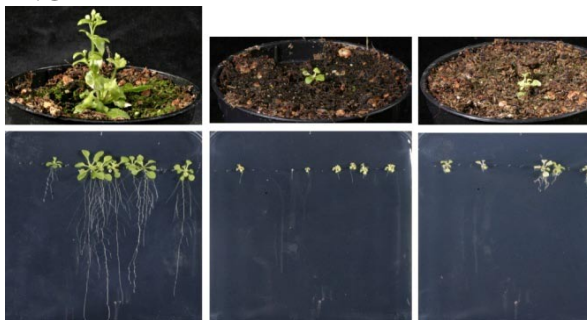
24.F



29.C



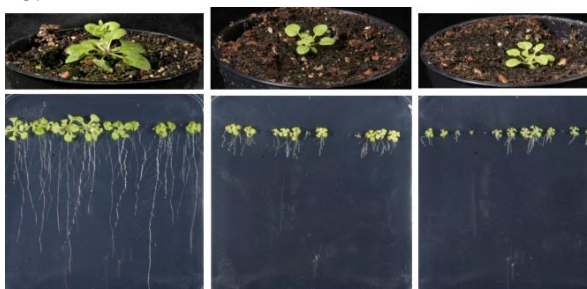
24.G



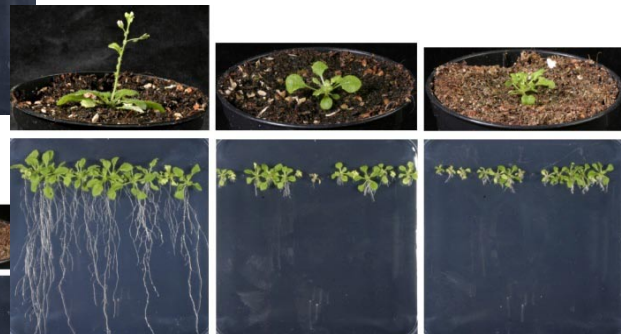
29.M



26.F



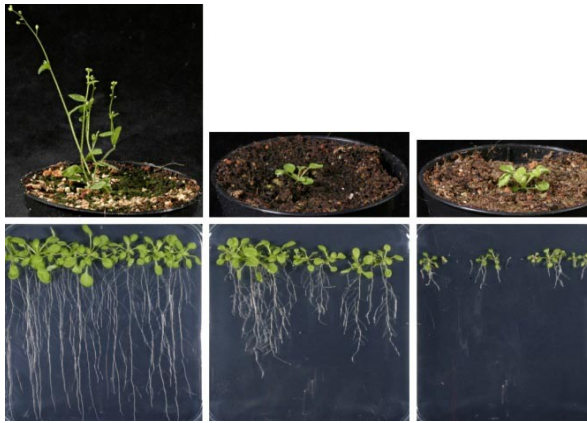
29.F



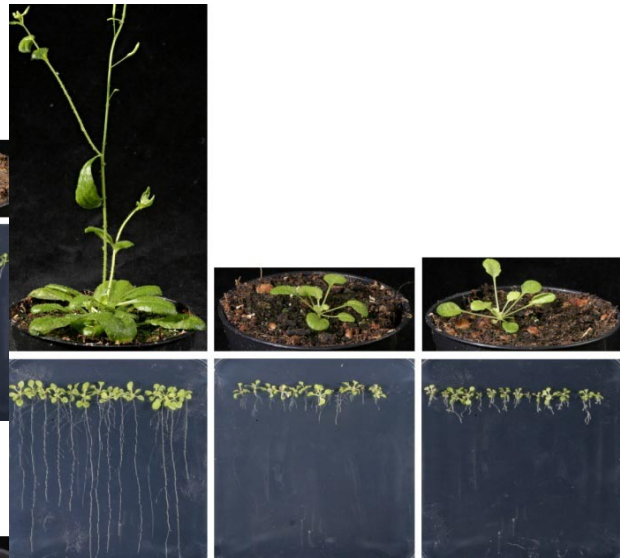
30.L



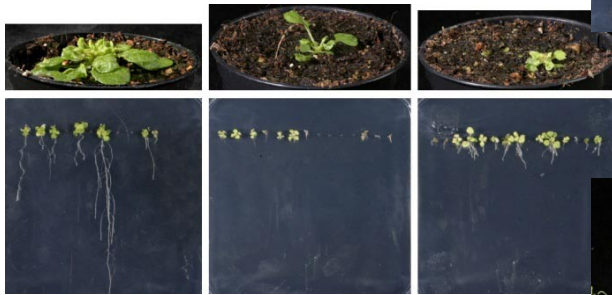
31.A



35.A



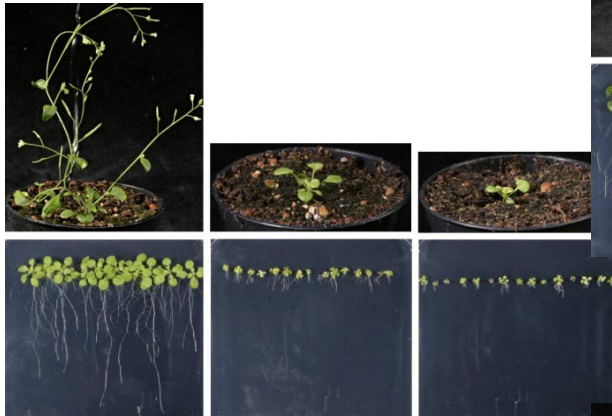
34.D



.D



34.G



.F



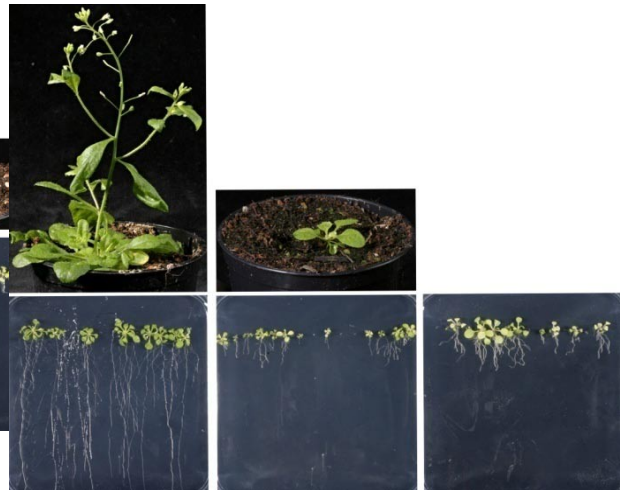
35.J



35.K



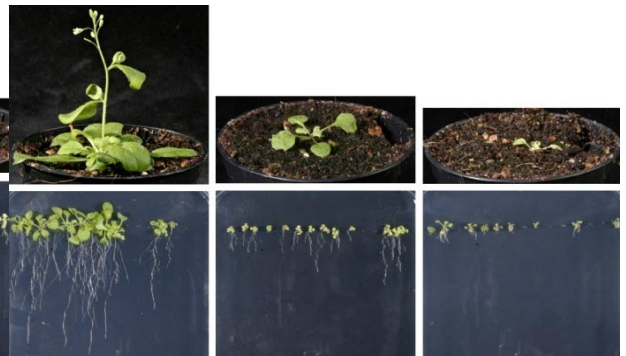
38.H



37.H



39.D



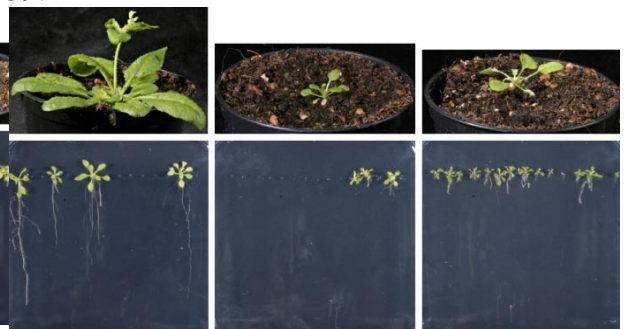
39.E



37.J



39.H



39.C



6.2. Reporter lines

Clone	Abbreviation	Localization
CD3-960	ER-rb	ER-mCherry
CD3-968	G-rb	Golgi-mCherry
CD3-976	vac-rb	tonoplast-mCherry
CD3-984	px-rb	peroxisome-mCherry
CD3-992	mt-rb	mitochondria-mCherry
CD3-1000	pt-rb	plastid-mCherry
CD3-1008	pm-rb	plasma membrane-mCherry

All constructs [123] are available via TAIR.

Plant Line		donated from
AKT1prom-GUS	root hair specific promoter	Uta Anschütz, Würzburg
ARR7::GUS	Response Regulator 7 (At1g19050)	Rosalia Deeken, Würzburg
AtKC::GUS	root hair specific promoter	Uta Anschütz, Würzburg
aux1p::GUS (ll4)	Auxin Resistant 1 (At2g38120)	Rosalia Deeken, Würzburg Klaus Palme, MPIZ
DR5::GUS	artificial auxin-responsive promoter	MPIZ
GSTF2::GUS	hypocotyl specific expression, ethylene response	Markus Geisler, Zürich
IAA2::GUS	auxin-inducible transcription factor, promoter-GUS-fusion	Klaus Palme, MPIZ
LAX1::GUS	Auxin Transporter-like 1 (At5g01240)	Rosalia Deeken, Würzburg
LAX2::GUS	Auxin Transporter-like 2 (At2g21050)	Rosalia Deeken/Würzburg
LAX3::GUS	Auxin Transporter-like 3 (At1g77690)	Rosalia Deeken, Würzburg
NIT1::GUS	Nitrilase, IAA sensitive	Klaus Palme, MPIZ
NIT2::GUS	Nitrilase, IAA sensitive	Klaus Palme, MPIZ
NIT3::GUS	Nitrilase, IAA sensitive	Klaus Palme, MPIZ
NIT4::GUS	Nitrilase	Klaus Palme, MPIZ
Pin1::GUS	auxin efflux carrier	Klaus Palme, MPIZ
Pin6::GUS	auxin efflux carrier	Klaus Palme, MPIZ

6.3. Phytohormone mutants

Plant Line		donated from
aux1/lax3	aux1/lax3-Doppelmutante,	Malcolm Bennett, Nottingham
aux1-100	Auxin Resistant 1 (At2g38120)	Rosalia Deeken, Würzburg
aux1-21	Auxin Resistant 1 (At2g38120)	Malcolm Bennett, Nottingham
aux1-7 (ll4)	Auxin Resistant 1 (At2g38120)	Rosalia Deeken, Würzburg
axr1-3	Auxin Resistant 1 (At1g05180)	Rosalia Deeken, Würzburg
lax1	Auxin Transporter-like 1 (At5g01240)	Rosalia Deeken, Würzburg
lax2	Auxin Transporter-like 2 (At2g21050)	Rosalia Deeken, Würzburg
lax3	Auxin Transporter-like 3 (At1g77690)	Rosalia Deeken, Würzburg
lax3	Auxin Transporter-like 3 (At1g77690)	Malcolm Bennett, Nottingham
N24607	At5g20730 (arf7), Auxin regulated TF	Eva Winkelbauer, Tübingen
N24617	At1g19220 (arf19), Auxin response factor	Eva Winkelbauer, Tübingen
N24629	arf7/arf19-double mutant	Eva Winkelbauer, Tübingen
nahG	Overexpression of a bacterial Salicylate Hydroxylase	Rosalia Deeken, Würzburg
nph1-5	Non Phototropic Hypocotyl 1 (At3g45780)	Rosalia Deeken, Würzburg
nph3	Non Phototropic Hypocotyl 3 (At5g64330)	Rosalia Deeken, Würzburg
nph4-1 (ARF7)	Non Phototropic Hypocotyl 3 (At5g20730)	Rosalia Deeken, Würzburg
pin1oid	Pin-formed 1 (At1g73590)	Rosalia Deeken, Würzburg
pin3	Pin-formed 3 (At1g70940), Col-0	Rosalia Deeken, Würzburg
shy2-2	SHY2/IAA3 (At1g04240)	Rosalia Deeken, Würzburg
tir1-1	Transport Inhibitor Response 1 (At3g62980)	Rosalia Deeken, Würzburg

6.4. Primer Sequences

All primer sequences are given in 5' → 3' orientation.

6.4.1. Screening

Primer	Sequence
LB-F (SALK)	GTCCGCAATGTGTTATTAAGTTGTC
RB-F (SALK)	CAACGTTGCGGTTCTGTCAGTTCC
RB-RB (SALK)	GAGCAAGGTGAGATGACAGGAG
At2g01170scrFOR	GTTGCTGTGTTTTTCTGTGGC
At2g01170scrREV	GTGTTGATTATTATTCATTCGC
At2g02000scr2f (GAD 3)	TCGGAGGCAGTGATGTTGGC
At2g02000scrFOR (GAD 3)	GGGCTGCCTTATGATAGACC
At2g02000scrREV (GAD 3)	GGCAATTATCCATCACGTTGCG
At2g02010scrFOR (GAD 4)	ATGGTTTTGTCTAAGACAGTTTCC
At2g02010scrREV (GAD 4)	CTCGAATCCAAGACGAATCAGC
At2g41190for	GAGGACAAGAACAATGATAAGG
At2g41190rev	GAGAGGTAGGAAATGATGCG
At3g17760scrFOR (GAD 5)	GCAAGGTACTTTGAGGTAGAGC
At3g17760scrREV (GAD 5)	CCAATACTTAGTGATATCCTCC
AtProT1 - for	GCCATTGCTGGTTTTGATTTGTGCG
AtProT1 - rev	GCTTACAGGAGAAAATAAACCTGCC
AtProT2 - for	TGAACAATTCGATCTCGAAGTCCC
AtProT2 - rev	GAGGACCCGTAAGCCAAATATCCG
AtProT3 - for	GATTTCTCACCATAGTCTGTCCCG
AtProT3 - rev	TGCCTGAATTTCTGGAAGCATCCC
GAD 1 F2 (At5g17330)	GGCAGAACAAGCGCAAAGCTG
GAD 1 R (At5g17330)	GGCCCAATCGGTAAGTTGG
GAD 1.b F2 (At5g17330)	ACAAGTGGCACTCCCTGCTCC
GAD 2 F (At1g65960)	CTTTGCAAATCGTGAATACCCG
GAD 2 R (At1g65960)	GTTCTGGTGATCTTGCCGG
GAT 1 F (At1g08230)	CTATCTTCTTGCAACGCAGGC
GAT 1 hom F (At5g41800)	CCGGTTATTGTGATGTGGTGC
GAT 1 hom R (At5g41800)	TAAAAACTTTCCCTGAATCCG
GAT 1 R (At1g08230)	GCTACCATAGCAATCACCCC
ghbdh.2 for	TGCTGTGTATAGAGAGTTTCCTCC
ghbdh.2 rev	CATCACACCTAACAACCAAGCCCC
SSADH F	GCCCTGCTCTTGCTTCTGG
SSADH F (SALK)	GTCTCTGGTCACATCTAGATGGATTTC
SSADH F .a	GGAGTTCCTCCGGTAATCTTTTAT
SSADH F .b	TGGAGTTCCTCCGGTAATCTT
SSADH R	CAGCTACATCCAGGCTGTC
SSADH R (SALK)	GTACCAGGGGTATTCAATCTAGATTC
SSADH R .a	TCTTTTGGATAAAGAAATGCCTTC
SSADH R .b	GCACGAGAAACAAAAGCAGTC

LB-F (Gabi-Kat)	ATATTGACCATCATACTCATTGC
RB-F (Gabi-Kat)	GTGGATTGATGTGATATCTCC
RB-RB (Gabi-Kat)	CGCCAGGGTTTTCCAGTCACGACG
GABA-T F (At3g22200)	CTTTCCCTTTTGGTGTCATTTTTA
GABA-T R (At3g22200)	GGCTAATCTGGTTGAGAACTCC
GHBDH for (At3g25530)	TCAGTATGTGAGAGTCCAGC
GHBDH rev (At3g25530)	AGAGTGTGAGAGCTAAGTCC
ghbdh.2 for (GK)	CATCAATACTAATCAGCAAGC
ghbdh.2 rev (GK)	GCGCATTGATAGCTCCCTGTG
SSADH F-2 (At1g79440)	TTGGAGCAGATTGACTGCTGG
SSADH R-2 (At1g79440)	CTTGGGAAGGTGTGGGAATGC
LB-F (WiscDSLox)	AACGTCCGCAATGTGTTATTAAGTTGTC
450E1 (At2g19890) for	CTGCTCAAGAGTGGGCTGGGGC
450E1 (At2g19890) rev	GGACAGCATCATGAAGATGAGCG
453-456K22 (At2g02050) for	TCGTCTTAGCAATTTTGTGTC
453-456K22 (At2g02050) rev	GTTCCAGAGAATCCCTGTCC
LBal (Syngenta)	ATGGTTCACGTAGTGGGCCATC
ssadh-3 f1	CTTTGTTTCGATTGAAGTTTGGG
ssadh-3 r1	CATGATGTCAACATAAAGCATTC

6.4.2. Cloning

Primer

AtGHBDH.1-GFP for
 AtGHBDH.1-GFP rev
 AtGHBDH.2-GFP for
 AtGHBDH.2-GFP rev

Sequence

CACCATGGAAGTAGGGTTTCTGGGTT
 TTCGCGGGAGAATTTACAGC
 CACCATGCCTTTGGTTTCATATATCTTTTGC
 AGCTTCTCGGGATTTTGCAGCTT

6.4.3. RT-PCR

Primer

At2g01170 RT for.a
 At2g01170 RT rev.b
 At2g01170FOR
 At2g01170REV
 At2g02000f (GAD 3)
 At2g02000FOR (GAD 3)
 At2g02000REV (GAD 3)
 At2g02010FOR (GAD 4)

Sequence

GAGTGTGGTGTACGGATGGTTC
 CCACAGAAAAACACAGCAACCGC
 GTTGCTGTGTTTTTCTGTGGC
 GTGTTGATTATTATTCCATTTCG
 TCGGAGGCAGTGATGTTGGC
 GGGCTGCCTTATGATAGACC
 GGCAATTATCCATCACGTTGCG
 ATGGTTTTGTCTAAGACAGTTTCC

At2g02010REV (GAD 4)	CTCGAATCCAAGACGAATCAGC
At2g41190for	GAGGACAAGAACAATGATAAGG
At2g41190rev	GAGAGGTAGGAAATGATGCG
At3g17760FOR (GAD 5)	GCAAGGTACTTTGAGGTAGAGC
At3g17760REV (GAD 5)	CCAATACTTAGTGATATCCTCC
GABA-T F	ATGGTCGTTATCAACAGTCTC
GABA-T R	CTTCTTGTGCTGAGCCTTGAG
GABA-T RT for.b	CATGGATTTACTTATTCTGGTC
GABA-T RT rev.a	AAATCAGCACTCTGCCATCCAGC
GAD 1pro F	CTTGAAAGATAGCAGCTGTC
GAD 1pro R	CTCGTCTTCTTCTGTCGGCG
GAD 2pro F	TCTCAAGGACCATAGTTTCC
GAD 2pro R	TTCATCTTCTTCTCCTCTC
GHBDH-1 for (RT-PCR)	TAGGAAGTAGGGTTTCTGGG
GHBDH-1 rev (RT-PCR)	CTACGAACCGACCACCCTTCCCG
GHBDH1 RT for.a	CAGACCATCATCACTAAGCAG
GHBDH1 RT rev.b	CAAATACCGAAAGAGCAGCAC
GHBDH-2 for (RT-PCR)	CTGCAATCTACTACTCCCTCTACC
GHBDH-2 rev (RT-PCR)	CTCGTTCGCAGCGGCTGCAATCGG
SSADH for (RT-PCR)	ATGGACGCACAAAGCGTTTCTG
SSADH rev (RT-PCR)	GCACCAACAACACCGACAGG
SSADH RT for.a	ATGGTAATAGGAGCAGCAGCG
SSADH RT rev.a	CTCTCCAGCAGTCAATCTGCTCC

6.4.4. Sequencing

gaba-t 1	TACTTTATTCTCTCTCTAGGG
gaba-t 1.2	AGGGGATATGTGTGTGAACG
gaba-t 2	AGTTTTTCCTACTATCCCTCC
gaba-t 3	AATAAAAACACCAACTAGGCC
gaba-t 4	CTACTGCACCAGTTACAACC
gaba-t 5	TTTATTTAATCTTTTCGAGTTCC
gaba-t 5.2	GATTGTTTGAGAGGGAGAGC
gaba-t 6	CCAAATTGACGTGGATCAGG
gaba-t 7	GGTTAGGATATAATGATCTCC
gaba-t 8	GTGACGTTTTTCTTACAGGG
gaba-t 9	AGAAGGAAGAATACCTAAGGC
gaba-t 10	ATCAGATGCCAACGATACCC
gaba-t 11	ATAAACTTTTTCTTCTCGGGC
gaba-t 12	AGGCGAAACGGAAGAGGAG
gaba-t 13	TGGTTCAGCTATAAAAGCACC
gaba-t 14	GCTCGGGACAATGTTTGGC
gaba-t 15	TGGCTCATAAGAATGGCTCC
gaba-t 16	ATGTCGCCAAAGTTGCCCC
gaba-t 17	TCAGTCCCAAGAATCAAACC
gaba-t 18	GAAAGCATTGAAGGCAACGG
gaba-t 19	CATCGTCAGATGTTGTCCC
gaba-t 20	GAAGGGATAAGCCATATCGC
ghbdh.1 1	GAATTGTAGGGAAGAACAACCTGC
ghbdh.1 2	GTTGATTCCAGCAGGCACTG
ghbdh.1 3	CCATCATCGCTGAAGAAAGGC
ghbdh.1 4	GTGGCGAAATCCTGTTCTGTTT
ghbdh.1 5	TTACTGCTTAGTGATGATGGAC
ghbdh.1 6	ATCCTTGTGCTGCTCTTTTCGG
ghbdh.1 7	TATCTGCTCCAAAACACGGCC
ghbdh.1 8	GGACAAGTTGGAAACGGAGC
ghbdh.1 9	TGTCAGCCAATACAAGCCCC
ghbdh.1 10	CTTCTCTGCTGTGATTGAAGC
ghbdh.1 11	ACATAGATTTGAGTATCTCAGCC
ghbdh.1 12	GTGAAGAGAAGCAAGAGGCGG
ghbdh.2 1	ATCTTCCTTTGACCGACTTCG
ghbdh.2 2	GAGCACAGAGTTAGACAATCC
ghbdh.2 3	TAATAAGCTTGAGGAGAGATGG
ghbdh.2 4	GAGTATCGTACATAGTGAGGC
ghbdh.2 5	AACTGACAGATTTTTACTGAGG
ghbdh.2 6	TTGGGGTAGTCTTATCTGAGG
ghbdh.2 7	GATTCCCATAACCCAGAAACCC

ghbdh.2 8	GCTTGCTGATCCTGAAAGTGC
ghbdh.2 9	GGCTCCATTCTTTCCACATGC
ghbdh.2 10	TATCAGATTATTTTGTCTTCGC
ghbdh.2 11	TCACCTAAAATGTCAAGTGCC
ghbdh.2 12	ATCCAAATGTACTTGTGCGAGG
ghbdh.2 13	ACACAAACCTTCTGCTGATGC
ghbdh.2 14	CGTTGACTACAATAAATACGGC
ghbdh.2 15	AAGTGGAAACGGCAACGAGC
ghbdh.2 16	GCACCACAAGAAACCTCCCC
At2g01170 1	TTCGTAAGTGGTGATGGTAGG
At2g01170 2	GCAGCCCTTGCTAGSCCSGCC
At2g01170 3	ATCTGAAGCCTTATGCAGAAGC
At2g01170 4	GTTTGTGTATCAAGGAGTAGGC
At2g01170 5	GGACTCTCAAAAATATTCATGTCC
At2g01170 6	ATCTCTCGTCTGTCTCCGCC
At2g01170 7	TAGACCAGAGTGACAGTGCCG
At2g01170 8	CTCTTCTCAACAGCCTCCCC
At2g01170 9	CAGAGACAAAAGAGAGATTGGG
At2g01170 10	GTGCTTAGGC GTTGTTCGG
At2g01170 11	ATCAAGTCCTAAATGCAGACAG
At2g01170 12	GGCAGTTGCTGGTTTGGTGCC
At2g01170 13	CTTAAATGGGCTTCGTCGAGGC
At2g01170 14	AAGTTGAAATGTGGGTGTTATC
At2g01170 15	TTATTGTAAAGACTGTCTGTGTC
At2g01170 16	GAGAGAAGAAGATGGAGGGAGG
At2g41190 1	TCGTAATTTTCTTCCACC
At2g41190 2	AAATGTGACACCTATGAG
At2g41190 3	ACCCATAGTTTATCCCCTG
At2g41190 4	ACCATTAAGGAGCAAATC
At2g41190 5	TTCTAAGAACAGCACTCG
At2g41190 6	TTATCAGCCATGGATTGGT
At2g41190 7	TTGATAGCAGTAAGCGTG
At2g41190 8	CATAACATTGCAGAAACC
At2g41190 9	TGATATTGGAGAAGCAGC
At2g41190 10	TCGTATAAGAATCAGTCG
At2g41190 11	TTCCTTGTAACCCATCTC
At2g41190 12	TGATTGCTCTTGTCTCCG
At2g41190 13	ACTTGTCGTCGATCAAAAAG
At2g41190 14	TTCTAAATCTAAGTGTCTCGC
At2g41190 15	TAACACGATTACATTTACACC
At2g41190 16	TTTTGGAGACCGTACTTGTG

6.4.5. Mapping

6.4.5.1. SSLP-Marker

SSLPs (simple sequence length polymorphisms) are short stretches of simple sequences, that differ in the repeat number between *Arabidopsis* ecotypes and can therefore be used to distinguish between them [17].

Marker	Size (Col-0)	Size (Ler)	Primer 1	Primer 2
NGA 63	111	89	ACCCAAGTGATCGCCACC	AACCAAGGCACAGAAGCG
NGA 392	170	162	GGTGTAAATGCGGTGTTC	TTGAATAATTTGTAGCCATG
NGA 280	105	85	GGCTCCATAAAAAGTGCACC	CTCCAGTTGGAAGCTAAAGGG
GENEA	209	205	ACATAACCACAAATAGGGGTGC	ACCATGCATAGCTTAAACTTCTTG
NGA 111	128	162	TGTTTTTTTAGGACAAATGGCG	CTCCAGTTGGAAGCTAAAGGG
NGA 1145	213	217	GCACATACCCACAACCAGAA	CCTTCACATCCAAAACCCAC
NGA 1126	191	199	GCACAGTCCAAGTCACAACC	CGCTACGCTTTTCGGTAAAG
CZSOD 2	183	187	GAATCTCAATATGTGTCAAC	GCATTACTCCGGTGTCTGTC
NGA361	114	120	ACATATCAATATATTTAAAGTAGC	AAAGAGATGAGAATTTGGAC
NGA 168	151/150	135/130	GAGGACATGTATAGGAGCCTCG	TCGTCTACTGCACTGCCG
NGA 172	162	136	CATCCGAATGCCATTGTTC	AGCTGCTTCCTTATAGCGTCC
NGA126	107/110	85/89	CTCTGTCACTCTTTTCCTCTGG	CATGCAATTTGCATCTGAGG
GAPAB	142	150	TCCTGAGAATTCAGTGAAACCC	CACCATGGCTTCGGTTACTT
NGA 6	143	123/128	ATGGAGAAGCTTACACTGATC	TGGATTTCTTCCTCTCTTCAC
NGA12	247	234	TGATGCTCTCTGAAACAAGAGC	AATGTTGTCTCCCTCCTC
NGA8	154	198	TGGCTTTCGTTTATAAACATCC	GAGGGCAAATCTTTATTTTCGG
NGA1111	148	154	AGTTCAGATTGAGCTTTGAGC	GGGTTTCGGTTACAATCGTGT
DET1.2	138	136	GGTGAAAATGGAGGAGACGA	TTCAAACACCAATATCAGGCC
NGA1139	114	118	TTTTTCCTTGTGTTGCATTC	TAGCCGATGAGTTGGTACC
NGA1107	150	140	CGACGAATCGACAGAATTAGG	GCGAAAAACAAAAAATCCA
NGA 249	125	115	GGATCCCTAACTGTAAAATCCC	TACCGTCAATTTTCATCGCC
CA72	124	110	CCCAGTCTAACCACGACCAC	AATCCCAGTAACCAAACACACA
NGA 151	150	120	CAGTCTAAAAGCGAGATATGATG	GTTTTGGGAAGTTTTGCTGG
NGA106	157	123	TGCCCAATTTTGTTCCTTCTC	GTTATGGAGTTTCTAGGGCAGC
CDPK9	106	104	TCAATCATTTGTCCAAAACCTGG	GAAACTGACTTGGAGAAGGCA
NGA 139	174	132	GGTTTCGTTTCACTATCCAGG	AGAGCTACCAGATCCGATGG
SO262	220/231	300/>250	ATCATCTTCCCATGGTTTTT	TTGCTTTTTGGTTATATTCGGA
NGA 76	145	159	AGGCATGGGAGACATTTACG	GGAGAAAATGTCACTCTCCACC
NGA129	177	179	CACACTGAAGATGGTCTTGAGG	TCAGGAGGAACTAAAGTGAGGG
CIW 10	140	130	CCACATTTCTTCTTTTCATA	CAACATTTAGCAAATCAACTT

6.4.5.2. CAPS-Marker

CAPS (cleaved amplified polymorphic sites) are DNA fragments amplified by PCR and subsequently digested with specific restriction endonucleases. The number of recognitions sites varies for each marker between *Arabidopsis* ecotypes and the resulting fragment pattern can therefore be used to distinguish between them [99].

6.4.5.2.1. Line 4.D

Gene	Primer A	Primer B	Enzyme	Col	Ler
At4g00895	GAAAGGCCTGCAATTGTTT	AATTCCTTGTGGAAGCTAAATCA	XbaI	808	275 533
At4g01750	GACCCTTCACCAACAACGAC	GCCAATCTACTCATTGCGAGT	XbaI	233 346	579
At4g02000	TCATACAAGAAAGGTCGGACA	GAGGTTTCAGAATCCCTCCA	HindIII	409 591	1000
At4g08390	TCAGCAATCTTGGAGCAGAA	TGAATAATCACTTCCGCAATTT	XbaI	590	198 392

6.4.5.2.2. Line 17.J

Gene	Primer A	Primer B	Enzyme	Col	Ler
At5g39600	CCTGACAATTGGGATTCGAT	TGATGGAATCTCTTATATCTTCACG	MseI	59 332	391
At5g44110	AACCAGCAGTTTTACTCCATGA	TGCAGTTTTCTTACGATGTTCAA	SnaBI	533	265 268
At5g45280	CAAAGTTCGGTATTGCGATG	TTCATGTAAACAAACATTTTAAATTCC	DraI	21 361	21 119 242
At5g47050	TCCATCATCATCATCATGTCC	AACTGAGATTTATGCGGCTGA	HindIII	92 127	219

6.4.5.2.3. Line 21.H

Gene	Primer A	Primer B	Enzyme	Col	Ler
At2g28970	GGCACTAAAAATTGTTATGTAGGTTT	GGGATCACCTCGGTGTCAAT	NcoI	708	40 668
At2g39725	TCTCGTTGAATCAGATACTGTCA	GAGTTGTGGCGGAACCTCTGT	XhoI	535	47 488
At2g47485	CGCATAGTGAGCAGAGATCG	ACTCCTTCGACGCCAAAC	HindIII	127 202	329
At2g41910	GGTTCATACGGTTCGGTGAG	TTCTCGAGAGACTCAGCGTTT	SacII	45 61	106

6.5. Vector Maps

The fragments were first cloned into pDONR207, and then the inserts were recombined using LR-Clonase into the binary vector pGWB5.

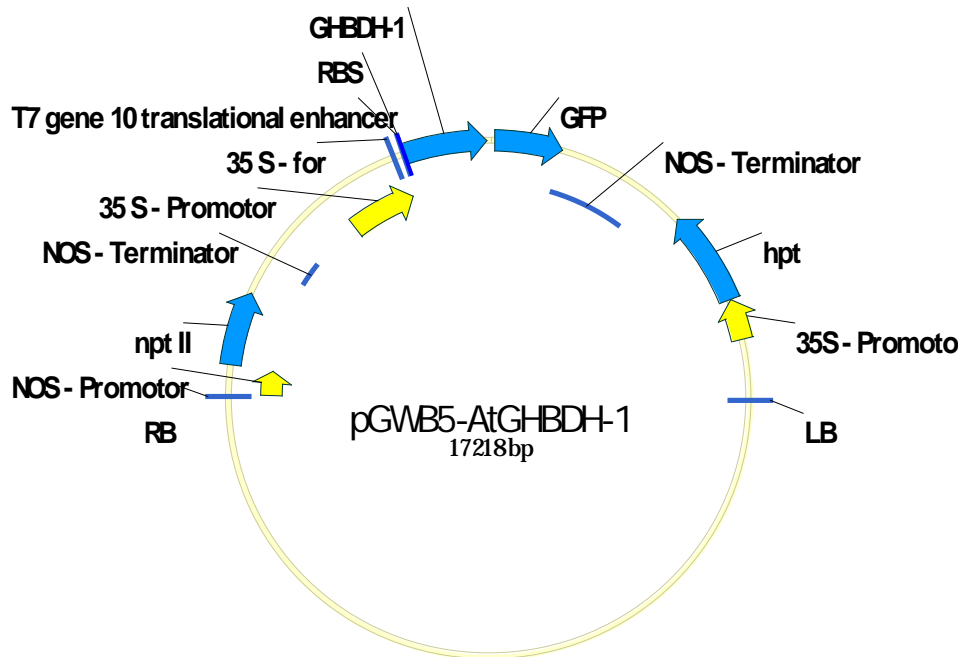


Figure 44: Map of the AtGHBDH-1-GFP fusion construct

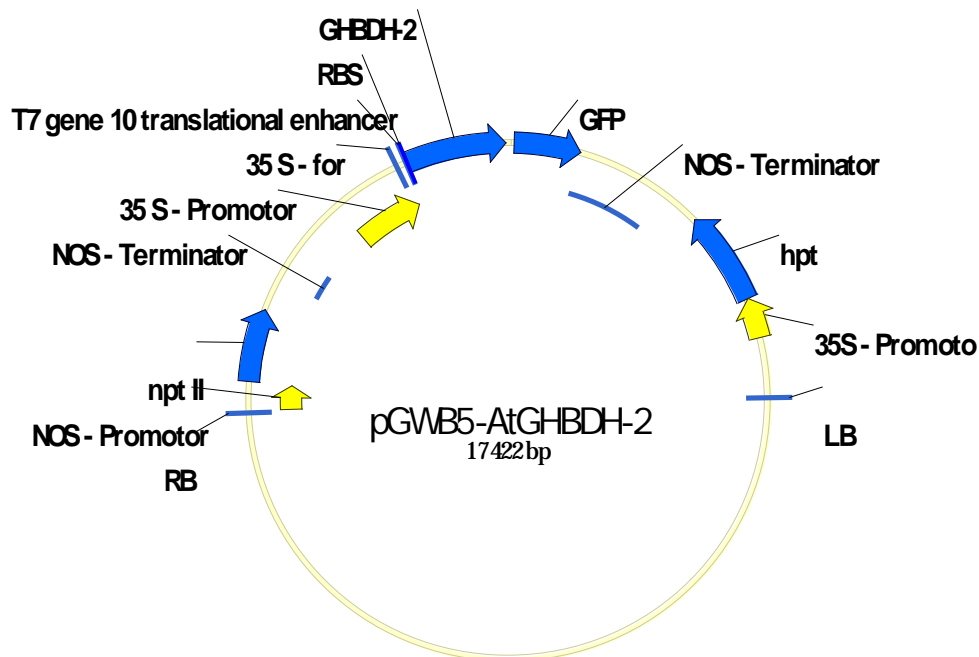


Figure 45: Map of the AtGHBDH-2-GFP fusion construct

Abbreviations

α -C-Atom	first carbon atom following the highest functional group
%	Percent
°C	Temperature (in Grad Celsius)
μ	micro-
1/2 MS	half strength MS medium
A	Absorption
AHL	N-acyl-homoserine lactone
ATP	Adenosintriphosphate
bd.	distilled twice
bp	base pairs
BSA	bovine serum albumin
C	carbon
c	Concentration
ca.	circa
Ca ²⁺	Calcium
CaM	Calmodulin
CBL	Calcineurin B-like Proteins
cDNA	copy DNA
CDPK	Ca ²⁺ -dependent protein kinase
cGMP	cyclic Guanidine monophosphate
dATP	2-Desoxyadenosintriphosphate
DEPC	Diethylpyrocarbonat
DMSO	Dimethylsulfoxyd
DNA	Desoxyribonucleic acid
dNTP	2-Desoxynukleosidtriphosphat
DTT	1,4-Dithiothreitol
EDTA	Ethylendiamine tetraacetate
F ₂	second generation from crossings
FW	Fresh weight
g	Gramm
GABA	γ -amino butyric acid
GABA-T	GABA transaminase
GAD	Glutamatate decarboxylase
GDH	Glutamate dehydrogenase
GHB	γ -Hydroxybutyric acid
GHBDH	γ - Hydroxybutyric acid dehydrogenase
HPLC-H ₂ O	pure water
IPTG	Isopropyl- β -D-thiogalactopyranoside
conc.	concentrated
L	Liter
LB	T-DNA Left border
LB	Luria/Bertani (Medium für Bakterienkultur)
M	Molar (mol/l)
m	milli-

mA	Milliampere
MES	4-Morpholinoethan-sulfonic acid
min	Minutes
MOPS	4-morpholinopropan-sulfonic acid
mRNA	messenger RNA
MS-Medium	Murashige & Skoog-Medium
n	nano
N	nitrogen
NAD(H)	Nicotine amide adenine dinucleotide (reduced)
NADP(H)	Nicotine amide adenine dinucleotidephosphate (reduced)
nm	Nanometer
OD	Optical density
p	Pico
PCR	polymerase-chain reaction
pI	Isoelectric point
QS	Quorum sensing
RB	T-DNA right border
RNA	Ribonucleic acid
rpm	rounds per minute
rRNA	ribosomal RNA
RT	Reverse Transcription
SAP	Shrimps Alkaline Phosphatase
SDS	sodium dodecylsulfate
SSA	Succinic semialdehyde
SSADH	Succinic semialdehyde dehydrogenase
Taq	DNA polymerase (from <i>Thermophilus aquaticus</i>)
TCA	Citric acid cycle
T-DNA	Transfer-DNA
Tris	Tris-(hydroxymethyl)-aminomethane
UV	ultraviolet
w/v	Weight per volume
WT	Wild type

Publications

Ludewig, F., Hüser, A., Fromm, H., Beauclair, L., and Bouche, N.
Mutants of GABA transaminase (POP2) suppress the severe phenotype of succinic semialdehyde dehydrogenase (ssadh) mutants in arabidopsis.
PLoS ONE, 2008. 3:e3383.

Conference Abstracts

Analysis of GABA-shunt metabolites in *Arabidopsis thaliana*

19th International Conference on Arabidopsis Research,
July 23 – 27, 2008 – Montréal, Canada
Poster presentation, ICAR 1008

Do GABA-shunt intermediates act as signaling molecules in *Arabidopsis thaliana*?

Botanikertagung
September 3-7, 2007 - Hamburg, Germany
Poster presentation

Analysis of metabolite contents in Arabidopsis GABA shunt mutants

2nd International Symposium on Plant Neurobiology
May 22-27, 2006 - Beijing, China
Poster presentation
Invited talk at the Normal University of He'nan, Xinxiang, China

Gamma Aminobutyric Acid (GABA) Metabolism in Plants: Analysis of knock-out Mutants

2nd International Symposium on Plant Neurobiology
May 22-27, 2006 - Beijing, China

Arabidopsis knock-out mutants of GABA metabolism and their response to different growth conditions

1st International Symposium on Plant Neurobiology
May 17-20, 2005 - Florence, Italy

γ -aminobutyric acid (GABA) metabolism in plants

Botanikertagung
September , 2004 - Braunschweig, Germany
Poster presentation

Danksagung

Bedanken möchte ich mich bei

Prof. Dr. U.-I. Flügge für die Möglichkeit, sowohl meine Diplom- als auch meine Doktorarbeit in seiner Arbeitsgruppe anzufertigen

Prof. Dr. U. Höcker für die Erstellung des Zweitgutachtens

Prof. Dr. H.W. Klein für die Übernahme des Prüfungsvorsitzes

Dr. Frank Ludewig für die Überlassung des Themas und seine Betreuung

Bei Dennis, Annemarie, Steffi und Sophie bedanke ich mich für die Hilfe bei unzähligen Screenings, Kreuzungen, DNA- und GC-Präps, Platten-Aussaaten und sonstigen kleinen oder größeren Ansätzen – ohne das mir „Beschwerden“ über „Anke-typische“ Größenordnungen zu Ohren gekommen sind – ohne euch wäre mir so manches einfach nicht möglich gewesen.

Allen Mitgliedern der AG Flügge danke ich für das einmalige Arbeitsklima, ich habe mich hier immer sehr wohl gefühlt.

Bei der International Graduate School in Genetics and Functional Genomics bedanke ich mich für die Unterstützung während meiner gesamten Promotionszeit.

Ohne Kirstens Angebot der „offenen Labortür“ wäre mein PCR-Rekord beim Mapping wohl deutlich kleiner ausgefallen....

Bei Klaus Palme (Köln), Markus Geisler (Zürich), Eva Winkelbauer (Tübingen), Malcolm Bennett (Nottingham), Rosalia Deeken und Uta Anschütz (Würzburg) bedanke ich mich für die freundliche Überlassung diverser Mutanten und Reporter-Linien.

Nicht vergessen möchte ich die Mitarbeiter der Gärtnerei für die Pflege meiner Pflanzen und Siggie Werth für die Hilfe bei unzähligen Pflanzenfotos.

Bei meiner Familie möchte ich mich für die Unterstützung während meines gesamten Studiums bedanken.

Lebenslauf

Name Hüser, Anke Christine
Geburtsdatum 28. August 1980
Nationalität Deutsch

Telefon 49-221-4703388
Email AnkeHueser@uni-koeln.de

Adresse Botanisches Institut, LS II
Universität zu Köln
Gyrhofstr. 15
50931 Köln

Ausbildung

ab April 2005 Botanisches Institut der Universität zu Köln, Deutschland
Gruppenleiter: Prof. Dr. U.-I. Flügge
Anfertigung einer Doktorarbeit zum Thema
“GABA metabolism in *A.thaliana*“

ab September 2004 Stipendiatin der “International Graduate School in
Genetics and functional Genomics”,
Universität zu Köln

Juni 2003 – Juli 2004 Botanisches Institut der Universität zu Köln, Deutschland
Gruppenleiter: Prof. Dr. U.-I. Flügge
Anfertigung einer Diplomarbeit zum Thema
“Analyse von Insertionsmutanten des γ -Aminobuttersäure
(GABA)-Stoffwechsels in *A.thaliana*“

Oktober 1999 – Mai 2003 Universität zu Köln, Deutschland
Studium der Biologie, Studienziel Diplom

Juli 1990 – Juni 1999 Gymnasium Schulstrasse, Köln, Deutschland

Erklärung

Ich versichere, dass ich die von mir vorgelegte Dissertation selbständig angefertigt, die benutzten Quellen und Hilfsmittel vollständig angegeben und die Stellen der Arbeit – einschließlich Tabellen, Karten und Abbildungen –, die anderen Werken im Wortlaut oder dem Sinn nach entnommen sind, in jedem Einzelfall als Entlehnung kenntlich gemacht habe; dass diese Dissertation noch keiner anderen Fakultät oder Universität zur Prüfung vorgelegen hat; dass sie – abgesehen von unten angegebenen Teilpublikationen – noch nicht veröffentlicht worden ist sowie, dass ich eine solche Veröffentlichung vor Abschluss des Promotionsverfahrens nicht vornehmen werde. Die Bestimmungen der Promotionsordnung sind mir bekannt. Die von mir vorgelegte Dissertation ist von Prof. Dr. U.-I. Flügge betreut worden.

Köln, den 28.02.2009